NASA order W-13,452 DRA

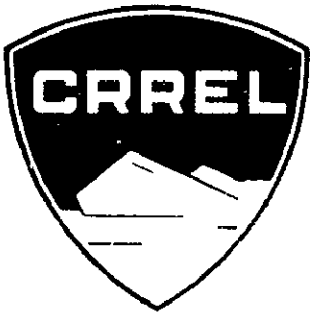

FINAL REPORT
SR/T Contract No.160-75-89-02-10
April 1972-February 1975

Baseline Data on the Oceanography of Cook Inlet, Alaska

L.W. Gatto

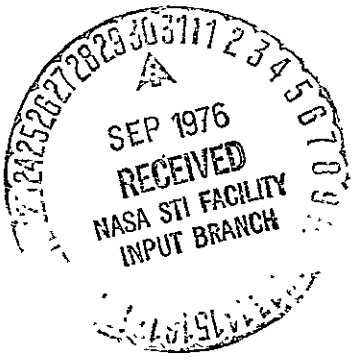

PREPARED FOR
NATIONAL AERONAUTICS AND SPACE ADMINISTRATION
BY
CORPS OF ENGINEERS, U.S. ARMY
COLD REGIONS RESEARCH AND ENGINEERING LABORATORY
HANOVER, NEW HAMPSHIRE

BASELINE DATA ON THE OCEANOGRAPHY OF COOK INLET, ALASKA

Lawrence W. Gatto

U.S. Army Cold Regions Research and Engineering Laboratory
Hanover, New Hampshire 03755

Final Report
for
NASA SR/T Project 160-75-89-02-10

February 1975

Prepared for

National Aeronautics and Space Administration

PREFACE

This report was prepared by Lawrence W. Gatto, Research Geologist, Earth Sciences Branch, Research Division, U.S. Army Cold Regions Research and Engineering Laboratory. The work was funded by the National Aeronautics and Space Administration under NASA-Defense Purchase Request W-13,452, SR/T Project 160-75-89-02-10, Tidal Flushing in Cook Inlet, Alaska.

The author expresses appreciation to Dr. Duwayne Anderson for assistance, critical suggestions and support throughout the project and for guidance in preparing and review of the manuscript; to Michael Hutton for technical review of the manuscript and assistance in data reduction and calculations of flushing rates; to Dr. Harlan McKim, Carolyn Merry and Thomas Marlar for technical review of the manuscript; to Dr. Fredrick Wright, University of Alaska Marine Institute, Messrs Isiah Fitzgerald, Coastal Mapping Division and Robert Muirhead, Oceanographic Division, National Ocean Survey, National Oceanic and Atmospheric Administration for providing ground truth data; to Duncan Chisholm for compiling background material for the section, "Physical and Cultural Setting"; to Eleanor Huke and Carl Martinson for their assistance in layout and drafting; to Robert Demars and Thomas Vaughn for photographic processing; and, to numerous colleagues for encouragement and support.

ABSTRACT

The primary objective of this investigation was to compile baseline information pertaining to the ocean circulation, especially the extent and patterns of tidal currents and tidal flushing, in Cook Inlet utilizing aircraft and satellite imagery with corroborative ground truth data. Earth Resources Technology Satellite (ERTS) -1 and N.O.A.A. -2 and -3 imagery provided repetitive, synoptic views of surface currents, water mass migration and sediment distribution during different seasons and tides. Color, color infrared and thermal infrared imagery acquired on 22 July 1972 with the NASA NP-3A aircraft was used to analyze currents, mixing patterns and sediment dispersion in selected areas. Temperature (°C), salinity ($^{o}/_{oo}$) and suspended sediment concentration (mg/ℓ) data and hand-held photography were utilized as ground truth information in the interpretation of the aircraft and satellite imagery.

Coriolis effect, semidiurnal tides and the Alaska current govern the estuary circulation. Clear, oceanic water enters the inlet on the southeast during flood tide, progresses northward along the east shore with minor lateral mixing, and remains a distinct water mass to the latitude of Kasilof-Ninilchik. South of the forelands, mixing with turbid inlet water becomes extensive. Turbid water moves south primarily along the north shore during ebb tide and a shear zone between the two water masses forms in mid-inlet south of Kalgin Island. Currents adjacent to and north of the forelands are complicated by tidal action, coastal configuration and bottom effects. Turbulence is greatest throughout the water column along the south shore and stratification is more pronounced in Kamishak and Kachemak Bays, especially when fresh water runoff is high. Most of the sediment discharged into the inlet is deposited on the extensive tidal flats or removed by tidal currents along the west side during ebb flow. Bottom scouring is evident along the east shore south of Pt. Possession.

Regional relationships between river hydrology, sediment transport, circulation and coastal processes were analyzed utilizing aircraft, ERTS-1 and N.O.A.A. -2 and -3 imagery and corroborative ground truth data. The use of satellite and aircraft imagery provides a means of acquiring synoptic information for analyzing the dynamic processes of Cook Inlet in a fashion not previously possible.

TABLE OF CONTENTS

ILLUSTRATIONS

TABLES

INTRODUCTION

The Cook Inlet area in south central Alaska (Fig. 1) is currently undergoing the most rapid development in the state and will play an increasingly important role in the future of Alaska. Anchorage, the state's most populated city, located at the head of Cook Inlet, is presently the center of transportation, commerce, recreation and industry. The use of Cook Inlet as a water road to this growing region will increase as the areal development continues. A particular concern of many governmental agencies, especially the Corps of Engineers, is to control and alleviate the environmental disturbances associated with this rapid coastal zone development. Increased estuarine pollution will be a direct result of this future development.

This governmental interest in estuarine and nearshore environments has increased over the last several years as illustrated by new federal legislation and enactment of state laws protecting the fragile ecology of the coasts. As a result, the importance of acquiring adequate baseline data prior to further development in the marine environment was emphasized recently by the Environmental Protection Agency (Carter 1973). In addition, an international symposium on the physical processes responsible for the dispersal of pollutants in the sea with special reference to the nearshore zone was convened at the University of Aarhus, Denmark in July 1972. Subjects of particular concern were advective processes (currents and circulation), turbulent processes (diffusion, shear effects and stratification), effects of ice cover, water entrainment, beach and estuarine processes and modelling (Hansen 1973). A coastal zone workshop sponsored by the Institute of Ecology and Woods Hole Oceanographic Institution was also held in Woods Hole, Massachusetts from 22 May to 3 June 1972. The primary objectives were to identify problems of the coastal zone, assess effects of man's activities and identify scientific, legal, social and economic constraints that prevent rational management of coastal resources. A general conclusion of this workshop was that "maximum rational use of coastal resources consistent with the retention of life-support systems, beauties and amenities of the coastal zone for the enjoyment of future generations must be the objective of coastal zone management" (Ketchum and Tripp 1972). A specific recommendation of the workshop, "the acceleration and expansion of baseline surveys", was addressed during this investigation.

Suspended sediment is currently the dominant pollutant in Cook Inlet and will increase as previously undisturbed areas become affected. Knik and Matanuska Rivers alone discharge up to 150,000 tons of glacial silt per day into the inlet during the summer months (Carlson 1970). It is estimated that in newly developed areas as much as 20,000-30,000 times more sediment is produced than in natural undisturbed areas

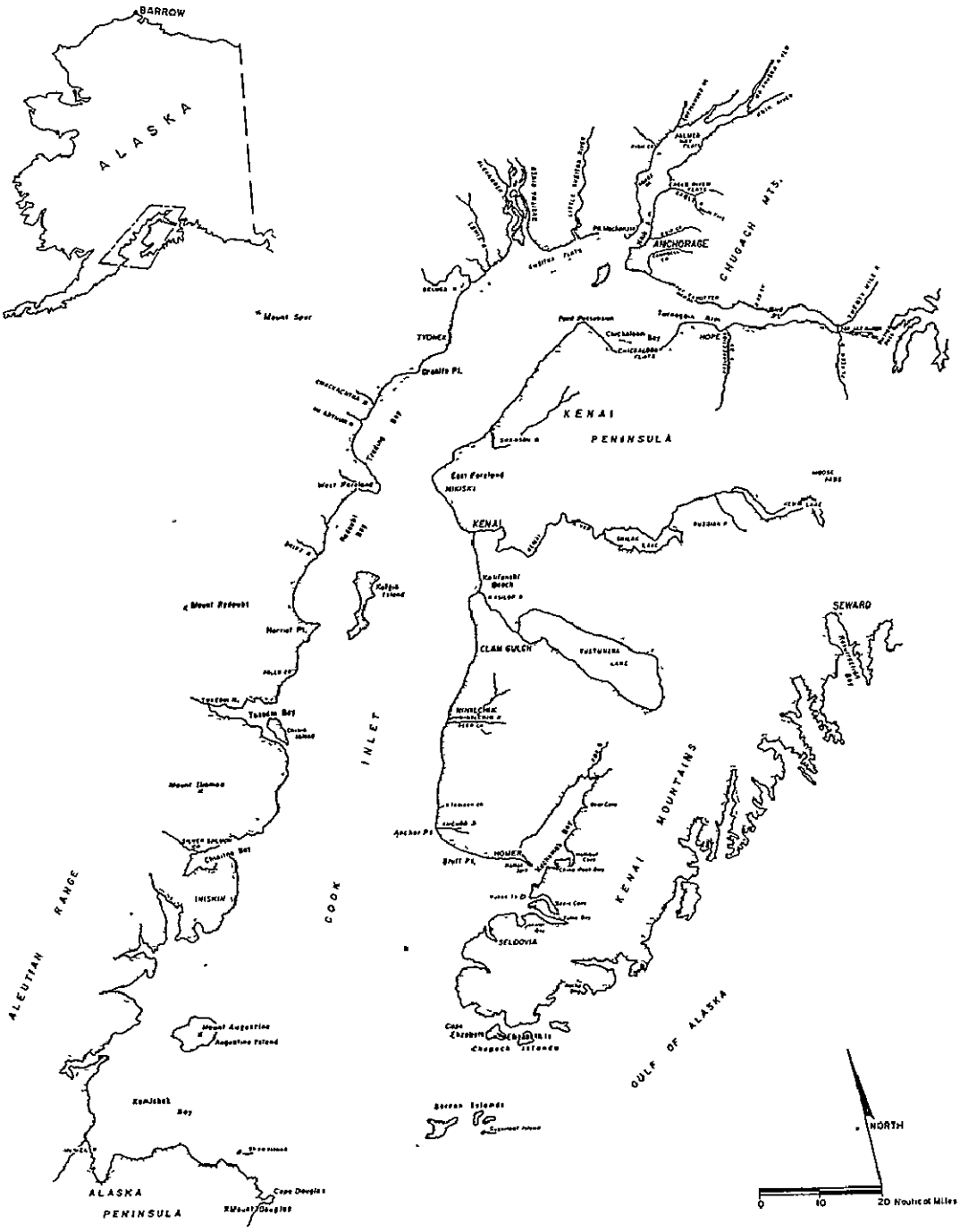

Figure 1. Regional map of Cook Inlet.

(Environmental Currents 1972). Other pollutants include municipal sewage, waste from canneries and natural or manmade oil spills. Baseline data on the ocean currents, particularly tidal currents and the patterns of tidal flushing, are needed to determine the extent that these pollutants remain in the inlet (Bartlett 1973).

Background

Oceanographic processes in the following specific areas of Cook Inlet have been investigated using data collected by conventional ship board methods: Nikiski (Rosenberg et al. 1967 and 1969); the mouth of the Drift River and Trading Bay (Marine Advisers 1966a and b); and, Knik Arm (Murphy et al. 1972). Data for regional areas are sparse; Sharma and Burrell (1970) mapped the distribution of bottom sediments in a large portion of the inlet; available environmental and oceanographic data were compiled by Wagner et al. (1969) and Evans et al. (1972). Although regional oceanographic relationships are beginning to emerge, considerably more data are required to develop a more detailed understanding of the oceanographic processes. A synoptic analysis of the oceanographic processes in large portions of the inlet can be accomplished by correlating interpretations made from remote sensing imagery with ground truth data.

The application of imagery in monitoring surface water circulation and sedimentation processes has been demonstrated in the Straits of Georgia (Tabata 1972), at South Pass, Mississippi River (Coleman et al. 1972), near the Mississippi River Delta (Walsh 1969), along the north and south shore of Long Island (Pluhowski 1972), and in the area around Anchorage and Knik Arm (Barnwell and Zenone 1969). Traditional data collection procedures from aboard ship are expensive, time consuming and exclude the possibility of acquiring synoptic data. Conversely, analyses of patterns of surface circulation and sediment distribution over a large portion of the inlet can be made synoptically with aircraft and satellite imagery and limited ground truth data. In addition, less time is required to observe a given area on the imagery than is needed for sampling while on the sea surface.

The improved understanding of inlet circulation, especially tidal flushing processes as natural mechanisms for dissipating pollutants, will result in more intelligent and efficient planning and performance of construction, maintenance, design and related engineering activities in this marine environment. In addition, new remote sensing interpretation techniques developed during this investigation would be useful in guiding improvements in sensor selection and analysis methods for future aircraft and satellite programs.

Objectives

When this project was originally conceived the following objectives were established:

1. Compile baseline information pertaining to the ocean circulation, especially the extent and patterns of tidal currents and tidal flushing in Cook Inlet.

2. Obtain new remote sensing data on the circulation patterns, sediment transport and deposition under different seasonal and tidal conditions.

3. Validate the most suitable combination of sensors, altitudes, and seasons for ocean and tidal current studies.

4. Develop appropriate maps, charts, diagrams and reports describing and documenting the oceanographic processes to prepare a baseline data package.

5. Improve techniques and develop ideas that will advance our capability for improvements in future remote sensing studies of arctic and subarctic oceanography.

Objectives 1 through 4 have been accomplished and the results reported herein. A baseline data package has been compiled on circulation patterns, extent and patterns of tidal flushing and sediment transport under various seasonal and tidal conditions. These data were acquired using remote sensing methods (i.e. aircraft photography and IR scanner imagery and medium and high altitude satellite multispectral imagery) and corroborative ground truth data. This combination of sensors provided the means to acquire the most useful data and each sensor attributed a unique capability to the investigation. Objective 5 was indirectly addressed in that limitations of the sensor systems used during this project were enumerated. Techniques were improved and ideas developed by illustrating the utility of remote sensing data in areas where existing data are sparse.

Project History

A chronological listing of the events that occurred and the milestones that were accomplished during the project is presented in Table 1. Interim and related reports prepared and presentations made during the project are summarized in Table 2. A preliminary cost analysis (enclosed in the Seventh Quarterly Management and Financial Report, 1 October-31 December 1973) was prepared to evaluate the benefits and utility of remote sensing data in the investigation of Cook Inlet oceanographic processes.

Table 1. Project history, chronological listing of events and milestones.

Milestones	CY72* 1	2	3	4	CY73 1	2	3	4	CY74 1	2	3
Project commencement/Receipt of NASA-DPR, W-13452	▲		(22 Mar)								
Compilation of existing photography and data	▬	▬									
Literature review	▬	▬	▬	▬	▬	▬	▬	▬	▬	▬	▬
Reconnaissance of study area/establish field methods		▲	(29 May/3 June)								
Acquistion of aerial imagery											
Hand-held B/W and color infrared (CIR)		▲	▲	(29 May/3 June; 5-7Aug)							
NASA NP-3A color, CIR and RS-14 thermal scanner imagery			▲	(22 July)							
Acquisition of ground truth data		▬	▬		▬	▬					
Receipt of ground truth data (6 June, 9 Mar, 12 July, 1 Feb)		▲			▲	▲		▲			
1st Quarterly Management/Financial Report			▲	(25 July)							
Acquisition of ERTS-1 imagery			▬	▬	▬	▬	▬	▬	▬		
Receipt of NASA aircraft imagery				▲	▲	(13Oct; 20 Mar)					
2nd Quarterly Management/Financial Report				▲	(2 Nov)						
Thematic mapping with ERTS-1 imagery				▬	▬	▬	▬	▬	▬	▬	▬
Surface circulation											
Water masses/sediment distribution											
Tidal flats											
River plumes											
Sea ice movement											
Acquisition of N. O. A. A. -2 and -3 imagery					▬	▬	▬	▬			
Sea ice regime/N. O. A. A. -2 and -3 imagery					▬	▬	▬	▬			
3rd Quarterly Management/Financial Report					▲	(8 Feb)					
Presentation at 2nd ERTS-1 Symposium, "Sediment distribution and coastal processes in Cook Inlet, Alaska"					▲	(5-9 Mar)					
Project review at Office of Chief of Engineers, Systems Analysis Branch.					▲	(9 Mar)					

Remarks

*Calendar year divided into quarters

Table 1 (Continued)

Milestones	CY72*				CY73				CY74		
	1	2	3	4	1	2	3	4	1	2	3
First look interpretation/evaluation of aircraft imagery						▬					
Thematic mapping with NASA aircraft imagery						▬	▬	▬	▬		
Surface circulation											
Nearshore transport											
Thematic mapping with and analysis of ground truth data						▬	▬	▬	▬	▬	
Surface temperature, salinity and suspended sediment distributions											
Temperature and salinity profiles											
T-S diagrams/characterize water types											
Analyze changes with seasons/tides											
4th Quarterly Management/Financial Report						▲ (31 May)					
Preliminary analysis report							▲ (10 July)				
5th Quarterly Management/Financial Report							▲ (13 Aug)				
U.S. Army Corps of Engineers Remote Sensing Symposium, L. B. J. Space Center, Houston, Texas, "Coastal processes, Cook Inlet"				(26-30 Nov) ▲							
Preliminary Cost/Benefit Analysis					(13 Dec) ▲						
6th Quarterly Management/Financial Report					(27 Dec) ▲						
Seattle District remote sensing briefing					(28 Jan) ▲						
7th Quarterly Management/Financial Report							(3 Apr) ▲				
8th Quarterly Management/Financial Report							(18 June) ▲				
Final Report (Draft)						(30 September) ▲					

Remarks

*Calendar year divided into quarters

Table 2. Reports prepared and presentations made during the project.

Reports

Preliminary Analysis Report, "Baseline data on tidal flushing in Cook Inlet, Alaska", June 1973, 11 p.

"Sediment distribution and coastal processes in Cook Inlet, Alaska": in Symposium on Significant Results Obtained from the Earth Resources Technology Satellite-1, NASA SP-327, March 1973, p. 1323-1339.

"Cook Inlet, Alaska, Bay Processes," in Remote Sensing for Environmental Analysis, A Reference Document for Planners and Engineers, Office of Chief of Engineers Handbook, Washington, D.C., August 1974, Chapter 4, p. 33.

Presentations

Second ERTS-1 Principal Investigator's Symposium, Goddard Space Flight Center, 5-9 March 1973, "Sediment Distribution and Coastal Processes in Cook Inlet, Alaska."

Project review, Office of Chief of Engineers, Systems Analysis Branch, Washington, D.C., 9 March 1973.

U. S. Army Corps of Engineers Remote Sensing Symposium, L.B. Johnson Space Center, Houston, Texas, 26-30 November 1973, "Coastal processes."

"Applications of remote sensing data to Corps of Engineers projects," Seattle District, Corps of Engineers, 28 January 1974.

A review was made of current literature and unpublished reports pertaining to the oceanography of Cook Inlet. Oceanographic and bathymetric data were obtained from the National Ocean Survey and the University of Alaska Institute of Marine Science. Thematic maps were prepared of bottom topography, temperature and salinity distribution, surface currents and suspended sediment distribution. The temperature-salinity contour maps were used to characterize the water masses and the complex circulation patterns and were compared to interpretations from aircraft and satellite imagery. NASA NP-3A aircraft imagery obtained on 22 July 1972 was used to analyze surface circulation patterns, mixing patterns along river plumes, tidal flat morphology and coastline configuration. Late summer and fall water movement was monitored and regional circulation patterns determined with ERTS-1 imagery. N.O.A.A.-2 and -3 VHRR (Very High Resolution Radiometer) visible red and thermal infrared imagery was used to analyze the formation, movement and ablation of inlet ice. The repetitive and synoptic satellite imagery proved to be a necessary tool in analyzing estuarine processes.

Tidal flushing rates were calculated for Knik Arm and the inner portion of Kachemak Bay. Dissipation of inlet pollutants is dependent on tidal current velocities and the amount of freshwater inflow, which influence the net exchange of inlet and ocean water; where these factors are high, the dispersion and diffusion action is greatest. Current and mixing patterns were analyzed and areas delineated where tidal flushing mechanisms and suspended sediment dispersion are most active.

APPROACH

Suspended sediment concentrations in Cook Inlet vary from greater than 1700 mg/l near Anchorage (Wright et al. 1973) to as low as 0.4 mg/l near the inlet mouth (Kinney et al. 1970b). The suspended sediment acts as a natural tracer by which circulation patterns and water masses with different suspended sediment loads (temperatures and salinities) are visible from satellite and aircraft altitudes; thus, surface currents, water mass migration, sediment distribution and nearshore processes can be analyzed using remote sensing techniques and corroborative ground truth data.

Aircraft Imagery

The NASA Earth Resources Aircraft NP-3A (NASA 927) conducted a contingency flight on 22 July 1972 (Data Flight 7) over Cook Inlet during Mission 209. Seven flight lines (Fig. 2) totalling 292 nautical miles were flown at an altitude of approximately 20,000 feet from 1053 to 1233 Alaska Daylight Savings Time. Coverage includes the northern inlet from Harriet Point to the head of Knik Arm and the southern shore from Cape

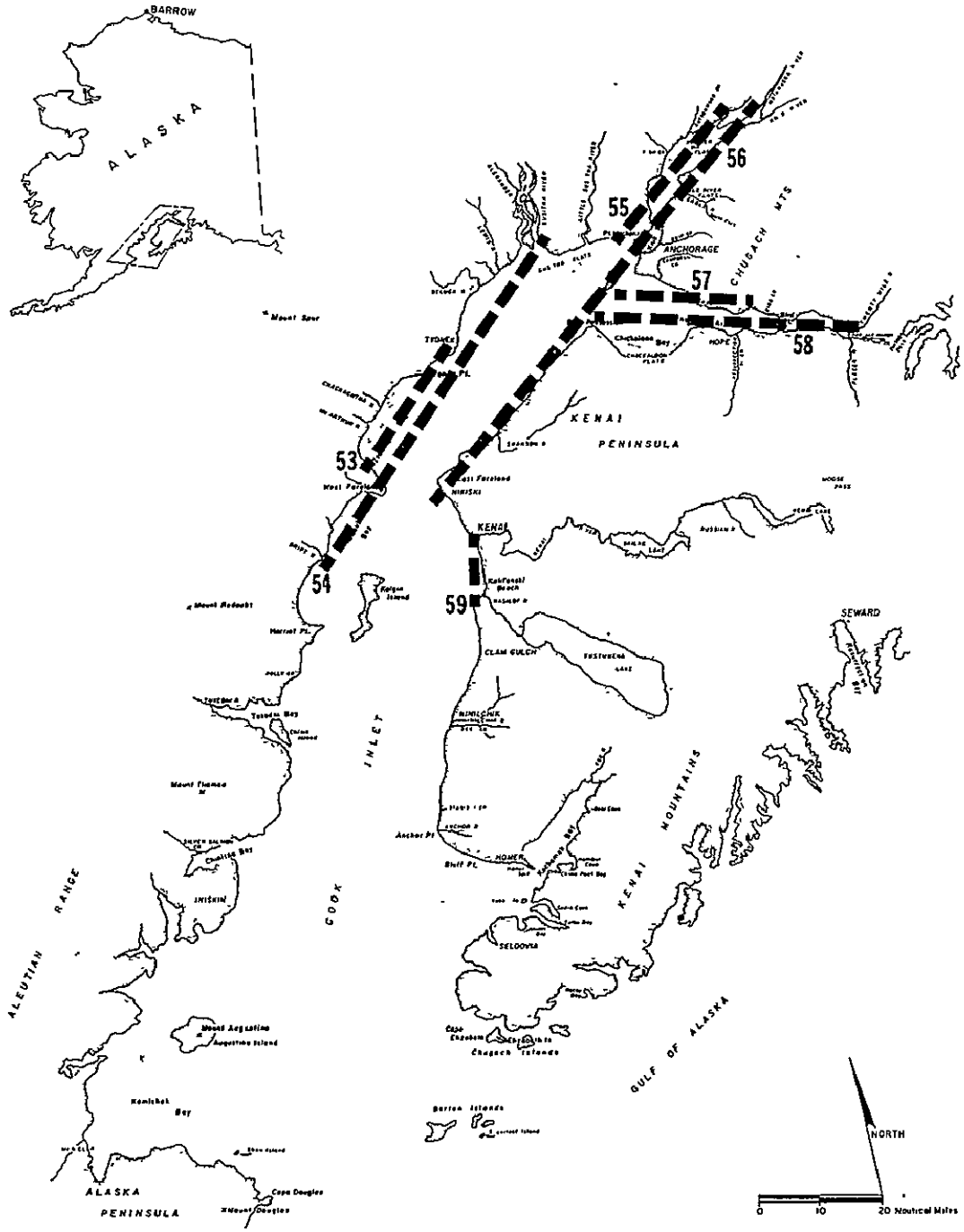

Figure 2. NASA NP-3A aircraft flight lines; mission 209 flown on 22 July 1972.

Kasilof to Anchorage including Turnagain Arm. Atmospheric conditions were ideal: ceiling unlimited, visibility 90 miles, air temperature 66°F, relative humidity 57%, wind southeast at 3 knots. Most of the imagery was acquired during early flood tide at Anchorage, but late flood at Seldovia; ebb tide occurred later in the day when the sun angle was too low and an overflight was not possible (Table 3). The tidal

Table 3. Tides at Anchorage and Seldovia on 22 July 1972 (from U.S. Department of Commerce 1971).

	TIME (Alaska Daylight Savings Time)	HEIGHT (m)*
Anchorage	0349	7.5
	1109	0.4
	1738	7.8
	2321	2.5
Seldovia	0601	0.7
	1242	4.0
	1748	2.1
	2342	4.7

* Above the datum of soundings, which is mean lower low water on charts of the locality.

stage differs at locations throughout the inlet because of its size; low tide can occur in the south while high tide is occurring in the north. For example, on 22 July 1972, high tide at Seldovia occurred one and a half hours after flood tide began in Anchorage.

Photography was acquired with two 9 inch format RC-8 metric cameras with 6 inch lenses (Table 4). One camera had a Wratten 16 filter with Kodak Plus-X Aerographic Black and White Film (Type 2402) and the other a Wratten 12 filter (minus blue) with Aerochrome Infrared Film (Type 2443). The scale of the photography was approximately 1:40,000 and the quality generally good*.

Features apparent on the photography include surface circulation patterns; relative differences in suspended sediment concentrations in the inlet and river plumes; water mass boundaries; foam and debris lines on the water surface which indicate local wind and/or surface current patterns; sun glint on the sea surface which enhances the view of wave front movement, wave refraction and long shore currents; areas of bottom

* Refer to Earth Resources Aircraft Mission Data Transmittal/Quick Look Reports dated 24 October 1972 and 23 March 1973.

Table 4. Data for NASA NP-3A aircraft flight 7, mission 209, 22 July 1972.

FLIGHT LINES	53	54	55	56	59	58	57	REMARKS
TIME - Start (Alaska Daylight	1053	1107	1127	1138	1159	1215	1229	
TIME - Stop Time)	1057	1120	1134	1154	1203	1223	1233	
ALTITUDE (m)	6212	6242	6272	6242	6272	6242	5393	
APPROXIMATE AIR TEMPERATURE AT ALTITUDE	-9°C							
GROUND SPEED (knots)	309	333	323	329	307	332	319	
TIDAL STAGE AT ANCHORAGE	Late ebb flow	Low at 1109 (ADT)	Early flood					
SYSTEM USED								
RC-8 camera No. 1	X (frames X 0-12)	X (frames X 13-48)	X (frames X 49-67)	X (frames X 68-109)	X (frames X 110-117)	X (frames X 118-139)	X (frames X 140-150)	Plus-X, 1/300 sec at f6.8
RC-8 camera No. 2	X	X	X	X	X	X	X	Aerochrome IR, 1/150 sec at f5.6
RS-14 scanner								Dual Channel: 3-5.5 μm, 8-14 μm
DATA OBTAINED	9 in. positive transparencies: Black and White Color IR							
	70 mm IR Scanner imagery strips							Electronic noise on imagery for lines 57 and 58

scouring and sediment reworking; nearshore bathymetry; tidal flat morphology; and coastal landforms. The above features are more distinct on the Aerochrome Infrared (Color Infrared, CIR) than on the Plus-X photography because atmospheric attenuation is less. The CIR photography records near-IR radiation which is less affected by haze. In addition, the amount of blue-green light produced by the haze that enters the camera is reduced by the Wratten 12 filter. The color infrared photography has been reproduced in black and white for this report. The approximate scales of these reproductions are indicated on the prints.

An RS-14 infrared scanner recording in two channels, 3-5.5 μm and 8-14 μm, produced 70 mm positive film strips for each flight line (in pocket at end of report). The scale of the original RS-14 scanner imagery is approximately 1 inch equals 2.25 miles and features 400 feet or larger in size can be seen. The quality is acceptable although some strips are marked with bright scan lines caused by instrument noise (these are not included in pocket). The scanner imagery shows thermal patterns in the water and was useful in interpreting 1) the surface thermal patterns in selected locations, 2) mixing patterns at the interface between colder river water and the inlet water, and 3) the sources of warm or cold water entering the inlet.

The correlation between patterns on the photography and the IR scanner imagery is very good*. These two NASA aircraft data products were used to verify patterns observed on ERTS imagery and to aid in analyzing surface currents which are the mechanisms of pollutant dispersion and diffusion at river mouths and along the coast.

Earth Resources Technology Satellite (ERTS)-1 Imagery

The multispectral scanner (MSS) on ERTS-1 has been the primary source of satellite imagery. The MSS records reflected radiation in four bands of the visible and near infrared region of the electromagnetic spectrum: band 4, 0.5-0.6 μm; band 5, 0.6-0.7 μm; band 6, 0.7-0.8 μm; and, band 7, 0.8-1.1 μm. Coastal landforms and cultural features are most distinct on ERTS MSS bands 5, 6 and 7, and suspended sediment distribution on bands 4 and 5. In general only one ERTS band is reproduced in this report. However, many of the conclusions are fully justified only by inspection of two or more spectral bands. In addition, the offset reproduction process has obscured some of the features discussed in the text or annotated on the photographs.

The satellite passes over Cook Inlet 4 successive days per orbital cycle, records 3 scenes of the inlet on each day (weather permitting),

* Refer to Preliminary Analysis Report for NASA SR/T Project 160-75-89-02-10, dated June 1973.

and, as of 7 August 1974 (end of analysis of ERTS imagery), had completed 41 cycles since launch on 23 July 1972. Each image covers 185 km on a side, has 10% overlap and approximately 50-60% sidelap at the latitude of Cook Inlet. Only 20% of the imagery is useful, however, because of frequent and extensive cloud cover and because of the low sun angle (<8°) from late November to mid-January. In spite of these interruptions in coverage, sufficient data are available for detailed analysis.

N.O.A.A.-2 and -3 Satellite Imagery

The very high resolution radiometer (VHRR) on board the NOAA-2 and -3 satellites, launched 15 October 1972 and 6 November 1973, respectively, into sun-synchronous polar orbits, provides imagery in two bands, visible red (0.6-0.7 μm) and thermal infrared (10.5-12.5 μm). The thermal IR imagery is useful in observing the formation, ablation and movement of sea ice in the inlet during the low sun angle periods when ERTS is not acquiring data. The VHRR imagery has a ground resolution of 1 km at nadir (ERTS ground resolution is approximately 70 m), is acquired several times during the day for the same area and serves as correlative information to the ERTS imagery.

Ground Truth Data

Ground truth data to be used in compiling a baseline data package and as corroborative information in interpreting satellite and aircraft imagery were obtained from two principal sources: the National Ocean Survey, N.O.A.A. and the University of Alaska Marine Institute. Oceanographic data were acquired with two ships from the Oceanographic and Coastal Mapping Divisions of the National Ocean Survey, N.O.A.A. Data collection was recently completed for the second season of a multiyear N.O.A.A. program to provide information for revision of the Cook Inlet navigational charts and to provide data for ecological, pollution, engineering and fisheries studies (Isiah Fitzgerald, personal communication, 1973).

Two types of surveys are being performed by N.O.A.A.: a tidal/current survey with instrumented buoys which measure currents and tidal fluctuations at selected locations in the inlet and a hydrographic survey of salinity, temperature, bathymetry and bottom sediment characteristics. Temperature and salinity (T-S) measurements were obtained from 15 May - 9 September 1973 using two instruments: a Plessey 9060 self-recording STD and an in-situ salinometer. Three types of stations were located at 62 sites in the inlet south of 60° north latitude (Fig. 3). Data were acquired from each site several times during the survey period. Four time series stations (S) were located in the south central part of the inlet. Data were acquired every half hour for 13 hours at these

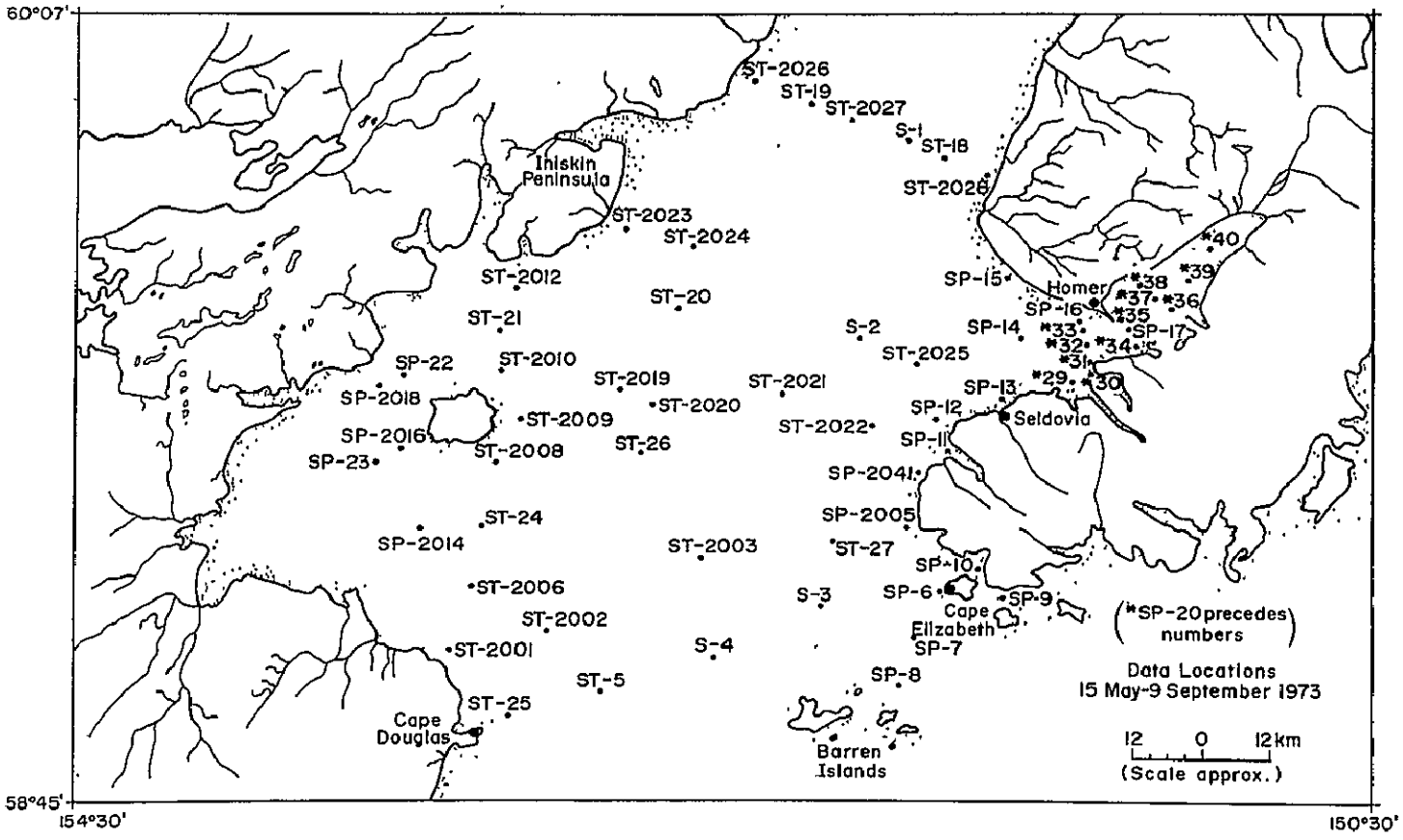

Figure 3. Data locations for N.O.A.A. survey from 15 May-9 September 1973.

locations. Thirty transect stations (ST) were located along four transects across the inlet and one across Kamishak Bay, east of Augustine Island. Thirty peripheral stations (SP) were scattered in Kamishak Bay, Kachemak Bay, Kennedy Entrance between the Barren and Chugach Islands and along the southeast coast from Elizabeth to Yukon Islands. Data were taken every 5 meters from the surface to 50 meters, then at 10 meter intervals from 50 meters to the bottom at deeper sites.

Additional temperature, salinity, pH, dissolved oxygen and nutrient (PO_4, NH_3, NO_2, NO_3, SiO_3) measurements from six cruises were provided by the University of Alaska Marine Institute. Data for surface and depth were collected throughout the inlet at 44 stations from 15-19 July 1966, 31 stations from 25-26 August 1966, 76 stations from 6-13 June 1967, 65 stations from 21-30 May 1968, 12 stations from 26-28 August 1969, and 14 stations from 17-18 August 1970. More recent surface salinity, temperature and suspended sediment concentration measurements* were obtained during 5 surveys from August 1972 to June 1973: 47 stations from 22-23 August 1972 in the northern inlet and on the eastern side of the southern inlet, 68 stations from 25-29 September 1972 throughout the inlet, 4 stations on 27 March 1973 from Tuxedni Bay to Anchor Point, 8 flood tide and 10 ebb tide stations on 14 April 1973 from Chinitna Bay to Homer, and 65 stations from 7-8 June 1973 in the southern inlet between 60°10' and 59°30' north latitude.

Aerial and ground surveys were made from 28 May - 2 June and 5-7 August 1972. Panchromatic, color and color infrared low-altitude aerial photographs were acquired of coastal topography, tidal flats, sediment plumes at river mouths, surface circulation patterns at ebb and flood tide, suspended sediment load at various locations, wave patterns and patterns of wind effect on the water surface. Beach profiles and surface features on exposed tidal flats were observed. The photographs acquired and observations made during the surveys were used as ground truth in analyzing the satellite and NASA aircraft imagery. Additional ground truth sources include current literature; unpublished reports from the U.S. Geological Survey, University of Alaska Marine Institute and private industry; and bathymetric data from the National Ocean Survey.

Imagery and Ground Truth Data Analysis

Satellite and aircraft imagery were analyzed and the interpretations correlated with data on currents, temperature, salinity, suspended sediment concentration and tides obtained from shipboard surveys during

* Data provided by F. F. Wright, University of Alaska.

overflights. Data were acquired at different seasons and tidal stages to detect respective changes. The current velocity and position, temperature, salinity and suspended sediment data were used to produce maps of surface circulation, isotherms, isohalines and sediment concentrations; the "at depth" data were used to prepare water profile diagrams to determine water column characteristics, and define subsurface processes and inlet stratification. This report constituted a preliminary baseline data package with direct application to many marine engineering problems. This approach has demonstrated the effectiveness of remote sensing techniques in providing data required for the solution of these problems.

PHYSICAL AND CULTURAL SETTING

Geography

Cook Inlet (Fig. 4) is oriented in a northeast-southwest direction and is approximately 330 km long, increasing in width from 37 km in the north to 83 km in the south. This mosaic was made with ERTS MSS band 6 images acquired during the sixth cycle over the inlet on 3 and 4 November 1972 when the sun angle was only 12°. These were the first cloud-free images of the entire inlet but the low sun angle caused the patterns on the flat water surface to be subdued, especially in bands 4 and 5. Various areas around the inlet were observed during the previous 5 cycles but generally clouds obscured most of the inlet and a synoptic view of surface circulation patterns and sediment distribution was not available until November. It was determined by inspection that band 6 provided the best rendition of coastline configuration and surface patterns.

The inlet is geographically divided into a northern and southern region by the East and West Forelands. It is bordered by extensive tidal marshes, lowlands with many lakes and glacier-carved mountains. Tidal marshes are prevalent around the mouth of the Susitna River, in Chickaloon, Trading and Redoubt Bays. The Chugach Mountains border the inlet on the east. The Kenai Lowland, a flat marshland of lakes and bogs, is situated east of and adjacent to the inlet. It separates the inlet from the Kenai Mountains on the southeast; the mountains trend southwesterly and border the inlet mouth on the southeast. The Susitna Lowland, similar in topography to the Kenai Lowland, is located at the head of the inlet and lies between the Talkeetna Mountains on the northeast and the southern Alaska Range on the northwest. The Alaska-Aleutian Range forms the western border.

The eastern mountains are generally lower (1000-2000 m) than those on the west (1000-3000 m). The mountains are steep and rugged with very distinct treelines. Above the treeline, bedrock is exposed and rock

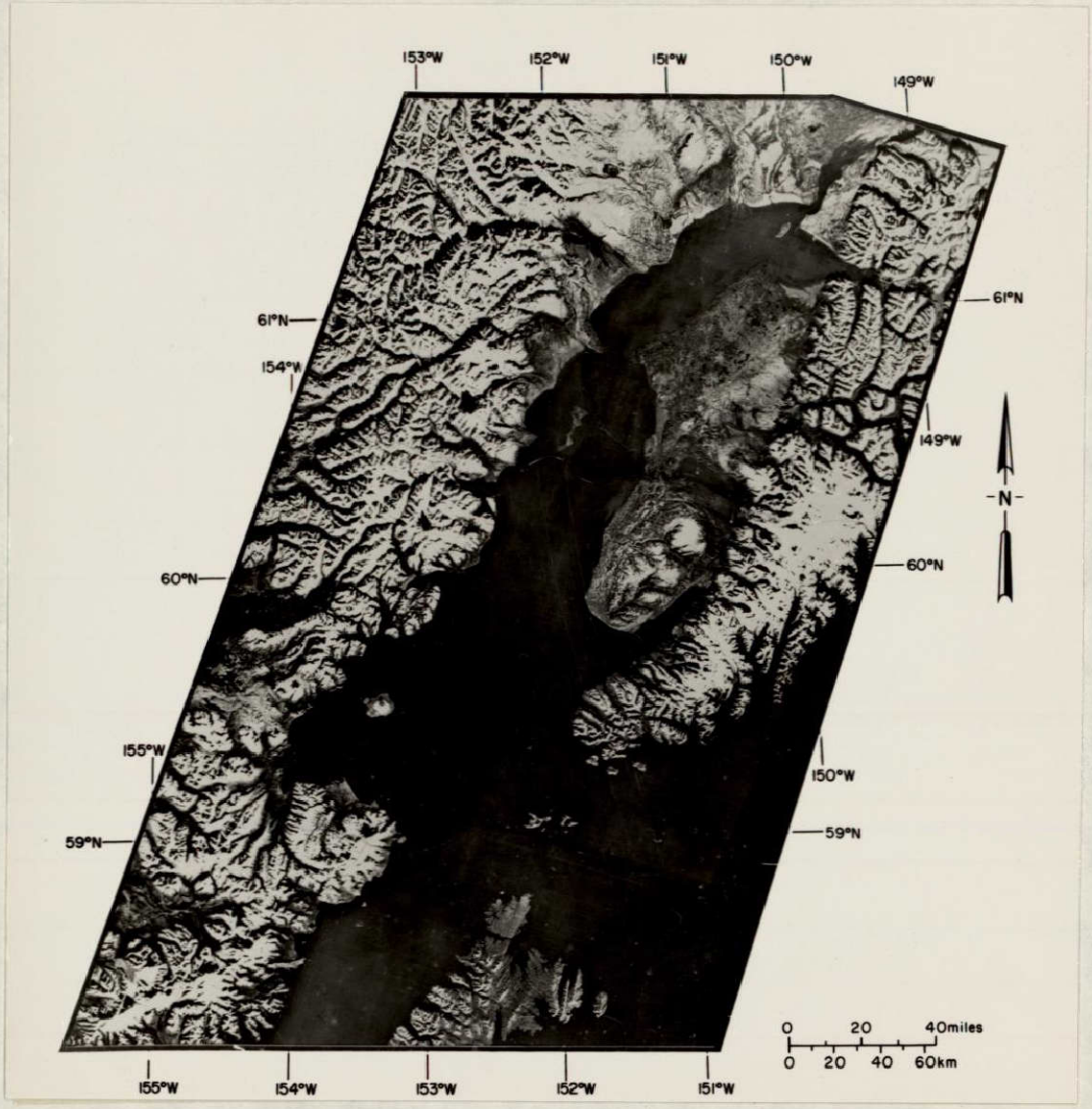

Figure 4. Geographic setting of Cook Inlet. Mosaic made from MSS band 6 images 1103-20513, 1103-20520, 1103-20522, 1104-20572, 1104-20574, 1104-20581 acquired 3 and 4 November 1972.

slides are common; scrubby alpine vegetation occurs on the lower slopes; black spruce forests or grasslands exist in a few areas. The higher portions of the surrounding ranges are covered with ice fields and valley glaciers; regional topography has been sculptured by extensive glaciation.

Approximately 90% of the Kenai, Chugach and Talkeetna Mountains is non-forested; however, approximately 70% of the forested areas in these mountains occur in the Chugach National Forest where sitka spruce and western hemlock are dominant species. The remaining forest lands located on lower slopes and in stream valleys are dominated by interior spruce-birch forests. Nearly 75% of the Cook Inlet-Susitna lowlands is forested with white spruce, paper birch, and quaking aspen. Sitka spruce is common around the mouth of the inlet and cottonwood along major streams. Black spruce occurs in wet or burned areas; muskeg, usually treeless, occasionally supports some stunted black spruce. Lowland vegetation changes to grasses, willow, and alder (Johnson and Hartman 1969) at elevations greater than 240 m at the inlet mouth and at 300 m to 455 m further north; scrubby alpine vegetation occurs at somewhat higher elevations.

Approximately 18,000 acres are cultivated for agriculture in the Matanuska River valley near Palmer and Wasilla northeast of Knik Arm. Virtually all of the remaining cultivated land is located in the coastal lowland area of the Kenai Peninsula and in the eastern portion of the Susitna River valley (U.S. Department of Agriculture et al. 1968).

Many of the natural features, major cities, towns and previously unmapped developments south of the mouth of Drift River and on the southern shore of the West Foreland are identifiable on the ERTS-1 image shown in Figure 5. Anchorage (1), the state's most populated city, is the center of transportation, commerce, recreation and industry and is situated between Knik (2) and Turnagain (3) Arms in the northern portion of the inlet. Fire Island (4) is located approximately 8 km off the coast west of Point Campbell. The Susitna River (5) with an average discharge of approximately 918 m^3/sec (Wagner et al. 1969) is a major contributor of sediment to the inlet. Note the well-defined tidal channels that have formed at the river mouth. Chickaloon Bay (6) and other areas around the northern inlet have extensive tidal flats (7). McArthur River (8), a glacial stream originating in the Chigmit Mountains to the west, drains into the inlet in Trading Bay (9). Trading Bay is presently the major site of active petroleum production in the area. An oil refinery and a tanker terminal are located at Nikiski (10), 24 km across the inlet. Kenai (11), at the mouth of the Kenai River, is a fishing and oil and gas processing center. Numerous submarine pipelines cross the inlet and several crude oil gathering facilities are located along the coast in this area. The Kenai Lowland (12), located east of

Figure 5. Northern portion of Cook Inlet. MSS band 6 image 1103-20513, acquired 3 November 1972.

Kenai, is a flat, glaciated plain marked by numerous lakes and swampy areas. The Kasilof River (13) begins at Tustumena Lake and discharges into the inlet approximately 21 km northeast of the lake. Kalgin Island (14) is located in the central portion of the inlet and separates two bathymetric channels found between Harriet Point and Kasilof. Near the mouth of the Drift River is a tanker terminal, an oil storage area and a landing strip (15). Sediment patterns and oceanic water (16) with a low suspended sediment concentration are discernible in the inlet. Differences in the concentrations are visible because turbid water causes more reflection of visible light and appears lighter.

The southern portion of Cook Inlet (Fig. 6) is less populated than the north. Nevertheless, there are numerous small towns and settlements. Ninilchik (1), Anchor Point (2) and Homer (3) at the base of the spit in Kachemak Bay (4) are located along the southern shore. Homer is a fishing town and is often used as a haven for ocean vessels caught in foul weather in the Gulf of Alaska. Seldovia (5) and English Bay (6) are small fishing villages on the northern side of the Kenai Range at the inlet mouth. The Chugach Islands (7) are clearly seen on the south side of the Kenai Mountains. The mountainous west shore of the inlet is marked by many embayments; Tuxedni (8), Chinitna (9) and Kamishak (11) Bays are the largest. Geologic structure on the Iniskin Peninsula (10) is recognizable in this image. Augustine Island (12) is an active composite volcano (strato-volcano) with a classic conical shape. It has a history of violent eruptions typical of an andesitic type volcano (Selkregg et al. 1972). Cape Douglas (13) is located on the western side of the inlet mouth, and between the Barren Islands (14) and the Kenai Peninsula to the north is the Kennedy Entrance to the inlet. Differences in sediment concentration are apparent between clear oceanic water on the east and turbid inlet water on the west; the boundary between these water masses is approximately at mid-inlet.

Geology

The Cook Inlet basin occupies a structural trough, is underlain by Late Paleozoic to Recent marine and nonmarine sedimentary and volcanic rocks and is mantled by unconsolidated deposits from five Pleistocene glaciations and recent deposition (Wagner et al. 1969, Karlstrom 1964). Local geologic history is characterized by extensive tectonism, deposition and glaciation. Five parallel, arcuate geosynclines and geanticlines were developed during the Mesozoic in south central Alaska (Grantz et al. 1963). Subsequent diastrophism further altered the southern Cook Inlet region during the Eocene when the subparallel Shelikof Trough was superimposed (Payne 1955) across the existing structures. As much as 4500 m of sediment was deposited during the Eocene following this subsidence.

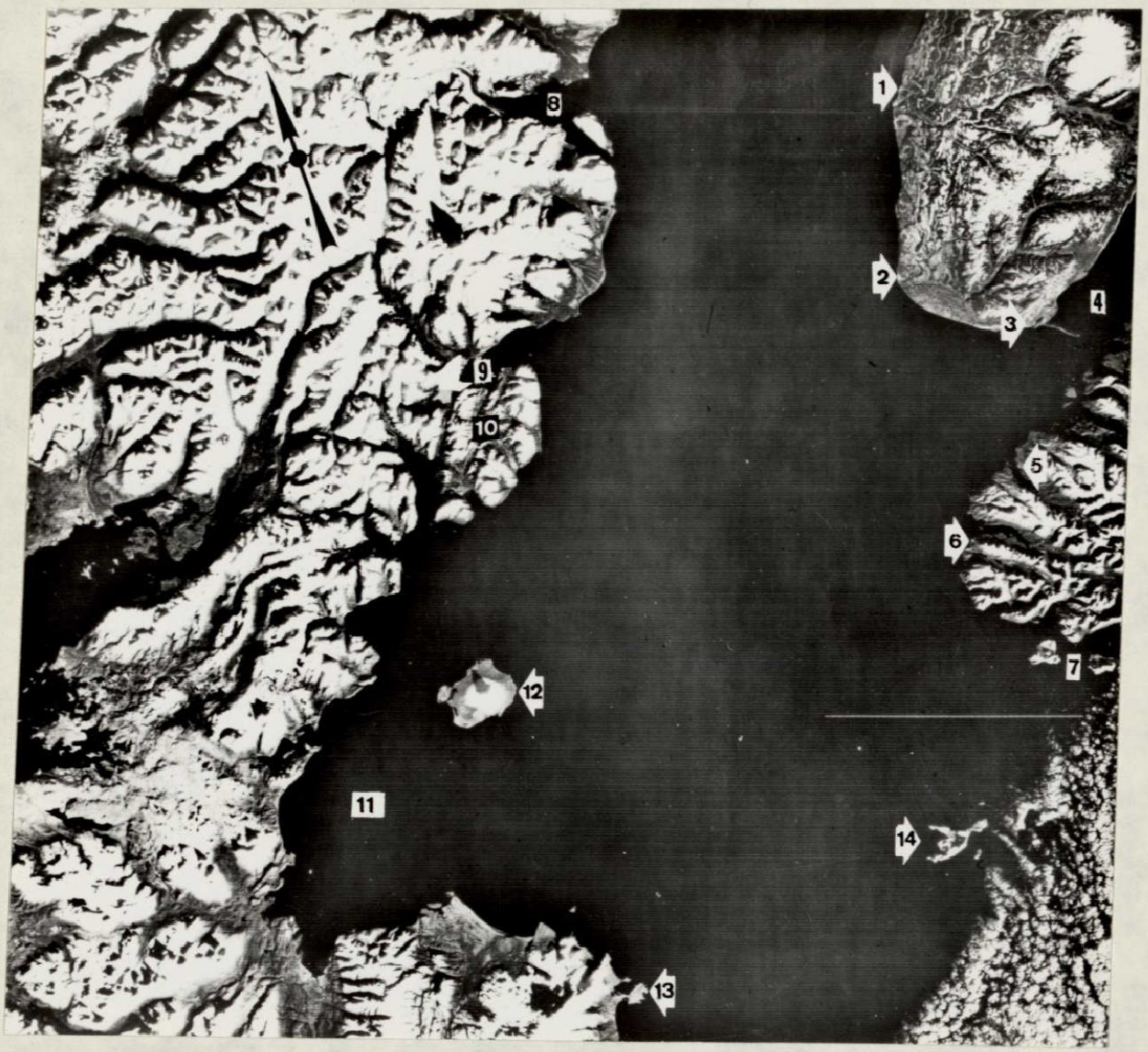

Figure 6. Southern portion of Cook Inlet. MSS band 6 image 1104-20574, acquired 4 November 1972.

The Cook Inlet area is highly faulted by both major and minor faults. Many of the major faults, such as the northwest dipping, reverse Bruin Bay and Castle Mountains faults, have offset the basal contacts between the sedimentary rocks of the regional geosynclines and geanticlines (Grantz et al. 1963); smaller faults have offset some of the surficial deposits. The abrupt change from lowlands to the steep flanks of the Chugach and Kenai Mountains (Fig. 4) and the relatively straight trenches within the mountains are attributed to faulting (Miller 1958, MacKevett and Plafker 1974).

This area is located in the trans-Pacific seismic zone and tectonism characteristic of the regional geologic history continues along many faults (Evans et al. 1972). The basin is included in seismic risk zone 3, defined as areas susceptible to earthquakes with magnitude 6.0-8.0 and where major structural damage could occur (Federal Field Committee 1971). Approximately 60 earthquakes $\geq$ 6.0 magnitude have occurred in the area from 1899-1964 (Evans et al. 1972); Anchorage alone has experienced 114 earthquakes from 1930 to 1954 (Porter et al. 1963).

Regional geologic structures in the Cook Inlet basin were formed by the end of the Tertiary (Wagner et al. 1969). Glaciation was extensive from the end of the Tertiary through the Pleistocene; five major and two minor glacial periods are recognized during the Quaternary (Karlstrom 1964). Glacial erosion sculptured the surrounding mountains and the lowlands are blanketed with glacial deposits; most of the present day topography was formed or modified during the Pleistocene. Thick alluvial, glacial and eolian deposits blanket the Tertiary, coal-bearing, non-marine sedimentary bedrock (Barnes 1958a) which underlies most of the lowlands to the north and east. The glacial deposits occur as extensive moraines, drumlin fields, eskers and broad outwash plains; marine and lacustrine deposits are not as extensive (Wahrhaftig 1965). Eolian silts from the glacial outwash and volcanic ash mantle the original glacial deposits (U.S. Department of Agriculture et al. 1968).

The mountains to the west are composed of large granitic batholiths which intrude highly deformed and slightly metamorphosed Paleozoic and Mesozoic sedimentary and volcanic rocks. Jurassic sedimentary rocks in the southern section of these mountains form hogbacks and cuestas dipping southward toward the inlet. Mounts Spurr, Iliamna and Redoubt are active volcanoes which border the inlet (Wahrhaftig 1965). The Bruin Bay fault trends northeast-southwest along the west shore of Kamishak Bay. A large Mesozoic granitic batholith is located north of the fault with folded and faulted Mesozoic and Cenozoic sedimentary rocks to the south (Wahrhaftig 1965).

The central and western Talkeetna Mountains are composed mainly of mid-Jurassic intrusives and Jurassic volcanics. The southern section is

predominantly Jurassic and Cretaceous sedimentary rocks capped by Tertiary basalt flows (Trainer 1953, Wahrhaftig 1965). Paleozoic and Mesozoic greenstone, greywacke and argillite are dominant in the northern portion (Wahrhaftig 1965).

The Kenai and Chugach Mountains are composed chiefly of slightly metamorphosed Mesozoic argillite and greywacke with Paleozoic and Mesozoic schist, greenstone, chert and limestone along the northern edge (Wahrhaftig 1965). Granitic intrusives are common. Lava flows, tuff and agglomerate are exposed along the western flank of both the Chugach and Kenai Mountains in the vicinity of Knik and Turnagain Arms (Porter et al. 1963).

Climate

The Cook Inlet area is located in a transitional zone between the interior, with its cold winters, hot summers, low precipitation and moderate winds and the maritime with cool summers, mild winters, high precipitation and frequent storms with high winds (Evans et al. 1972). Factors determining local climate are further complicated by topography; the surrounding mountains greatly affect the distribution of precipitation and the prevailing wind speed and direction.

Maritime characteristics predominate in the southern inlet region; winters are mild and summers are cool. Average winter temperatures in Homer are higher than 20°F; summers average 50°F (Fig. 7). Continental influences become somewhat more important in the northern section and the seasonal temperature range increases. In Anchorage, the average winter temperature is less than 15°F, the average summer temperature greater than 55°F. Temperatures at Kenai and Kasilof are transitional between those at Homer and Anchorage. Temperatures can vary considerably from the mean for the various locations (Trainer 1953).

Topographic effects on annual precipitation are well illustrated in the Chugach and Kenai Mountains. The mountains block the flow of moist air from the Gulf of Alaska and most of the precipitation carried by these easterly and southeasterly winds falls on the eastern slopes (Fig. 8) (Schoephorster 1968). The mean annual precipitation in Anchorage, Kenai, Kasilof and Homer is therefore relatively low, 14.4, 19.2, 16.4 and 22.1 inches, respectively (Fig. 7). Departures from the mean annual precipitation in these areas, however, can be as much as 1/3 of the local mean (Trainer 1953). Fifty percent of the annual precipitation for the period 1962-1971 fell from July through October. The driest period during the same 10 years, when about 20% of the precipitation fell, was January through May (Fig. 7).

Annual precipitation in the western portion of the basin is considerably greater and more consistent (Schoephorster 1968). Moist

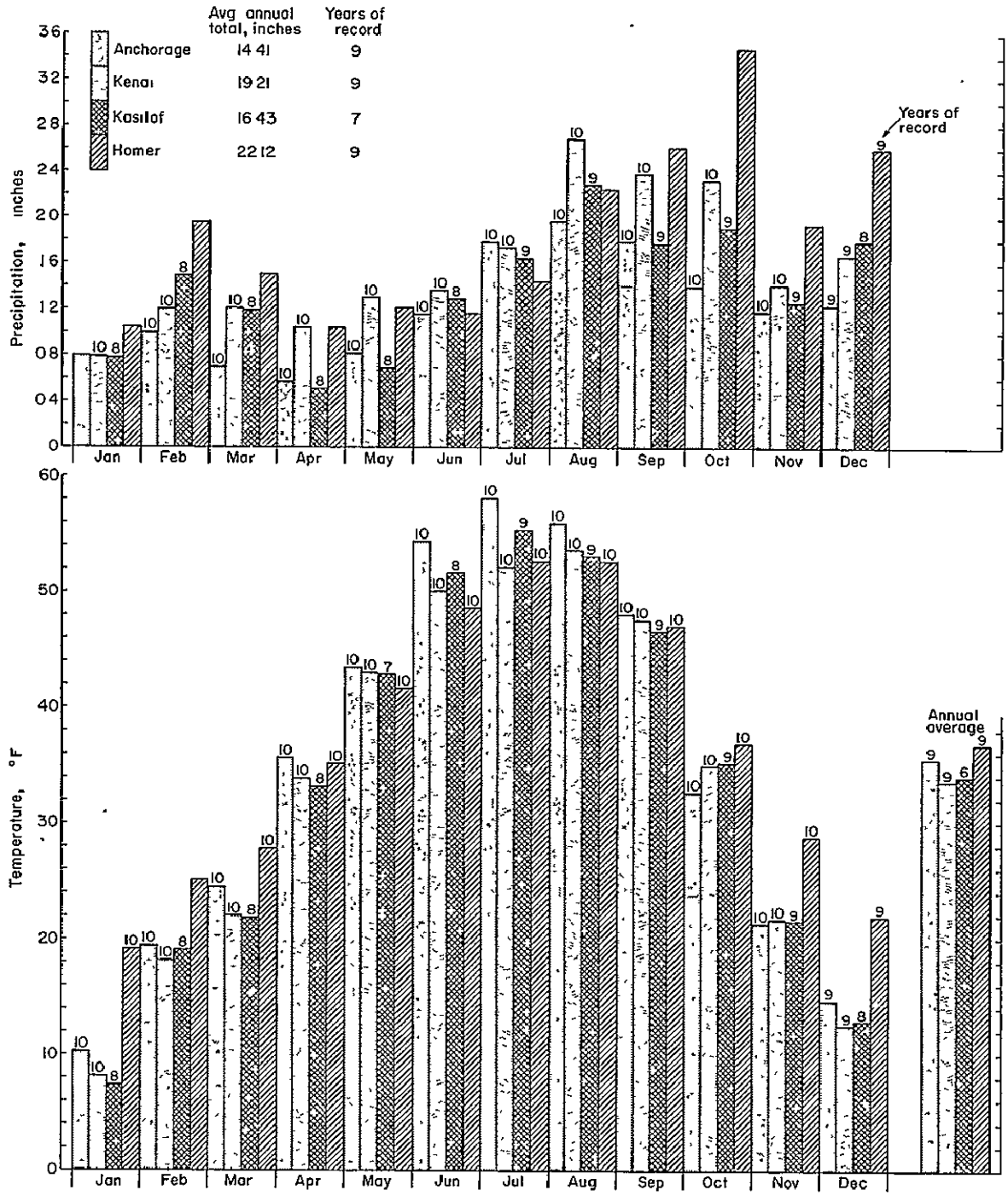

Figure 7. Average monthly temperatures and precipitation for Anchorage, Kenai, Kasilof and Homer (from Monthly Reports of Climatological Data: Alaska, U.S. Dept. of Commerce, NOAA, Environmental Data Service).

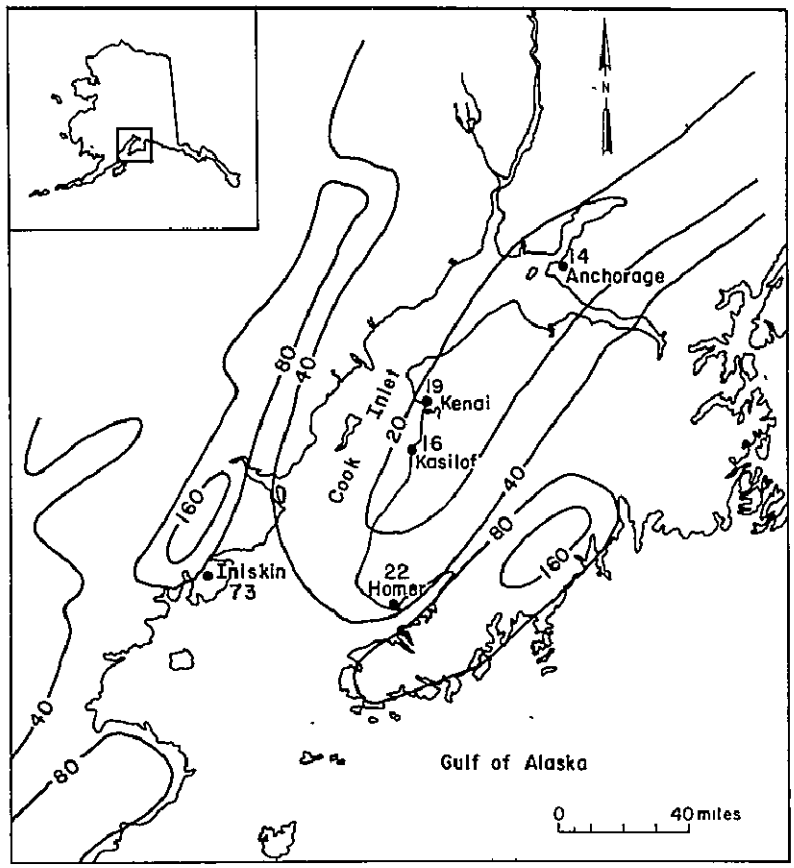

Figure 8. Mean annual precipitation in inches (adapted from Feulner et al. 1971).

southerly winds are directed up the inlet between the bordering eastern and western mountains where the sheltering effect of the Chugach and Kenai Mountains is reduced. Iniskin, located on the north shore of Kamishak Bay, records an average annual precipitation of 73.2 inches and an average annual snowfall of almost 188 inches. The average snowfalls in Homer and Kenai are only 53 and 69 inches, respectively (Wagner et al. 1969).

Complete cloud cover data are available only for the Anchorage area (Table 5). Average cloud cover is lowest during late fall and early winter with very little variation throughout the year.

Table 5. Average sky cover for Anchorage from sunrise to sunset, 1962-71 (from Monthly Reports of Climatological Data: Alaska, U.S. Dept. of Commerce, NOAA, Environmental Data Service).

Month	Sky Cover	Years of Record
Jan	6.0	9
Feb	7.7	10
Mar	6.8	9
Apr	7.3	10
May	7.3	
Jun	8.2	9
Jul	7.7	
Aug	8.1	
Sep	7.7	10
Oct	7.5	
Nov	6.6	
Dec	6.7	9

Annual average for seven years record: 7.3

Detailed wind speed and direction data for the region are limited to Anchorage. The data are not representative throughout the basin but indicate regional trends and several generalizations can be made. The eastern and western mountains block the winds from these directions; predominant winds are those funneled through the basin from the north or south. Forty-two percent of the prevailing winds in Anchorage are northerly (NNW-NNE) and 42% are southerly (SSW-SSE) (Marine Advisers 1964). High velocity winds occur throughout the basin when an atmospheric pressure gradient is established over the entire inlet; the winds are localized when the gradient is established through any of the

adjacent passes (Marine Advisers 1964). Strong gusts occur occasionally but the average wind speeds are low. Prevailing winds in December and January are northerly and have the lowest average wind speed. Southerly winds which prevail in May and June have the highest average velocity. Average daytime winds are approximately 10 to 20% greater than nighttime winds (Marine Advisers 1964). "Katabatic" or downslope winds occur periodically and are caused by cold air moving downslope from highland glaciers through adjacent valleys into the basin (Porter et al. 1963 and 1964). These winds are strongest when the temperature differences between the land and the inlet water are greatest (Marine Advisers 1964).

The following climatic generalizations can be made based on the previous discussion: January temperatures are warmer, July temperatures cooler toward the southern portion of the Inlet; total annual precipitation increases toward the inlet mouth (Evans et al. 1972); winds are strongly influenced by the surrounding mountainous terrain though the prevailing winds are from the north in fall, winter and spring, and from the south in summer (Wagner et al. 1969).

Hydrology

Approximate values* for the average annual discharge and the drainage areas for several of the major rivers and streams flowing into Cook Inlet are given in Table 6. Many streams with tributaries primarily in the mountains display similar yearly discharge cycles. The temperatures in the mountains are generally below freezing from October to May and most precipitation falls as snow during these months. The low flow period for these streams is in February and March; streamflow is mainly sustained by seepage of water into the stream from surrounding bedrock and alluvium (Barnwell et al. 1972). As average monthly temperatures rise above freezing, the stream flow fluctuates with the melting of the glacial ice and snow. Rapid melting generally begins in May and most of the snow is gone by August (Rosenberg et al. 1967). Streamflow is high from mid-July through August because precipitation is generally at its annual peak. The discharge of most streams increases 2-4 times in July and the suspended sediment concentrations generally increase equally. The only exceptions are Glacier Creek at Girdwood, where highest suspended sediment concentrations (1880 mg/l) occur in October, and Little Susitna River at Palmer, where highest concentrations (102 mg/l) occur in June (U.S. Geological Survey 1971). Precipitation and temperature decrease in the subsequent months, repeating the cycle (Barnwell et al. 1972).

* Approximate values because the gaging stations (in parenthesis) are usually located upstream from the river mouth.

Table 6. Drainage area and average annual discharge of rivers flowing into Cook Inlet.

River	Drainage Area (sq.km)	Average Discharge (cfs)	Discharge in July (cfs)	Ave. Suspended Sediment (mg/l)	Suspended Sediment in July mg/l[5]
Western Cook Inlet:					
Chakachatna River (near Tyonek)	2867	3,651	14,470	45	38
Susitna River (at Gold Creek)	15,770	9,797	23,950	--	1,934
Susitna River tributaries:					
Maclaren River (near Paxson)	707	--	--	--	--
Chulitna River (near Talkeetna)	6,579	--	--	--	--
Talkeetna River (near Talkeetna)	5,135	--	--	--	--
Skwentna River (near Skwentna)	5,760[1]	6,328	20,600	--	1,470
Little Susitna River (near Palmer)	1,065[1]	201	622	10	12
Knik Arm:					
Cottonwood Creek (near Wasilla)	64[1]	16[2]	--	--	--
Matanuska River (at Palmer)	5,299	3,891	11,890	--	2,203
Matanuska River tributary:					
Caribou Creek (near Sutton)	740	--	--	--	--
Knik River (near Palmer)	3,021[3]	6,905[3]	24,180	375	1,585
Eklutna River	305[3]	404[3]	--	--	--
Peters Creek	--	217[3]	--	--	--
Eagle River (at Eagle River)	492	535	--	110[3]	200[3]
Ship Creek (near Anchorage)	233	162	421	--	14
Ship Creek (at Elmendorf AFB)	289	113[3]	403	--[6]	15
Chester Creek (at Arctic Blvd at Anchorage)	74[4]	22[3]	20	200[6]	366
Turnagain Arm:	2,970[4]	3,500[4]	--	--	--
South Fork Campbell Creek (at canyon mouth near Anchorage)	64[4]	39	99	--	5.8
Campbell Creek (near Spenard)	179[4]	--	--	5	--
Bird Creek	--	163[3]	--	--	--
Glacier Creek (at Girdwood)	159[4]	289	883	326	72
Twenty-Mile River	425[4]	--	--	--	151
Portage River	282[4]	--	--	--	370
Placer River	317[4]	--	--	--	245
Sixmile Creek	673[4]	--	--	--	--
Resurrection Creek (near Hope)	381	--	--	--	--
Eastern Cook Inlet:					
Kenai River (at Soldotna)	5,146	5,775	15,240	44	--
Kasilof River (near Kasilof)	1,889	2,293	2,531	--	--
Ninilchik River (at Ninilchik)	335	103	90	--	--
Anchor River (near Anchor Point)	340	187	217	11	--
Bradley River (near Homer)	138	409	--	--	--

Data primarily from U. S. Geological Survey 1970 and 1971.

Additional references and notes:

1. Lawrence 1949.
2. Feulner 1971.
3. Barnwell et al. 1972.
4. Childers 1968.
5. Values based on 1-7 years data.
6. Feulner et al. 1971.

The precipitation-runoff cycle for rivers with large portions of the watershed in lowlands are different because these streams lose water to groundwater while flowing across the permeable glacial and alluvial deposits in the lowlands, and because there is less precipitation in the lowlands than in the mountains (Barnwell et al. 1972). As a result, streams with extensive lowland drainage exhibit low discharge rates, while streams with a large percentage of mountainous drainage area have high discharge rates (Feulner et al. 1971). The Chester and Cottonwood Creek watersheds are located completely in the permeable lowlands around Knik Arm. The average monthly discharges of these streams are virtually constant, deviating slightly from an annual average of 22 and 16 cubic feet per second, respectively (Marine Advisers 1965).

The Matanuska, Knik, and Susitna Rivers contribute approximately 70% of the fresh water discharged annually into the inlet (Table 6). These rivers originate in glaciers and consequently show large seasonal fluctuations in discharge (Rosenberg et al. 1967). The Knik River, for example, has a peak flow in July of 24000-27000 cfs and a minimum discharge in March of 454 cfs (Murphy et al. 1972). Much of the suspended sediment in these rivers originates at higher altitudes as glacial flour or by freezing and thawing of bedrock and unconsolidated material.* Additional sediment is produced by man's activities, i.e., industry, mining, highway and urban development and farming.

Suspended sediment data for Alaskan streams are sparse and derived from scattered analyses. However, the following generalizations are valid (Feulner et al. 1971). Nonglacial streams transport less than 100 mg/l suspended sediment during the summer; glacial streams carry as much as 2,000 mg/l. Nonglacial streams often transport highest concentrations during spring melt or heavy rainfall, whereas glacial streams carry their highest concentration at times of high melt water discharge in middle or late summer (Fig. 9). Less than 15% of the annual sediment load is carried during fall and winter when concentrations are $\leq$ 20 mg/l. Less than 50% of the material transported by nonglacial streams is finer than 0.062 mm (the silt-clay fraction), more than 50% by glacial streams. The percentage of fine material increases appreciably if a glacial stream flows through a lake. Many large streams form from glacial and nonglacial tributaries and transport suspended sediment that reflects this bi-modal origin in size distribution and concentration.

Glacial streams in the Matanuska-Susitna area normally contain as much as 2,000 mg/l suspended sediment during the summer while nonglacial streams generally contain about 50 mg/l. The rivers entering Knik Arm annually discharge 13-19 million tons of sediment, primarily in the summer

* Most information on suspended sediment loads from Feulner et al. 1971.

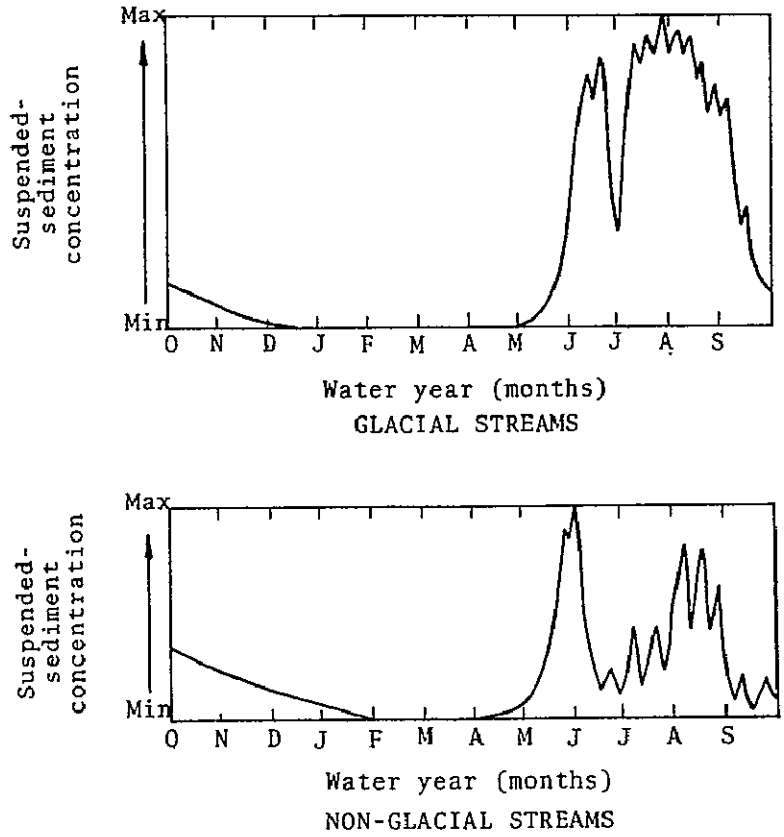

Figure 9. Relative suspended sediment load versus time of year for stream type (from Feulner et al. 1971).

(Rosenberg et al. 1967). Normal summer suspended sediment concentrations for the following streams in the Anchorage area are: Ship Creek, 15 mg/l; Campbell Creek, 5 mg/l; and Chester Creek, 25 mg/l. The concentrations in Campbell and Chester Creeks increase downstream to 45 mg/l and nearly 200 mg/l, respectively. In contrast, suspended sediment content in Ship Creek shows minor increase downstream where urban development has reduced the amount of erodable land. Turnagain Arm southeast of Anchorage receives approximately 2.5 million tons of sediment annually from surrounding rivers (Childers 1968). Most of the streams in the Kenai area head at glaciers and contain as much as 500 mg/l during a normal summer; nonglacial streams contain <50 mg/l; during the winter most streams transport <30 mg/l. Concentrations of several nonglacial streams in the Homer-Ninilchik area are as high as 100 mg/l during the summer.

Local Industry and Population Density

Virtually one half of the 302,173 people (1970 census) in Alaska reside in the Cook Inlet basin (Feulner et al. 1971, Selkregg et al. 1972). Most of these are located in the Anchorage metropolitan area and the smaller cities and towns bordering Knik and Turnagain Arms and along the southeastern shore; scattered villages are located on the northwestern coast. Commercial activities associated with the main industries in the basin, petroleum exploration and production, fishing, transportation, recreation, tourism, timber and agriculture, are centered in these populated areas. These industries are the major competitors for utilization of the natural resources in the region.

Petroleum and gas exploration and production are presently the primary economic activities in the basin (Evans et al. 1972). The rapid growth of the Kenai-Nikiski region, for example, is attributed to the discovery of petroleum in the Swanson River area in 1957 and the subsequent development of petroleum production facilities (Wagner et al. 1969). Figure 10 shows currently producing oil fields within the basin: Granite Point (1), Trading Bay (2), McArthur River (oil and gas) (3), Middle Ground Shoal (4), Redoubt Shoal (5) and Swanson River (oil and gas) (6); gas fields are: North Cook Inlet (7), North Middle Ground Shoal (8), Falls Creek (9), Ivan River (10), Beluga River (11), Moquamkie (12), Nicolai Creek (13), Albert Kaloa (14), West Foreland (15), Birch Hill (16), Beaver Creek (17), West Fork (18), Sterling (19), Kenai (20) and North Fork (21). Petroleum facilities presently located within the basin include 14 offshore platforms (Fig. 11), off- and on-shore gas and oil pipelines, tank farms, gathering facilities, refineries, petrochemical plants and tanker terminals.

The estimated petroleum and gas reserves of the Cook Inlet area are 7.9 billion barrels (bbl) and 14.6 trillion cubic feet, respectively

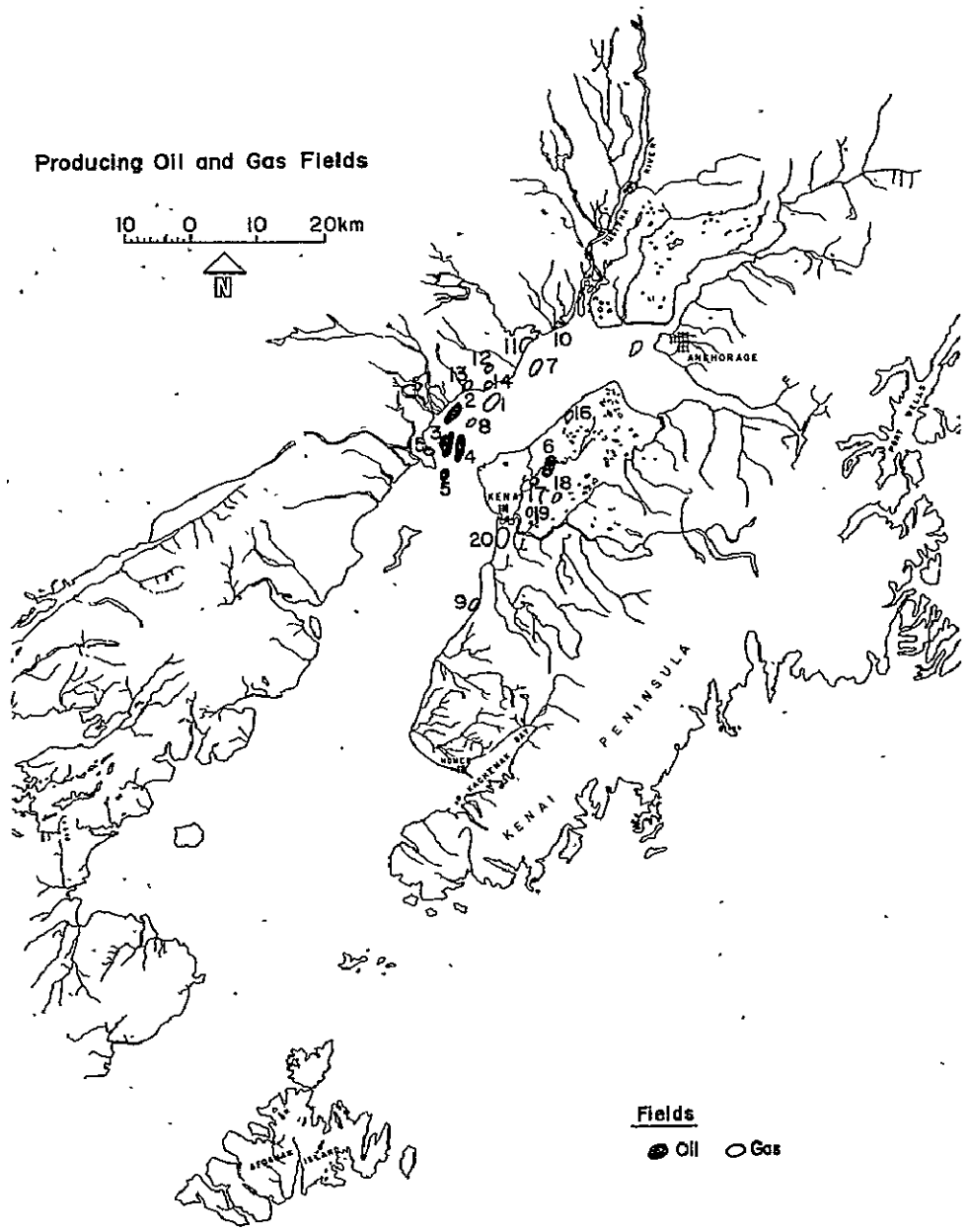

Figure 10. Producing oil and gas fields in the Cook Inlet basin (after Evans et al. 1972).

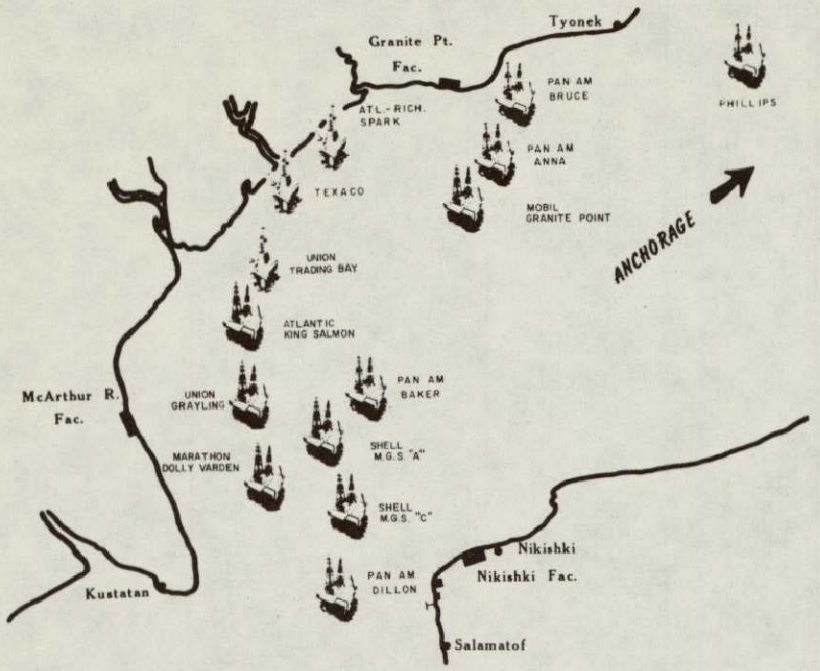

(a)

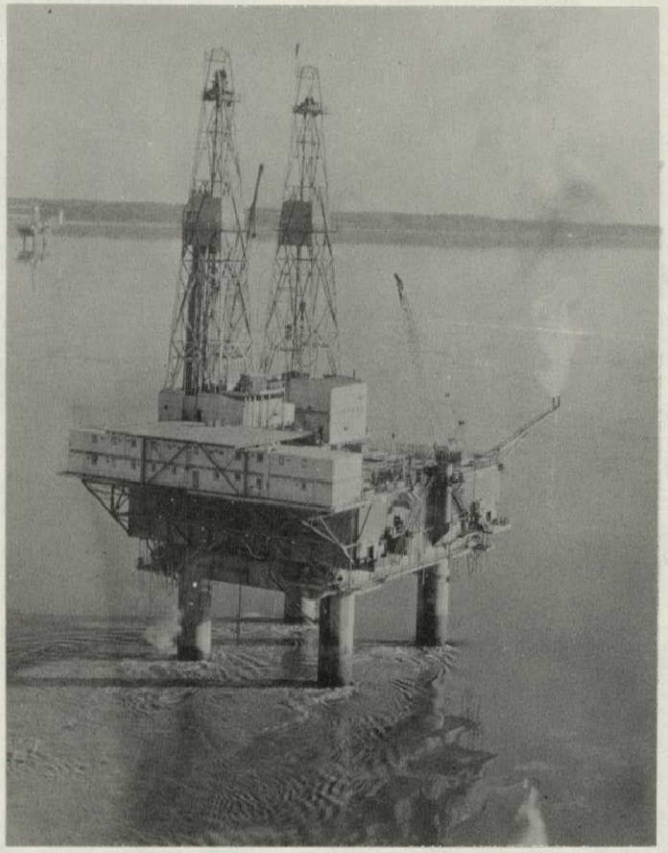

(b)

Figure 11. (a) Platform locations in Cook Inlet; (b) Granite Point Platform Anna during combined drilling and producing operations (from Owens and Allard 1970).

(Crick 1971). Coal deposits in the Beluga River region north of Trading Bay are estimated at more than 2.3 billion tons, equivalent to approximately 7 billion barrels of oil (Evans et al. 1972). In view of present acute energy requirements, rapid development of these resources and subsequent industrial expansion along the coast are inevitable (Oil and Gas Journal 1974a and b).

Commerical fishing activities are concentrated in the lower inlet south of the forelands. The economies of Kasilof, Ninilchik, Anchor Point, Homer and Seldovia are based upon commercial fishing of salmon, crabs and shrimp (Wagner et al. 1969). Fish canneries are located in Kenai, Homer, Seldovia, Ninilchik and Anchorage. Present projections indicate that the Cook Inlet commercial fishery could continue to produce indefinitely under proper management (Evans et al. 1972).

Marine transportation and shipping is also an important regional industry. Evans et al. (1972) report the categories of marine shipping and traffic within the inlet and indicate continued growth of this industry as the entire region develops. Major ports or terminals around the inlet are located at Anchorage, Drift River and Nikiski; Kenai, Homer, Seldovia, Halibut Cove and Ninilchik have small boat harbors. Figures and statistics indicating the main cargo and usage of these coastal facilities are available in reports by Evans et al. (1972) and Wagner et al. (1969).

Recreation in and along the upper inlet is somewhat limited due to the turbid water, fast current and extensive tidal flats. The shorelines of the lower inlet are more attractive and are often used for beachcombing, clamming and fishing (Evans et al. 1972). Federal and state resource areas, parks and campgrounds which border the inlet are used intensively for camping, sport fishing and hunting. Recreational boating is generally concentrated in the lower inlet, particularly in the Kachemak Bay area. As tourism is a major aspect of the recreational use of Cook Inlet, any activity which would reduce the scenic beauty of the inlet or of its shoreline would be detrimental to recreation and adversely affect the local economy (Evans et al. 1972).

The timber industry is presently active on a limited scale in the southeast near Seldovia (Evans et al. 1972). Though timber harvesting potential is great according to government sources, future production will probably fall due to the low grade of the resource in conjunction with marketing problems.

Agriculture in the inlet basin is concentrated in the Matanuska River valley and the Kenai Lowland close to Kachemak Bay (U.S. Department of Agriculture et al. 1968). The products are consumed primarily in the regional market and used as feed for the local beef herds; future agricultural growth is directly related to the increase in local population.

Sources of Estuarine Pollution

The effects on the inlet environment likely to result from future development must be assessed in order to formulate a rational coastal management plan for the Cook Inlet region. The present types and amounts of pollutants in the inlet will increase; therefore, it is important to evaluate the dispersion and flushing capability of the estuary at an early date. Glacial sediment is currently the dominant pollutant in the inlet. It is estimated that in developing areas as much as 20,000-30,000 times more sediment is produced than in natural undisturbed areas (Environmental Currents 1972). The Knik, Matanuska, Susitna, Beluga, McArthur, Drift and Tuxedni Rivers presently contribute the most sediment to the inlet; future development in these watersheds will increase the annual deposition throughout the inlet.

The coastal towns are additional sources of pollutants. With completion of the Asplund Water Pollution Control Facility the sewage from the Greater Anchorage Area Borough is treated prior to being discharged into the inlet near Point Woronzof. This project is the single most important environmental protection measure so far undertaken in the Anchorage area (Alaska Construction and Oil 1973). The remaining cities and villages, however, discharge untreated sewage directly into the inlet.

Petroleum pollution originates from numerous sources: oil producing offshore wells; the Drift River, Arness or Nikiski tanker terminals; submarine and coastal pipelines; gathering and handling facilities along the coast; and wastewater effluent from petroleum refineries. Approximately 9500-17500 bbl/yr or 0.3% (Kinney et al. 1970a) of the total crude oil produced is accidentally spilled, but, to date, the spills have not been noticeably detrimental to the coastal areas. From January through April 1972, 5 spills occurred in the inlet as a result of accidental disconnections at tanker terminals. Evidence of these spills had disappeared in 3-4 days (Evans et al. 1972). This is typical due to the high surface turbulence and mixing. Oil spills rarely reach shore; they simply evaporate and disperse as they move up and down the inlet with the exceptionally high tidal fluctuations.

Petrochemicals from the liquified natural gas plant and the ammonia plant at Nikiski presently are discharged directly into the inlet. However, the effluent outfalls from these plants are located in a region of high turbulence and dilution of these wastes is rapid (Fig. 39). As a result, concentrations remain below harmful levels even during the winter months when fresh water runoff is low (Rosenberg et al. 1967).

RESULTS AND DISCUSSION

Cook Inlet is an estuary as defined by Pritchard (1967): "a semi-enclosed coastal body of water which has a free connection with the open sea and within which sea water is measurably diluted with fresh water derived from land drainage." Estuaries are classified according to relative water balance, dominant physical processes of mixing and physical characteristics. Cook Inlet is considered a positive, tidal estuary formed by tectonic processes based on criteria for various estuary classes. This estuary is characterized by more runoff and precipitation than evaporation, resulting in dilution of sea water by fresh water. It is dominated by tidal action with strong tidal currents and mixing and was formed by faulting and local subsidence.

Coastal Configuration

The coast from the head of Kachemak Bay to Turnagain Arm is characterized by sea cliffs and pocket beaches (Refer to Figures 4, 5 and 6) which generally contain sand and/or coarser sediment; finer grained material is present along lower energy coasts. An extensive coastal plain borders a low lying, marshy coastline, with scattered sea cliffs along the northwest and west shore from Point MacKenzie to Harriet Point. Steep mountains slope directly into the inlet in most locations from Harriet Point to Cape Douglas. Bayhead beaches have formed in many of the small embayments and sea cliffs are found on the promontories along this coast. Tidal flats border much of the coast but are prevalent in the northern inlet.

The high sediment load in glacial rivers is the primary source of material for the tidal flats in the upper inlet. ERTS-1 MSS band 5 and 7 images were found to be ideal for a regional analysis of these tidal flats. However, to facilitate visualizing the relationships of these features throughout the inlet the locations of the tidal flats were superimposed on the band 6 mosaic and may not be easily distinguished in this representation (Fig. 12). The legend on this Figure may be misleading to some; extensive tidal flats are shown as white areas and river plumes are outlined by white lines. The most extensive flats formed north of the forelands. In the lower inlet tidal flats usually occur as bayhead bars in embayments along the western shore and northeast of Homer in Kachemak Bay. Strong, variable tidal currents cause significant changes in tidal flat configuration; migration of some of the major tidal channels in Knik and Turnagain Arms can be substantiated by comparing Figure 12 with the National Ocean Survey Navigational Chart 8553.

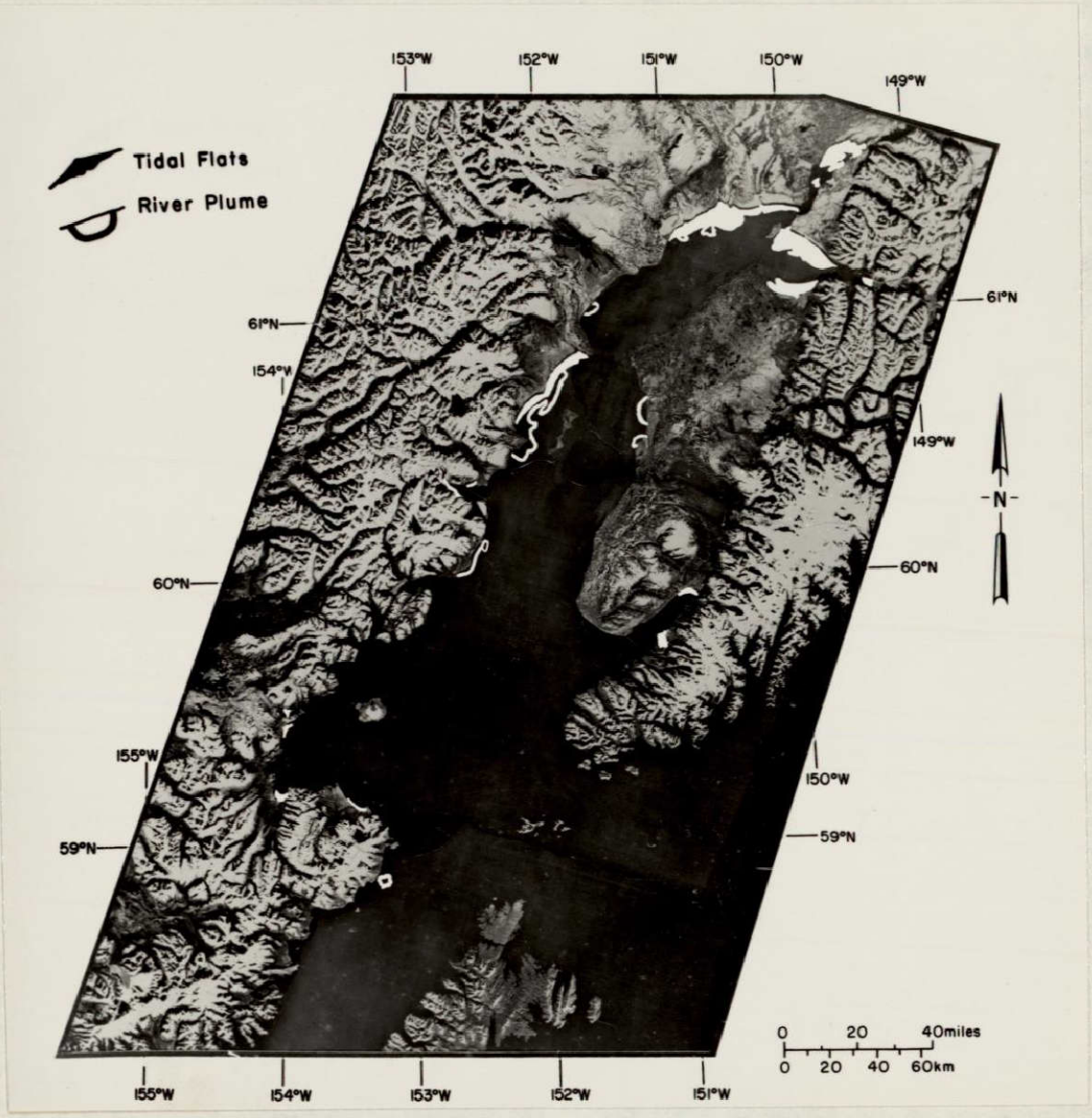

Figure 12. Tidal flat distribution and river plumes.

Bathymetry

Bottom topography is extremely rugged with many deep areas and shoals (Fig. 13). The depths in the upper inlet north of the forelands are generally less than 20 fathoms; the deepest portion is located in Trading Bay east of the mouth of the McArthur River. Turnagain and Knik Arms are the shallowest areas with much of the bottom exposed at low tide. South of the forelands two channels, one between Kalgin Island and Harriet Point and another between Kalgin Island and the east shore, extend southward in the inlet and join in an area west of Cape Ninilchik. The deepest portion of the western channel is greater than 40 fathoms. The eastern channel is deepest, 75 fathoms just south of a line between the forelands. It rapidly shoals to approximately 30 fathoms until it merges with the western branch. South of the Cape, the channel gradually deepens to approximately 80 fathoms and widens to extend across the mouth of the inlet between Cape Douglas and Cape Elizabeth.

The following reports contain more detailed bathymetric data. Rosenberg et al. (1967) presented a bathymetric profile across the inlet from Beshta Bay, just north of Granite Point, to the bay 2 miles south of the mouth of the Swanson River. Kinney et al. (1970b) prepared 8 east-west profiles from the inlet mouth to the forelands, 5 north-south profiles from the forelands to Point Possession, 1 longitudinal profile from the mouth of the Susitna River to Eagle Bay in Knik Arm and 1 longitudinal section from mid-inlet between the forelands to east of the Susitna River mouth. Armstrong Associates (1968) prepared 9 bathymetric cross-sections along Turnagain Arm from the Gull Rock area to 3 miles east of Girdwood. Marine Advisers (undated) prepared a bottom profile and bathymetric map for the area from Beluga to Moose Point. Carlson and Behlke (1972) presented a bathymetric map of the inlet in the Anchorage area and plotted 11 cross-sections for various stations along Cook Inlet and Knik Arm.

Bottom sediment distribution is determined by tidal action, hydrography, type of material, ice rafting and bottom topography (Wagner et al. 1969). Bottom sediments in the inlet have been divided into three groups on the basis of grain size: sand predominates in the upper inlet, sandy gravel with minor silt and clay in the middle inlet, and gravelly sand and minor interspersed silt and clay in the lower inlet (Sharma and Burrell 1970).

Tides

The tides in Cook Inlet are semi-diurnal with two unequal high tides and two unequal low tides per tidal day (24 hours, 50 minutes); high tide occurs approximately 4.5 hours later at Anchorage than at the inlet mouth. The results of a variable-boundary numerical tidal model

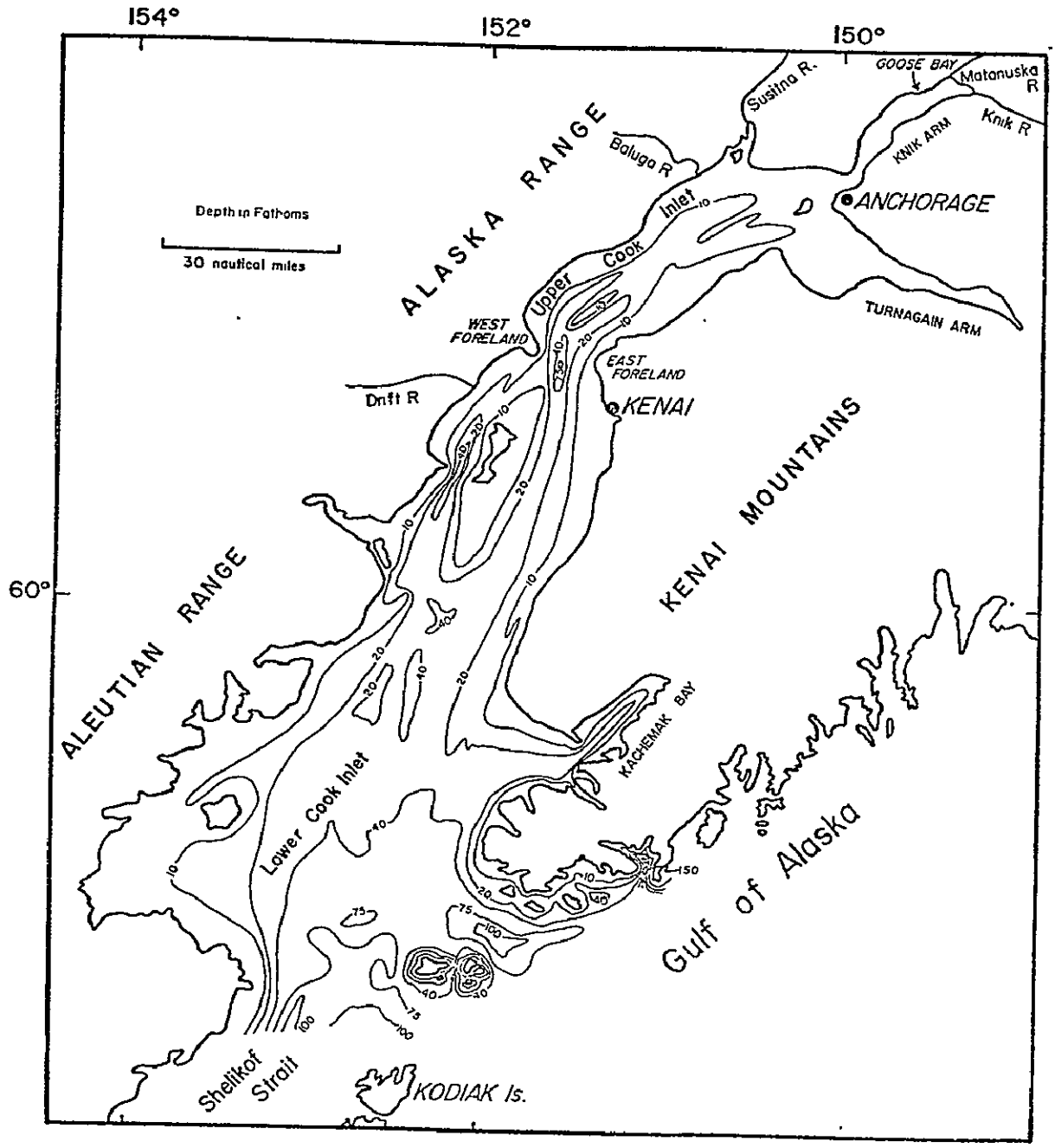

Figure 13. Generalized bathymetry of Cook Inlet (from Sharma and Burrell 1970).

study (Mungall and Matthews 1970) show that the tidal regime divides the inlet into two regions separated by the forelands. Tides in the south show characteristics of a progressive Kelvin wave. Co-range lines lie along the length of the inlet with higher amplitudes on the east (Fig. 14). Co-tidal lines lie perpendicular to co-range lines and slope upwards to the right indicating that the wave is not entirely progressive but tends toward a mixed type. If the tides in the south behaved as a standing wave there would be an increase in tidal range going north to the forelands; however, this is not the case. Lines being nearly perpendicular indicate that friction between the bottom and the moving water column is probably not an important factor in most of the southern inlet. Northern inlet tides appear more like the conventional standing waves; co-tidal and co-range lines are not perpendicular indicating that friction is increasingly important going north (decreasing depths). Also, the difference in tidal range across the inlet decreases going north because the phase difference between maximum tidal height and maximum current approaches 90°; therefore, if slack water occurs at maximum tide, no Coriolis force exists and no slope of the water surface exists across the inlet at that instant. Figure 14 also indicates that the tidal wave speed increases along the western inlet north of the Tuxedni Channel due to increased depth (less friction).

Mean diurnal tide range varies from 4.2 m at the mouth to 9.0 m at Anchorage. It varies within the lower portion of the inlet from 5.8 m on the east side to 5.1 m on the west (Wagner et al. 1969, Carlson 1970). The extreme tidal range produces currents typically 4 knots and occasionally 6 to 8 knots (Horrer 1967). The differences between the times of high tide and times of maximum flow at various locations are shown in Figure 15. The high Coriolis force at this latitude, the strong tidal currents and the inlet geometry produce considerable cross currents and turbulence within the water column during both ebb and flood (Burrell and Hood 1967). The tides are highly effective in expanding the dilution volume of the water by providing new water at an outfall and by increasing turbulence which increases dilution. Turbulence is especially strong along the eastern shore due to the high tidal range.

Suspended Sediment Distribution and Circulation

Turbid fresh water discharging into the inlet, especially from the north and west, produces sediment plumes which appear lighter in tone than the less turbid water in ERTS-1 MSS band 4 and 5 images. The suspended sediment in the fresh water functions as a natural tracer, marking water masses and making sediment distribution and current patterns visible. The transport and extent of surface plumes are influenced by river runoff, wind, tide, Coriolis force, centrifugal force and

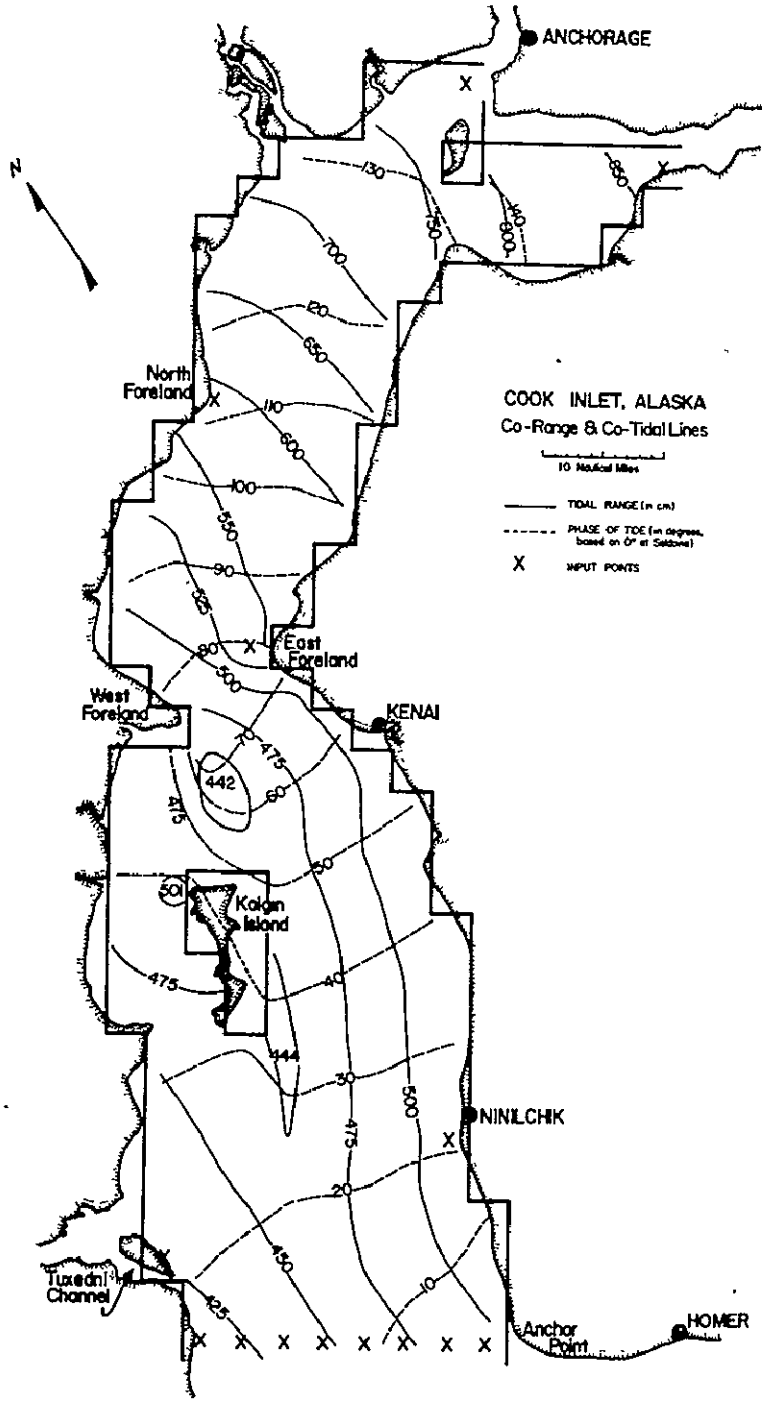

Figure 14. Co-tidal and co-range lines (from Mungall and Matthews 1970).

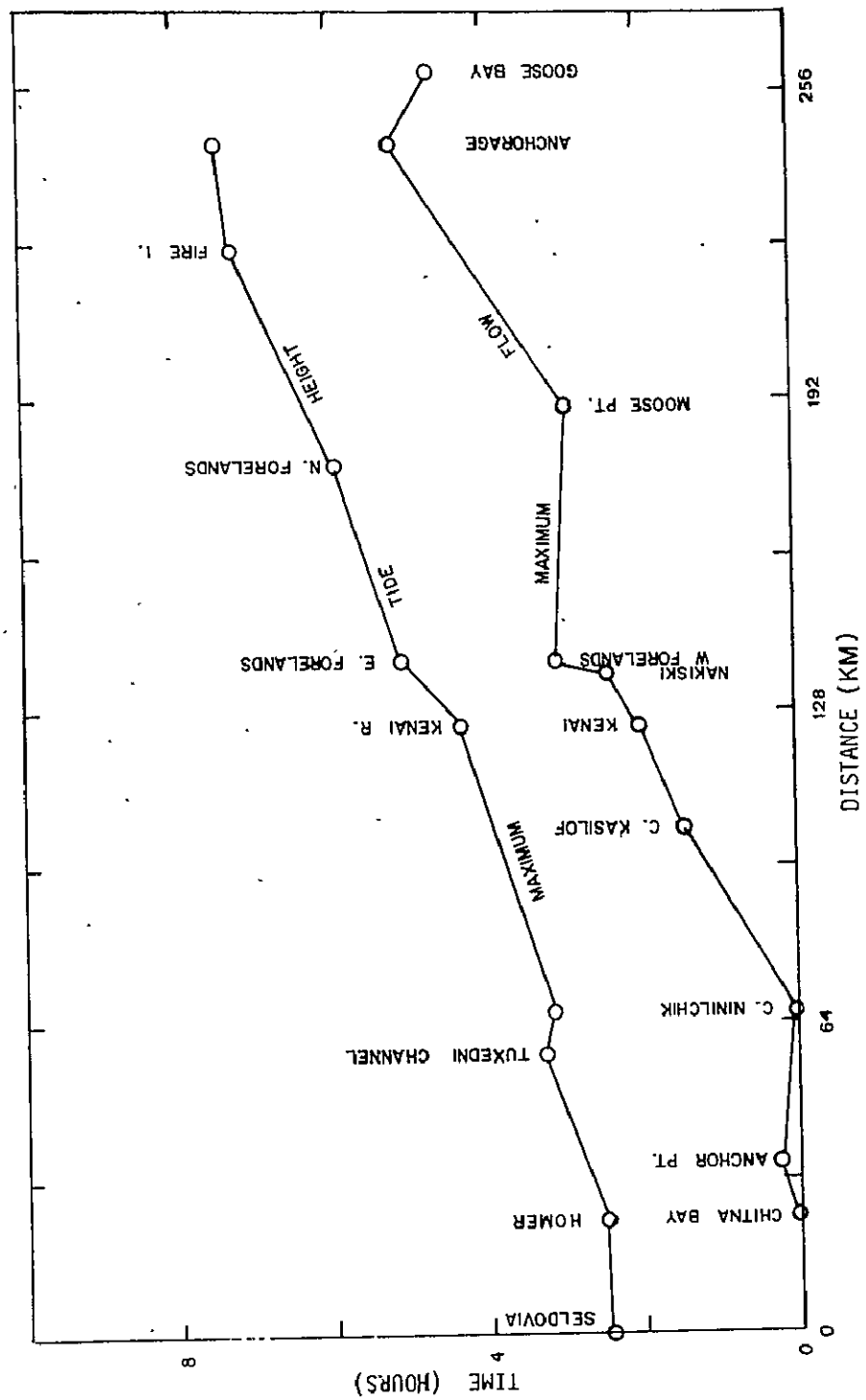

Figure 15. Difference between time of high tide and maximum flow (adapted from Carlson and Behlke 1972).

local topography. Qualitative descriptions of surface flow near river mouths can be made based on the shape of fresh water plumes and on mixing patterns observed on aircraft and satellite imagery. Figure 16, an ERTS-1 image acquired on 7 August 1972, shows the sediment plumes from the Drift (3) and Big (4) Rivers during flood tide at Seldovia. The shape and location of the plumes are convenient markers to determine current directions along the west shore between McArthur River (1) and Tuxedni bay (2). The plumes are clearly moving in a northerly direction. Relict sediment plumes from earlier tidal stages, visible far offshore, indicate water movement through several tide cycles. Relative differences in sediment concentration of the inlet water can also be distinguished. The darker tones apparent farther from shore indicate that the water is less turbid. Tidal flats (5) appear as a gray border along the coastline. Mt. Spurr (6), one of the many volcanoes in the Chigmit Mountains, Lake Chakachamna (7) and numerous glaciers (8) are also visible.

Figure 17 shows the movement of near-surface and surface water in the area of the Drift River tanker terminal during late flood at Seldovia, approximately the same tidal stage as shown in Figure 16. Tidal range at this location generally varies from 3-6 m and surface current velocities are 1-3 knots. Currents at depths of 8 and 15 m are generally lower but periodically reach velocities equal to those at the surface (Marine Advisers, 1966a). Turbid fresh water from the Drift (1) and Big (2) Rivers forms a distinct surface layer riding over and mixing with the saline inlet water (8). Turbulence caused by local tidal and wind currents produces the mixing as the fresh water is diverted to the north by the flood tide. Several mixing boundaries are evident between sediment laden and clearer, oceanic water. Turbid water (5) from the rivers rapidly mixes with the less turbid oceanic water (8) to form different water types of variable temperatures, salinities and sediment concentrations (6,7) within the mixing zone. More complete mixing has occurred in the southern portion of the area and the Drift River plume has migrated from the south during flood tide. The tanker at the terminal (4) roiled the more buoyant fresh water and brought deep, clear water up to the surface (dark area of clear water off the ship's stern). The surface foam lines (9) are common where different water types converge and mix. Internal waves (linear patterns) near density boundaries are also common in these locations and are obvious southeast of the tanker terminal. Compare the detail of tidal flats (3) to that observed on the ERTS image in Figure 16.

RS-14 Scanner imagery of the Drift River area (line 54; in pocket) has limited use; the gain control on the instrument was changed and surface water detail lost. The tanker terminal appears as a warm (light) spot surrounded by cold (dark) water. The cold water discharging from the Drift River is faintly visible; it forms a triangular plume with the

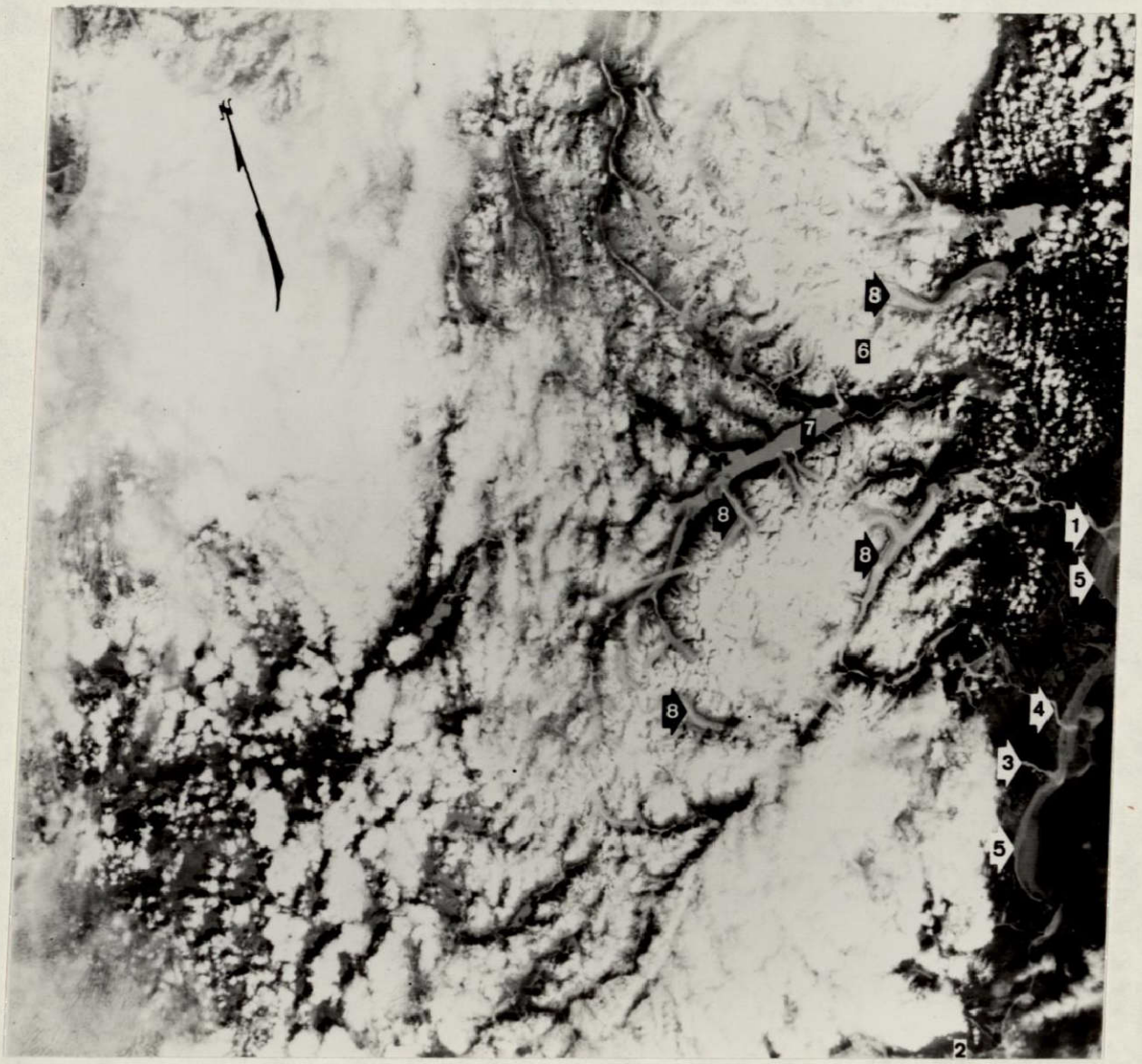

Figure 16. West shore of Cook Inlet between McArthur River and Tuxedni Bay. MSS band 5 image 1015-21022, acquired 7 August 1972.

Figure 17. Drift and Big Rivers area during flood tide (NASA NP-3A photographs).

apex at the river mouth. Cold water from Big River moves north, staying close to shore while mixing with warmer water farther offshore. The Big River plume remains distinctly cold for approximately 2-3 km offshore before mixing with warmer water. Comparisons to the NP-3A photography (Fig. 17) indicate that the coldest portion of the fresh water plume exists nearest the river mouth where mixing is minimal.

The plume from the McArthur river in Trading Bay (Line 53) is clearly colder than the surrounding inlet water. In this location the currents appear to be moving in two directions, nearshore currents moving north and currents approximately 4 km off shore moving south past the oil platforms. On the lee side of the platforms is a distinct mixing zone between cold river and bottom water and warm inlet water (more apparent in CIR photography). Between the North Foreland and the Susitna River on the northwest shore (line 54), nearshore northerly currents and offshore southerly currents are distinct. Complicated mixing patterns occur off the Susitna River mouth and a shear zone between opposite moving currents is discernible. Mixing between Point Possession and Boulder Point (line 56) about 48 km southwest of Anchorage shows a "feathered-edge" pattern, an indication of a high mixing area which occurs along most of the southeastern shore of Cook Inlet.

Sediment plume patterns of the Big (5) and Drift (6) Rivers on 10 September 1972 (Fig. 18) show a southerly direction of nearshore currents in Redoubt Bay (7) during ebb tide at Anchorage and flood in Seldovia. The shapes of the sediment plumes of the Kenai (15) and Kasilof (14) Rivers also indicate a southern current along the east shore. The plume shapes suggest that the ebb flow dominated the mid-inlet area at this time. Sediment laden water from the Tuxedni River (12) is being transported along the coast in a southerly direction between Chisik Island (13) and the mainland. Other features of interest in this scene are: the snowcapped Kenai Mountains (1), the Kenai Lowland (2), the East (3) and West (4) Forelands, a sediment pattern indicating a counterclockwise current (8) around Kalgin Island (9), tidal flats (10), Harriet Point (11), and turbid Lake Tustumena (16).

ERTS imagery acquired approximately one year later than that shown in Figure 18 shows changes in sediment distribution during different tides. Sediment patterns in Figure 19 were observed along the east shore on 17 August 1973 during early flood in Seldovia and early ebb in Anchorage. The shapes of the plumes from the Kenai (2) and Kasilof (3) Rivers suggest southerly moving nearshore currents. Note that the water from the Kasilof River is more turbid than that of the Kenai. The Kasilof originates in Tustumena Lake (6 in Fig. 20) which has a higher suspended sediment concentration than Skilak Lake (7 in Fig. 20), the source of the Kenai River. Turbid water (4) extends as far south as Cape Starichkof approximately 18 km south of Ninilchik.

Figure 18. Central portion of Cook Inlet. MSS band 5 image 1049-20512, acquired 10 September 1972.

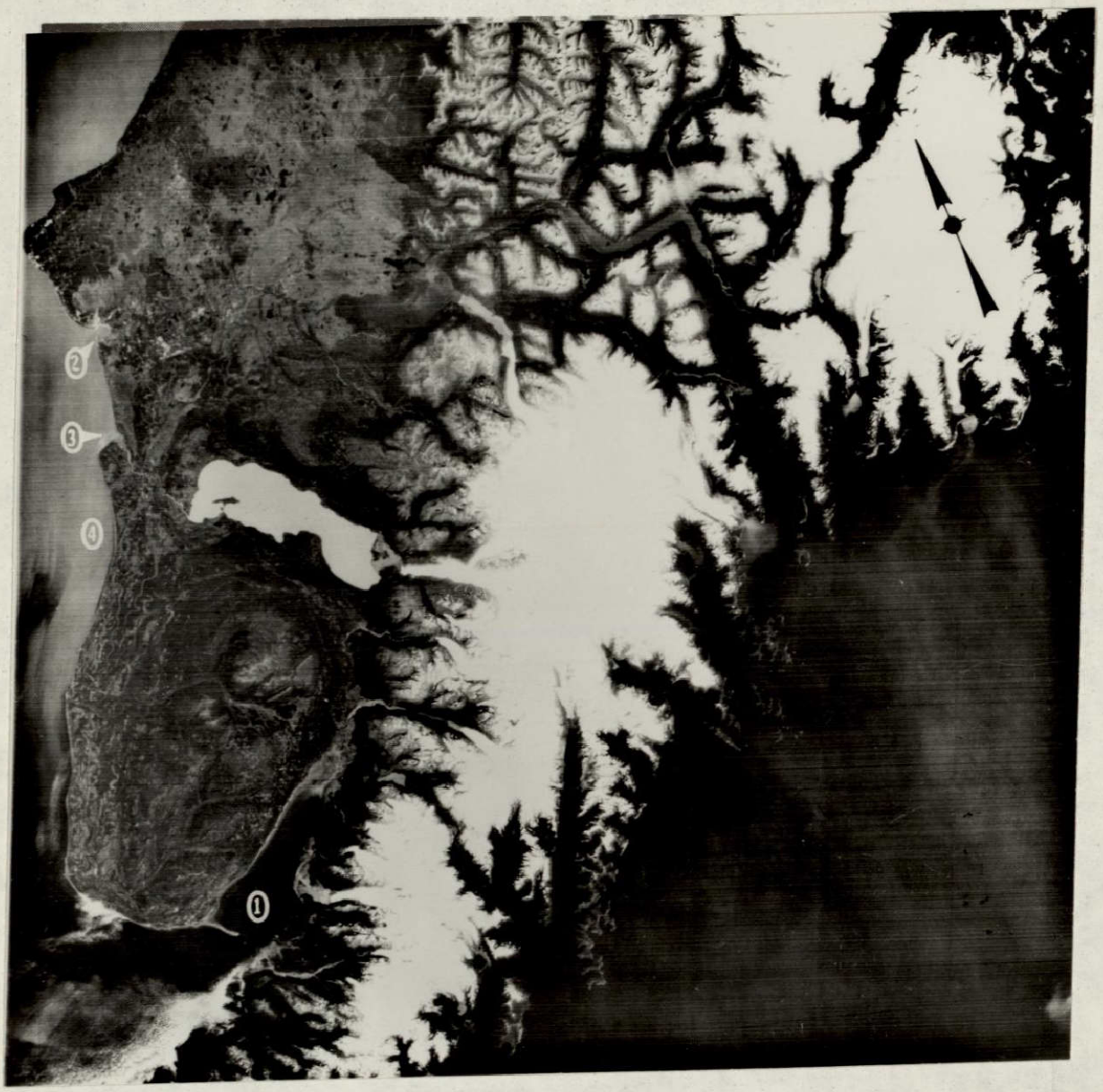

Figure 19. Southeastern Cook Inlet. MSS band 5 image 1390-20452, acquired 17 August 1973; early ebb at Anchorage, early flood at Seldovia.

Figure 20. Southeastern Cook Inlet. MSS band 4 image 1426-20444, acquired 22 September 1973; early ebb at Anchorage, high water at Seldovia.

Meltwater from the Fox River at the head of Kachemak Bay (1) appears concentrated along the north side; clear oceanic water occupies the southern portion.

Suspended sediment distributions at the same locations on 22 September 1973 (Fig. 20) indicate that the nearshore currents were moving north during high tide at Seldovia and early ebb at Anchorage when the image was acquired. Notice the change in the shape of the sediment plumes from the Kenai (2) and Kasilof (3) Rivers. The high turbidity of the water (4) south of the Kasilof River mouth may be caused primarily by bottom scouring of the shoals along this coast. Scouring was observed near Moose Point (5) on aircraft photography. Sediment patterns in Kachemak Bay (1) are similar to those observed in Figure 19.

Figure 21 shows the Kenai-Kasilof Rivers area during high tide at Seldovia and early flood at Anchorage on 22 July 1972. Plume shapes from the Kenai (1) and Kasilof (2) Rivers are similar to those on ERTS image 1426-20444 (Fig. 20). The plumes (3) from these rivers and the streaks (5) of sediment formed behind submerged rocks suggest northerly moving nearshore water (4). These streaks in the water are probably a result of bottom scouring on the lee side of rocks (much of this area is <4 fathoms). Differences in the turbidity of water in the mixing zone within the river plumes, foam lines along contacts between water of different densities, and internal waves along density boundaries were also present at the time of image acquisition. Local currents are strong and clearer saline water appears to intrude into the Kenai River. Note also that wind-generated waves are moving in a northeasterly direction (6) and reinforce the northward surface currents.

RS-14 imagery of this area (line 59; in pocket) shows that the Kenai River water is warmer than the surrounding inlet water on 22 July 1972. This may be due to heating as the river flows 48 km across the Kenai Lowland and/or to the introduction of warm wastes from the city of Kenai. Most pollutants introduced into the inlet at Kenai would be well mixed and rapidly dissipated because of the frequent changes in nearshore currents with each tidal cycle.

Relative differences in the suspended sediment concentrations of the surface water in Kachemak Bay (1) are shown in Figures 19 and 20. Kachemak Bay has been divided based on topography. The outer bay is from a line between Anchor Point and Point Bede (on western tip of Kenai Peninsula) to a line from Homer Spit south to Lancashire Rocks. The inner bay is from this Homer Spit line to the mouth of the Fox River (Knull and Williamson 1969). Suspended sediment load appears higher in the water on the north side of the inner bay; less turbid water is found along the south coast. The orientation of spits and bars along the south shore indicate that the predominant direction of flow for nearshore water is northeasterly. These ERTS scenes were acquired

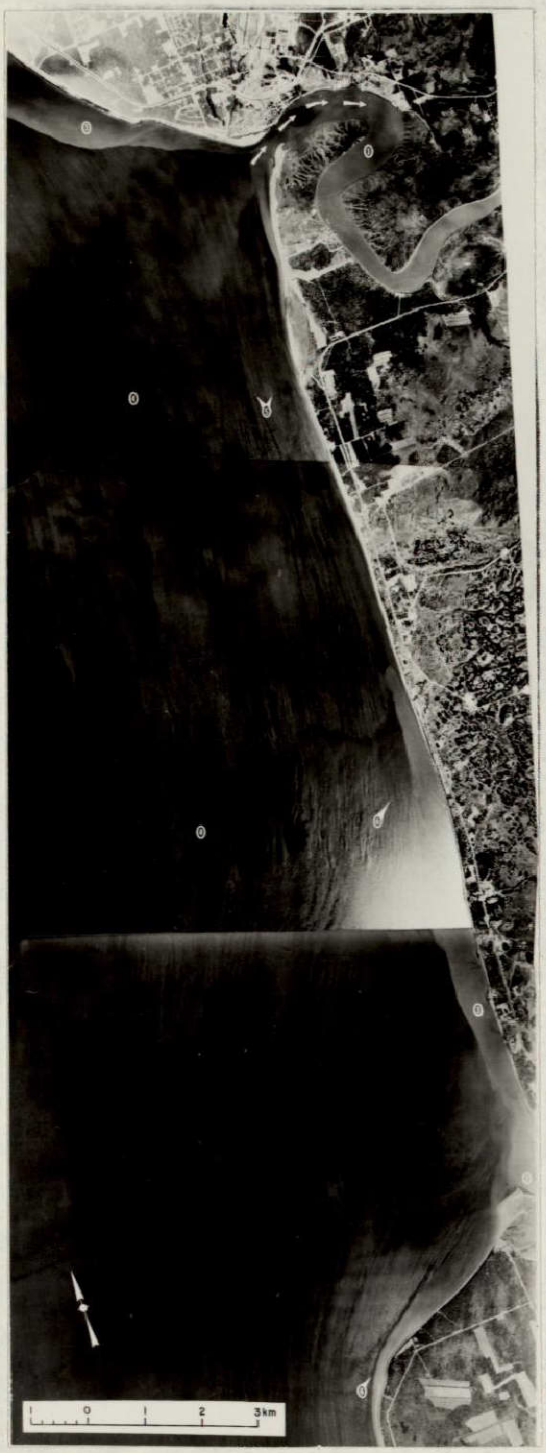

Figure 21. Kenai-Kasilof Rivers area during early flood at Anchorage, high tide at Seldovia (NASA NP-3a photographs).

during flood tide or high slack water in Seldovia and suggest that clear oceanic water intrudes into this bay along the south shore due to Coriolis effect. Currents past the mouth of the Bay during flood tide were estimated at 5 knots (Knull and Williamson 1969). The nearshore circulation continues counterclockwise around the bay and carries the turbid meltwater discharged from the glaciers in the Kenai Mountains along the north shore. Flood tide currents move northeasterly along the south coast of the bay at 1-2 knots, ebb flows are variable in velocity and direction from southwesterly to westerly (U. S. Department of Commerce 1964). The light tone of the water along the north shore may be partially due to bottom effects. The water depth here is variable from <1 to 12 m and bottom reflection may be significant especially in Figure 20 which is a band 4 image; the amount of water penetration is greatest in band 4.

Figure 22 shows the area around Homer Spit (1) in Kachemak Bay during flood tide at Seldovia on 22 July 1972. Turbid water (3) from the meltwater streams of the Wosnesenski and Doroshin Glaciers on the south shore moves across the bay, mixes with less turbid oceanic water (7) and forms water of variable turbidity (4) within the mixing zone. A similar pattern is evident near Homer Spit in Figure 20. The glacial meltwater moves on the surface of the oceanic water which is brought up from below by the mixing action (5) of the boat southwest of the spit. The dark bands (2) in the area of sun glint show areas where the water surface roughness has been reduced. This may reflect internal vertical circulation (Langmuir circulation) associated with streaks of windrows oriented approximately parallel to the wind (Scott and Stewart 1968). This circulation tends to dampen the roughness due to other factors. The distribution of surface sediment in inner Kachemak Bay (6) as observed on these medium altitude aircraft photographs verifies the observations made on the ERTS imagery that higher sediment concentrations occur along the north side.

Figure 12 shows the location of sediment plumes from some of the major rivers entering the inlet on 3 and 4 November 1972. Although the Knik and Matanuska Rivers at the head of Knik Arm contribute most of the sediment deposited in the inlet (Wagner et al. 1969) these rivers do not produce distinct sediment plumes on these dates. The river borne sediment is dispersed so quickly in this high energy area and the sediment concentration of the inlet water is so high (approximately 1350 mg/l, from Kinney et al. 1970b) at this location that a distinct plume is not visible. The Susitna River, another major sediment contributor, has only a small plume because the river discharge is reduced during the winter months (Fig. 23) and the inlet water at the river mouth has a high suspended sediment concentration (approximately 1540 mg/l, from Kinney et al. 1970b).

Figure 22. Homer Spit area during flood tide at Seldovia (NASA NP-3A photographs).

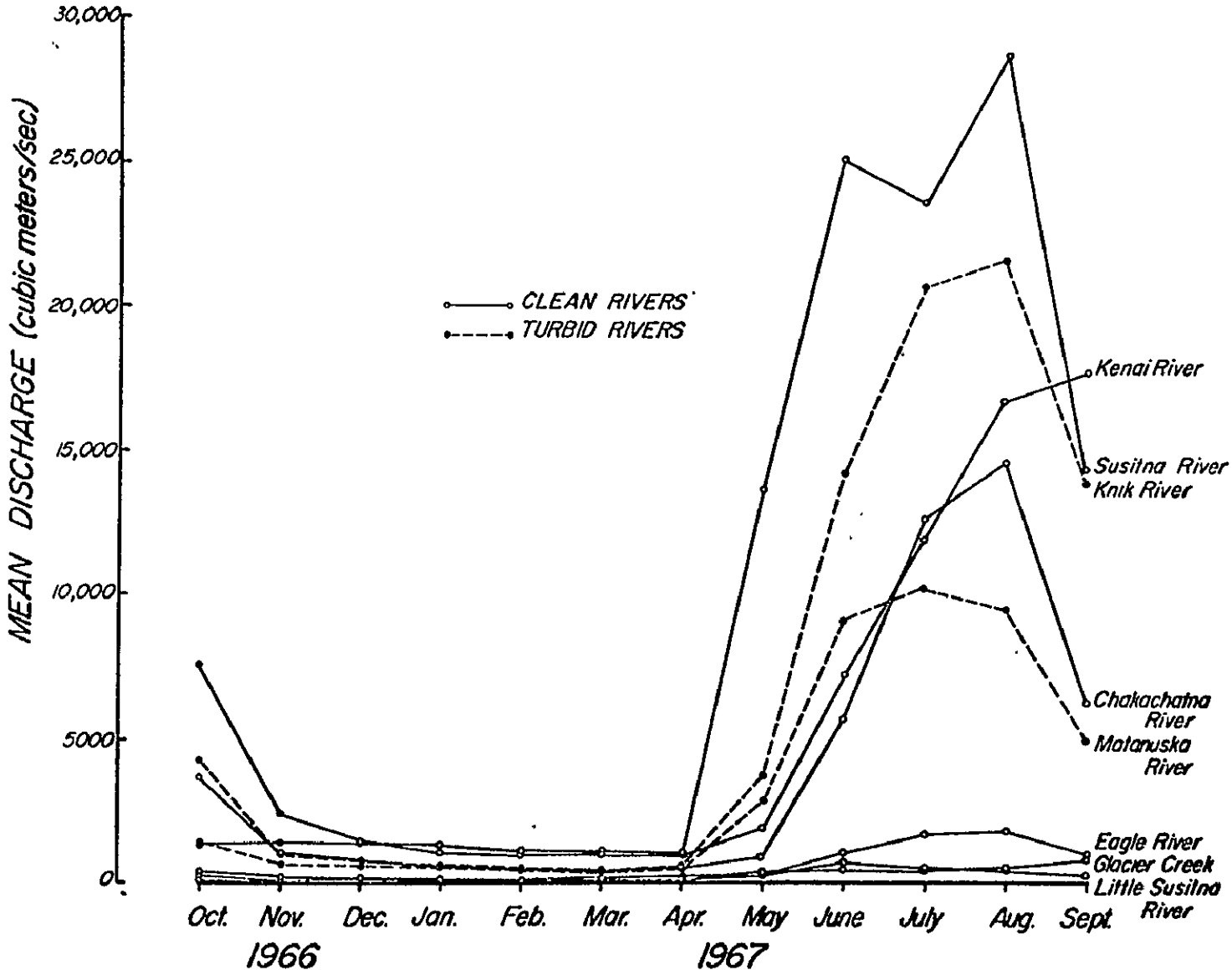

Figure 23. Seasonal changes in discharge for rivers entering Cook Inlet (from Sharma et al. 1974).

Circulation throughout the inlet is primarily governed by interactions between tides, Coriolis force, and the counterclockwise Alaska current; however, local currents are additionally influenced by local bathymetry, morphometry and fresh water influx (Evans et al. 1972). Generally tidal currents dominate and currents due to wind stress, surface waves, runoff and ordinary convective and advective processes are by comparison more local and of smaller magnitude (Marine Advisers 1965). Wind-driven currents may add approximately 2-3% of the wind speed to tidal current velocities in some localities (Marine Advisers 1964). The tidal currents are predominantly rectilinear or reversing currents which are common in elongated estuaries or bays. These currents produce turbulent mixing of sea and fresh water and the resulting mixing patterns are apparent on aircraft and satellite imagery. Current velocities increase from 2-3 knots near the inlet mouth to greater than 8 knots at topographic narrows (i.e. Harriet Point, the Forelands, Knik and Turnagain Arms) (U. S. Department of Commerce 1964).

In the past, surface temperature, salinity, oxygen and suspended sediment data acquired over several days during numerous ship surveys were used to diagram the regional circulation patterns of the inlet (Figs. 24, 25, and 26). These data do not provide a synoptic view and were not taken during the same tide stage. Several low and high tides occurred during the sampling period and the data do not reflect changes between times of low and high water. In spite of these shortcomings the data are useful for determining general patterns. The distributions indicate that surface water on the east side of the inlet south of the forelands differs considerably from that on the west.

Temperatures in May (Fig. 24) show a rapid decrease from 5.7°C to <4.9°C westward between Ninilchik and Tuxedni Bay; surface temperatures increase from 4.9°C east of Kalgin Island to >9.0°C at the mouth of the Susitna River, to 8.0°C on the west side of the inlet mouth. The mid-inlet cold water around Kalgin Island may result from upwelling of bottom water during flood tides (Evans et al. 1972, Kinney et al. 1970b). Some estuaries are characterized by a salt wedge that moves headward into the estuary along the bottom while the fresh water outflow moves over this wedge and out the estuary (Bowden 1967).

The low salinities north of the forelands and near Cape Douglas result from fresh water dilution. The salinity and temperature distributions near the mouth and along the eastern portion of the inlet to north of Ninilchik suggest that a distinct oceanic water mass exists in this location. The salinity data indicate that north of the forelands the saline water moves north in the eastern half of the inlet while fresher water progresses south on the west side; northeast of Kalgin Island ebbing waters from north of the forelands move south past the east side of the island. North of the forelands, temperature data

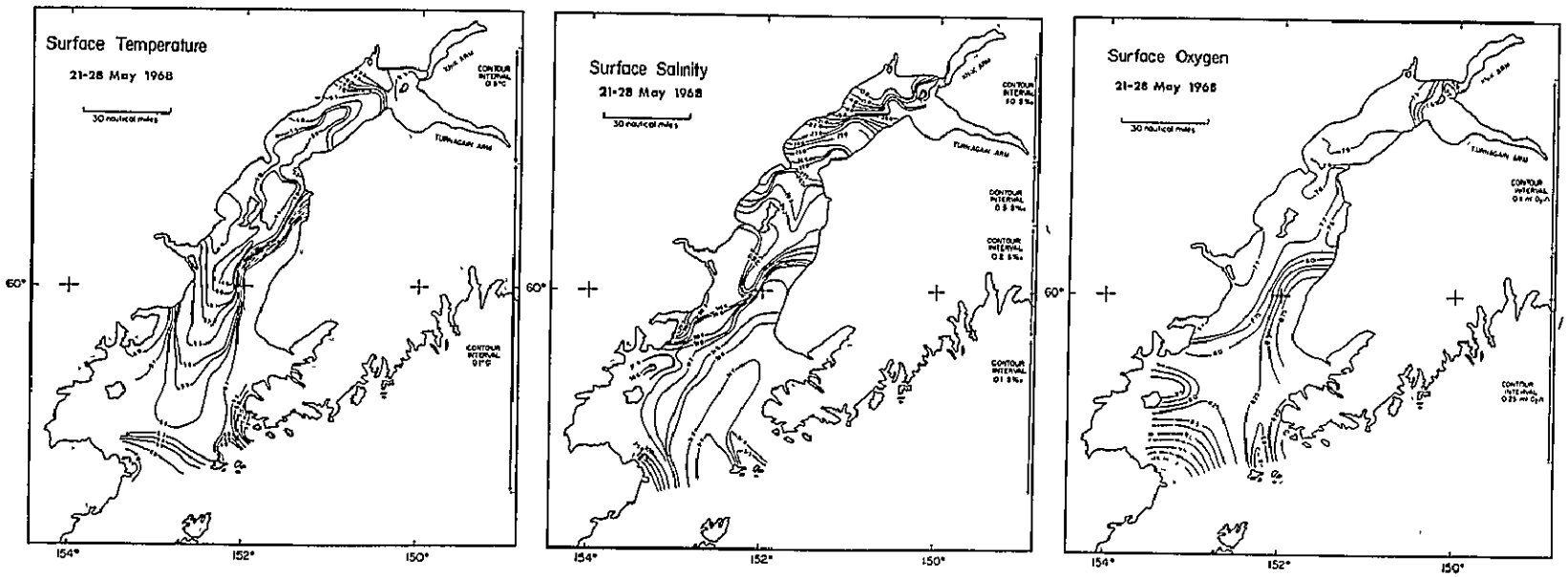

Figure 24. Surface temperature (°C), salinity ($^{o}/_{oo}$) and oxygen ($m\ell O_2/l$) in May 1968 (adapted from Kinney et al. 1970b).

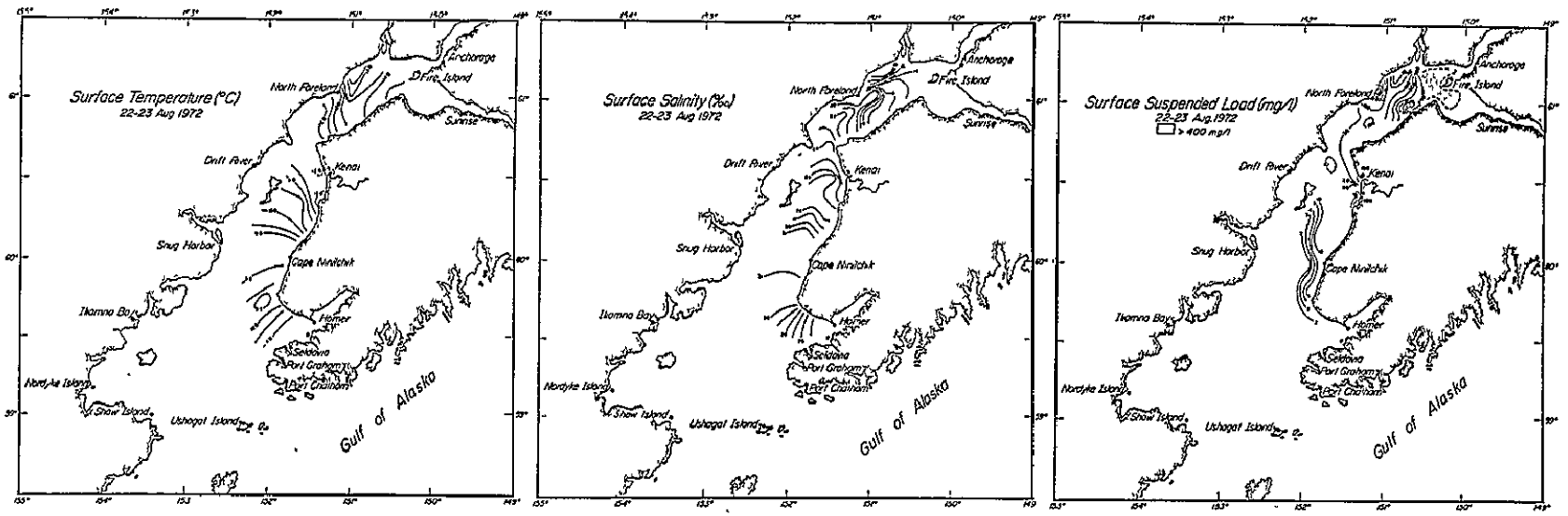

Figure 25. Surface temperature (°C), salinity (o/$_{oo}$) and suspended sediment (mg/l) in August 1972 (adapted from unpublished data provided by F.F. Wright).

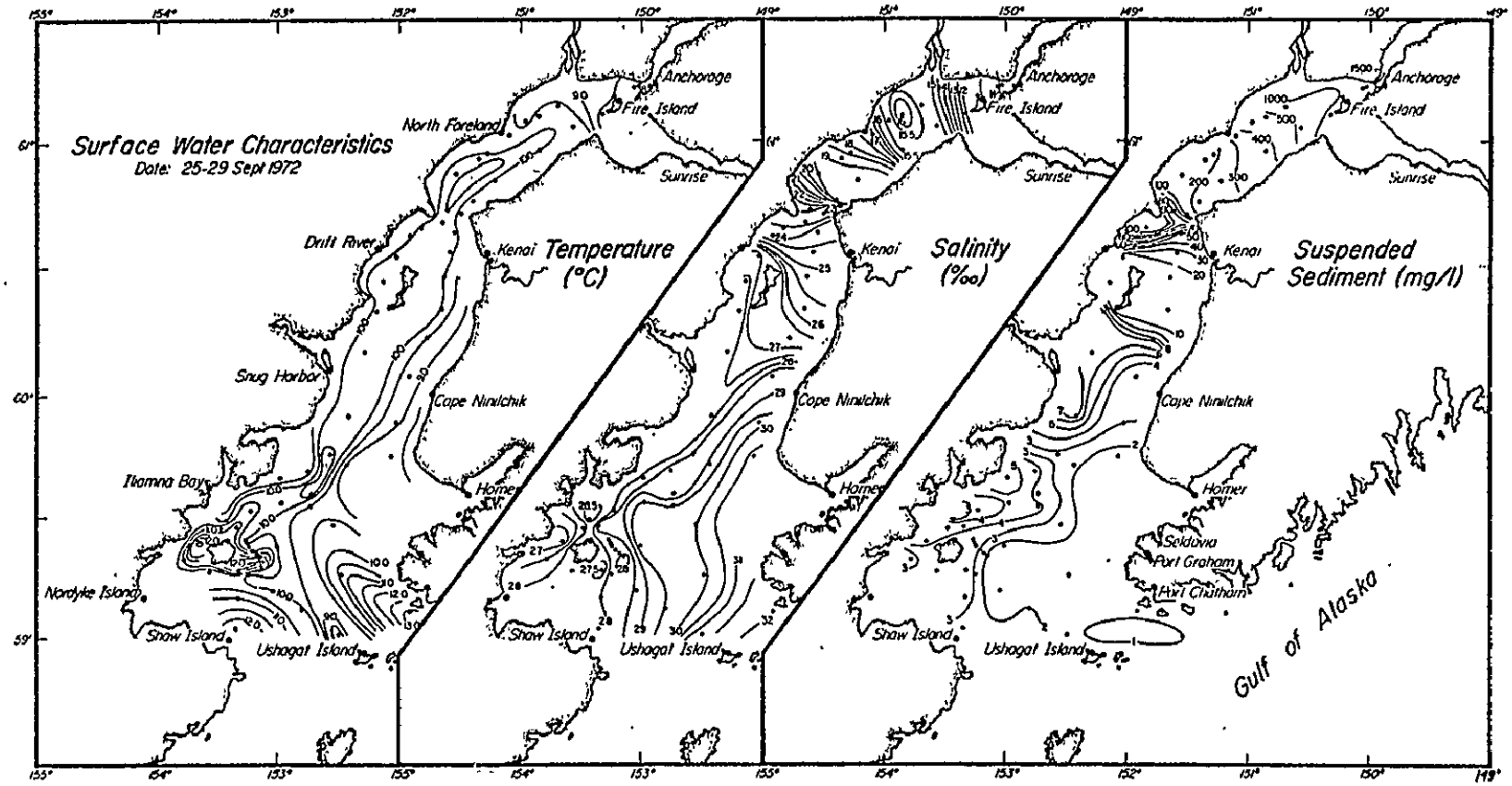

Figure 26. Surface temperature (°C), salinity (o/oo) and suspended sediment (mg/l) in September 1972 (adapted from Wright and Sharma 1973).

indicate that cold water moves north in the central part of the inlet. The cold water moves south past the east shore of Kalgin Island. This southerly movement is verified by the salinity data.

Surface oxygen data indicate that none of the water in the inlet is oxygen deficient; high concentrations occur at the mouth of the Susitna River and near Kamiskak Bay. The surface oxygen distribution also indicates a boundary zone between water types in the mid- and southern inlet as observed from the temperature and salinity data (Kinney et al. 1970b).

The August (Fig. 25) and September (Fig. 26) 1972 data show similar regional patterns; however, local differences are apparent. The oceanic water moving into the inlet on the southeast appears as a distinct tongue in September temperature data; north of the forelands August and September temperatures do not show the distinct water mass in the central portion as observed in May 1968. Salinity data from May 1968 and September 1972 show saline water throughout the southeastern half of the inlet and in September this water appears to progress nearly across the inlet northeast of Augustine Island. The tongue of less saline water east of Kalgin Island in May 1968 is less obvious in September 1972 and not present in August 1972. In addition, north of the forelands, the more saline water appears to move north through Trading Bay in the western inlet in August 1972 and does not appear in September 1972. These differences in distribution may result because the data were taken in different seasons and during different tides and, therefore, reflect changes caused by many tidal fluctuations.

In addition to these differences in distribution, the temperature and salinity ranges are lower. Water temperatures are higher in the northern inlet in August and in September temperatures decrease; oceanic water intruding at the inlet mouth is warmer in September than in August; water in Kamishak Bay was $\approx 6^{\circ}C$ warmer in September 1972 than in May 1968.

Suspended sediment concentrations were generally higher in September than August 1972. Abnormally low concentrations occurred at the mouth of the Susitna River, possibly a result of the low precipitation, 1.82 inches, in July and August (U. S. Department of Commerce 1973). Precipitation increased to 4.42 inches in September, resulting in increased runoff and suspended sediment concentrations. The low suspended sediment concentrations occur along the eastern portion of the inlet below the forelands because this area is dominated by clear oceanic water and rivers discharging into the inlet along this coast contain low sediment concentrations.

Based on this analysis the following observations can be made. The water in the upper inlet is well mixed due to the very large tidal fluctuations and high current velocities (Fig. 27) in this shallow, narrow basin. During summer, when surface runoff is high, there is a net outward movement of water from the upper inlet; with reduced runoff in the winter there is virtually no net outflow (Murphy et al. 1972). The middle inlet has a net inward circulation of cold, saline oceanic water up the eastern shore and a net outward flow of warmer and fresher inlet water along the western shore (Evans et al. 1972). These water masses are well mixed vertically along the eastern shore and are separated laterally by a well defined shear zone. In the lower inlet a lateral temperature and salinity separation is maintained, but in the western portion vertical stratification occurs with colder, saline oceanic water underlying warmer, less saline inlet water. During tidal inflow the deeper oceanic water rises to the surface at the latitude of Tuxedni Bay and mixes with the inlet water (Kinney et al. 1970b).

The repetitive ERTS-1 imagery has been used to analyze these regional surface circulation patterns (Anderson et al. 1973; Wright et al. 1973) and the imagery from October and November 1972 showed few changes in the patterns observed on the ground truth data (Fig. 28). The clear oceanic water from the Alaska Current enters the inlet at flood tide along the east side around the Barren Islands. This clear water becomes less distinct toward the north as it disperses and mixes with the turbid water in the middle inlet around Ninilchik. The tide front progresses up the inlet primarily along the east shore, being diverted in that direction by the Coriolis force. A back eddy not previously reported (dotted arrows) (Fig. 28) was apparent on the November 1972 ERTS frames just offshore from Clam Gulch. The eddy forms in the slack water northeast of Cape Ninilchik during flood. The tide front continues past the East Foreland, a large peninsula protruding some 16 km into the inlet, and is partially diverted across the inlet where it meets the West Foreland. At this location part of the front is diverted south of the West Foreland and the remainder moves north. The result is a counterclockwise circulation pattern around Kalgin Island. This pattern was verified by direct observation from 1800 m altitude during an aircraft underflight at the time the satellite passed. The circulation of surface water north of the forelands at this time appears to be similar to that previously reported (Evans et al. 1972). The ebbing water in the inlet moves predominantly along the northeastern shore past the forelands and was discernible on the November 1972 ERTS-1 imagery. However, the previously reported counterclockwise pattern north of the forelands, formed as ebbing waters strikes the West Foreland, are diverted across the inlet and become incorporated into the flood current along the east shore, was not observed (Anderson et al. 1973). South of the forelands as the sediment laden ebbing water moves past Chinitna Bay a portion appears to flow along the shoreline and

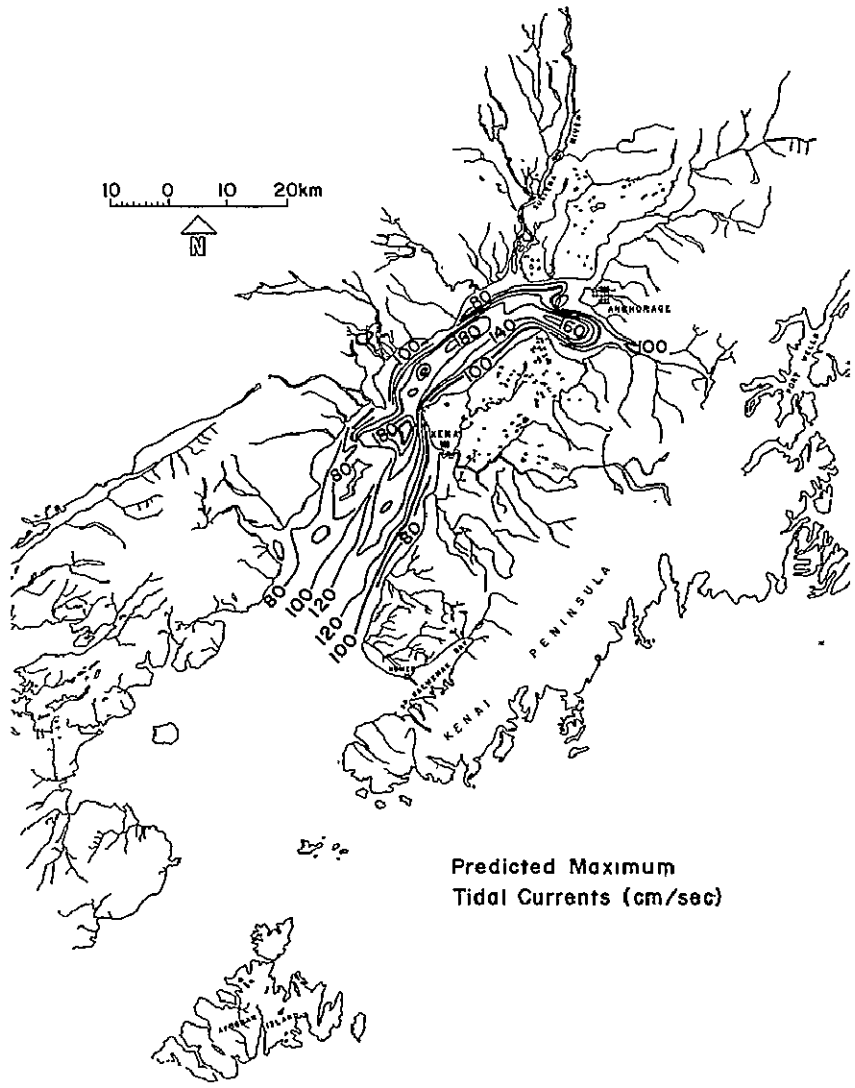

Figure 27. Predicted maximum tidal currents (cm/sec) (after Evans et al. 1972).

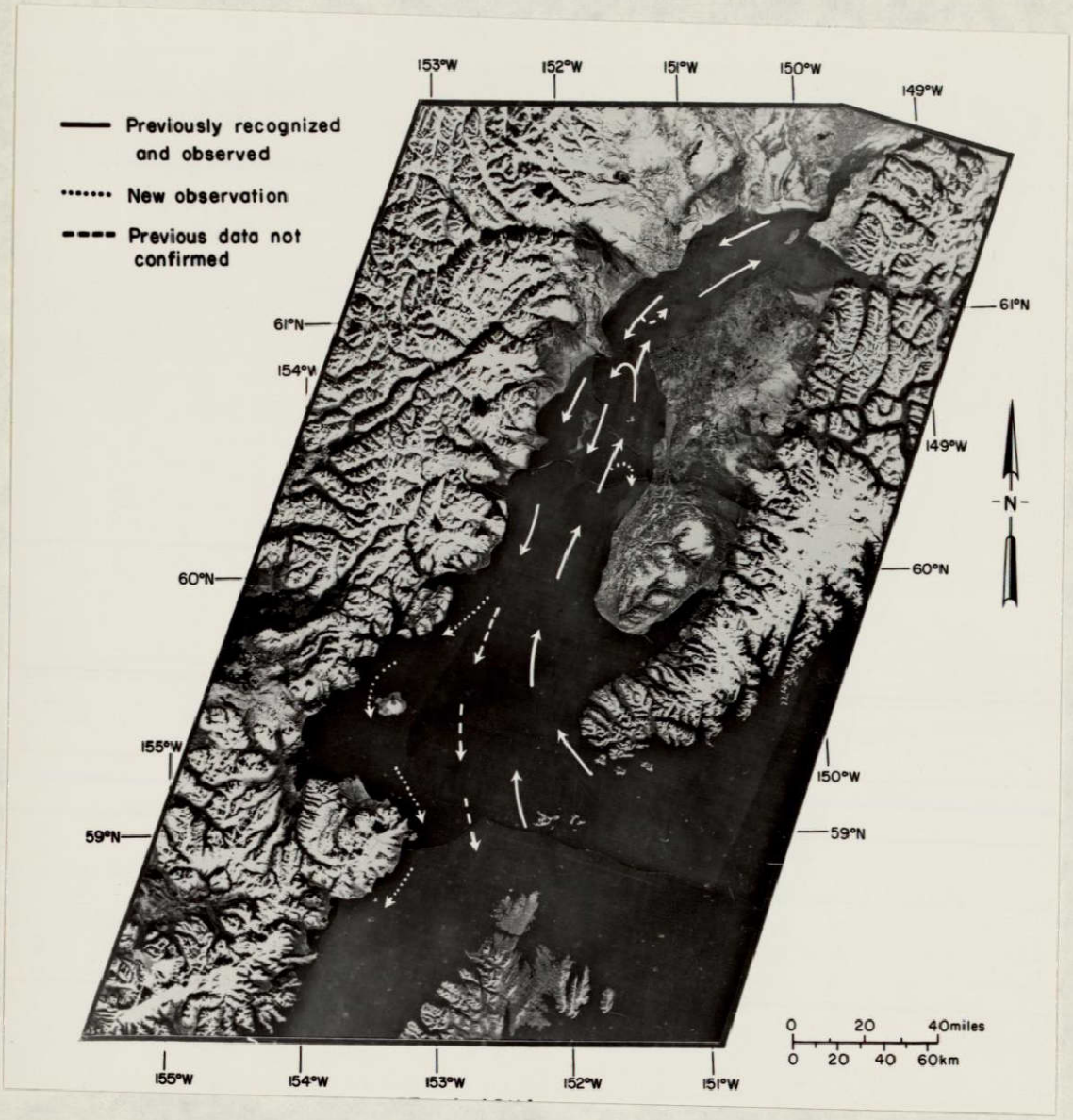

Figure 28. Generalized surface circulation patterns visible on MSS bands 4 and 5 imagery acquired in October and November 1972.

circulate around the west side of Augustine Island in Kamishak Bay while the remainder moves past the bay and continues parallel to the coast past Cape Douglas and progresses through Shelikof Strait. This circulation pattern in Kamishak Bay was not previously reported but is evident on the MSS imagery and verified with ground truth data. In the northern part of the bay, currents follow the coast, flooding northeastward and ebbing southwestward at about 1 knot (U. S. Department of Commerce 1964).

Changes in circulation and sediment distribution occurring during an 18 day ERTS cycle were detected and mapped (Fig. 29). Figure 29a shows differences in the position of the boundary between oceanic and inlet water in the southern inlet on two successive days; this boundary separates these two water types during late ebb tide in Anchorage and late flood in Seldovia. The irregularities and changes in the location of these lines may be due to changes in the mixing zone between these water types. The intrusion of the oceanic water appears to depend more or less on the tidal stage. Near the time of low water in Seldovia the boundary migrates toward the southeast, but near high water it moves more to the northwest. The irregularities in the northern portion of the 4 November boundary may also be due to upwelling of a subsurface salt wedge thought to occur in this portion of the inlet (Kinney et al. 1970b, Evans et al. 1972). This subsurface tongue of oceanic water may move headward up the shoaling bottom of the inlet to the latitude of Tuxedni Bay where it rises to the surface south of Kalgin Island during flood tide.

Changes in the boundary over an 18 day cycle are shown in Figure 29b. The 17-18 October imagery shows the position of the boundary during mid-flood tide in Anchorage and early ebb in Seldovia. The boundary is generally comparable to that shown in Figure 29a and the general relationships of the two water types appear from these observations to be consistent during the period October through November. Some confusion may result because the October boundary (small dots) was drawn from patterns observed on two successive days, not one day as in November. This was necessitated because October images were partially obscured by clouds. However, the observations on these two successive days were made at virtually identical tidal stages. In the areas of image overlap the two lines coincide, suggesting that the regional tidal changes from day to day were less significant than those over an 18 day period. This is in fact the conclusion illustrated in Figure 29b.

Surface water features were most apparent on the band 6 ERTS imagery acquired on 3 and 4 November 1972 because the low sun angle obscures the features on the band 4 and 5 images. Light recorded in the band 6 spectral region is reflected from the water surface with very minor water penetration. Notice that the surface water south of Cape Ninilchik (1) appears clear compared to the water to the north (Fig. 30). Much of

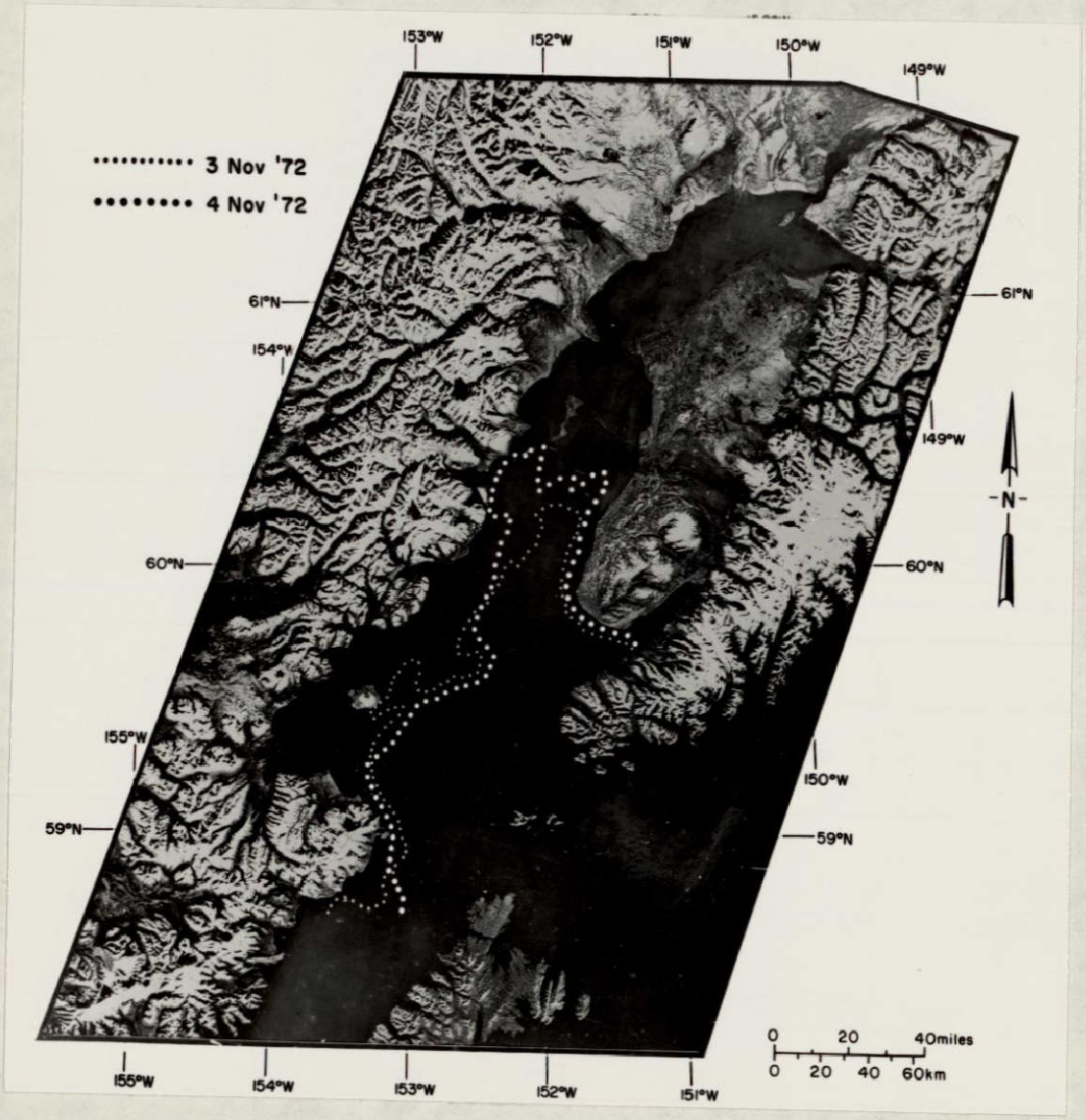

Figure 29. Boundaries separating oceanic and inlet water (from Anderson et al. 1973). a. Daily changes.

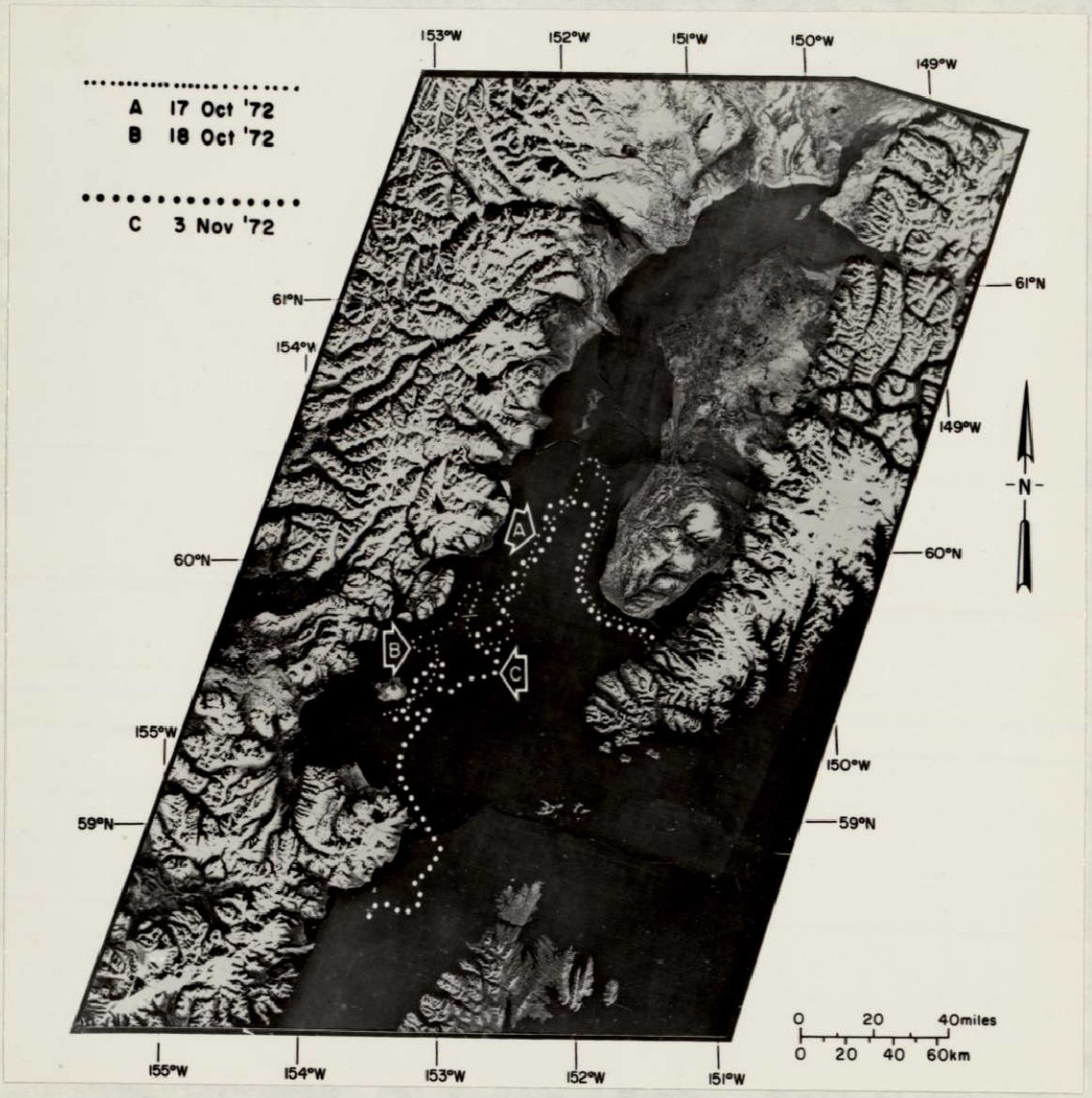

Figure 29 (cont'd). b. Changes over an 18 day period.

Figure 30. Surface water patterns on Cook Inlet on 3 November 1972. MSS band 6 images 1103-20513 (top) and 1103-20520 (bottom).

the turbidity along the coast from Point Possession (3) to the East Foreland (4) is caused by bottom scouring. The outlined area north of Moose Point (2) shows clear (dark) water surrounded by sediment laden water. Details of these patterns are shown in Figures 31-34. The turbid water (1) in Figure 31 results from resuspension of bottom sediment during flood tide. Moose Point shoals (2) are exposed and water of variable sediment concentration (3) occurs farther offshore. This zone between turbid and less turbid water may result from mixing of bottom water and inlet surface water. Note the thermal patterns in this area (line 56); the turbid water appears to produce a cold return (dark) on the scanner imagery. This is as expected since this water occurs in a turbulent zone where cold bottom water would be brought to the surface. The turbid streaks (4) form on the downstream side of submerged rocks because of increased turbulence and bottom scouring. The clearer (dark) water outlines an area where depths reach 10-15 m and scouring is reduced. Note the counterclockwise vortex in the slack water area formed on the lee side of the shoals.

Sediment patterns caused by bottom scouring are also shown in Figure 32. Rocks are scattered throughout this area on the tidal flats (3) and farther offshore (4) west of the sea cliffs (1) and the mouth (2) of Otter Creek (5). The rocks are known navigation hazards along the entire southern coast of Cook Inlet. The rocks are exposed during low tide (Fig. 32a) but are inundated during high water (Fig. 32b). The turbulence on the lee side of the submerged rocks causes bottom scouring and streaks of suspended sediment form behind the rocks. The pattern on Figure 32b is also apparent in the outlined area on Figure 30. Note the clearer water (7), the "feathered-edge" pattern (5) and the turbid water (6).

Currents moving past the West Foreland (1) parallel this coast and cause some bottom scouring (5) in the area around Knuttrain Rocks (Fig. 33). Erosion is active along the south side at the base of the sea cliff (3) and deposition has formed the tidal flats (4) farther west. The surface patterns to the northeast (2) may be wind slicks; the suspended sediment (6) may be reworked bottom sediment.

Across the inlet from Moose Point (2 on Figure 30) and east of the North Foreland several water types converge and mix near the offshore platform (1) (Fig. 34). The variability in sediment concentration shown in Figure 34 are not as obvious in Figure 30. The offshore water (2) appears to be moving north (note pattern behind platform) and overriding the less turbid water (6). Mixing between clear (6) and turbid (7) water is apparent. Plume patterns on the thermal scanner imagery (line 54) indicate that the water from Beluga, Theodore, Lewis and Ivan Rivers is moving north nearshore. The water about 4 km offshore appears to be moving south. The water types (3,4, and 5) nearshore in Figure 34 are from these rivers. Internal waves (8) occur along the front between these water types.

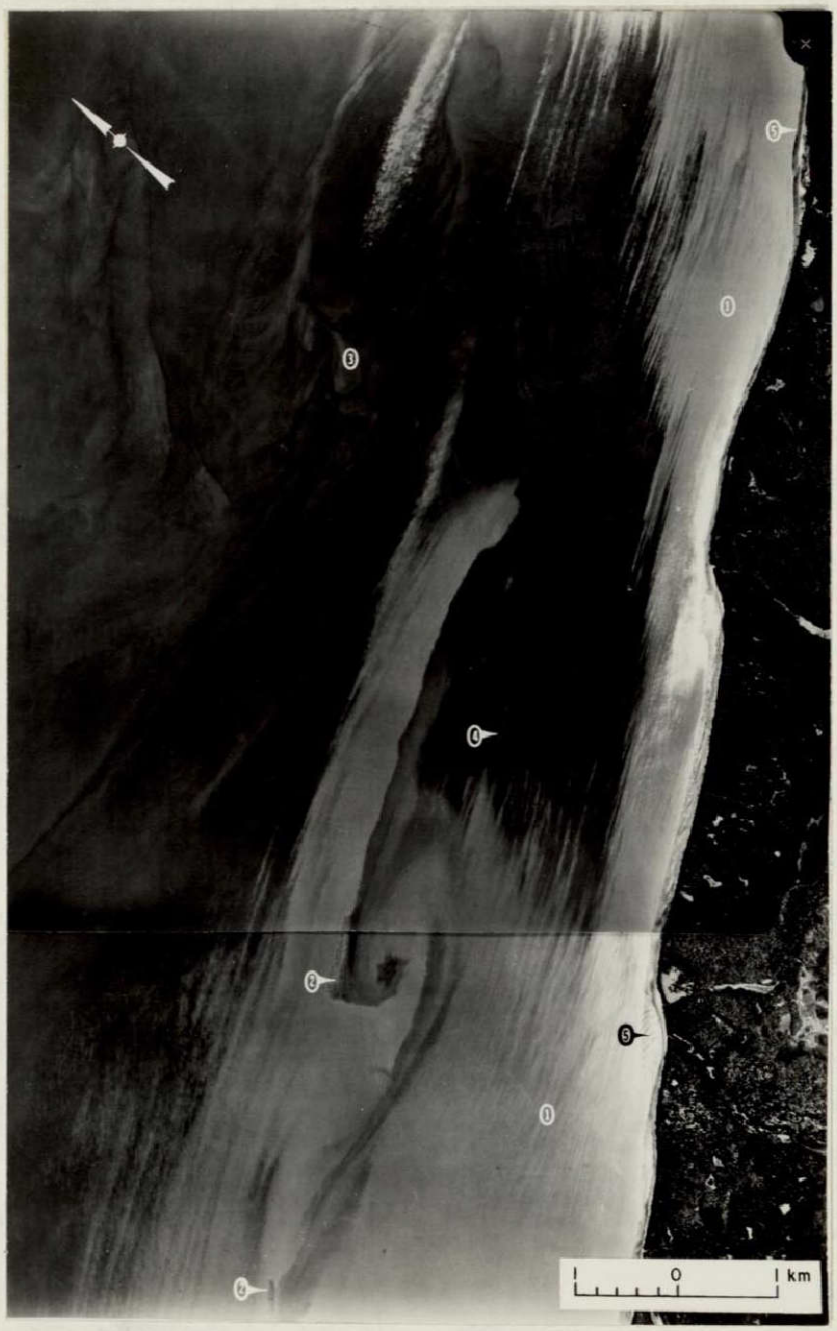

Figure 31. Cook Inlet coast approximately 13 km southwest of Point Possession (outlined on Figure 30; NASA NP-3A photographs).

Figure 32. Coast south of Moose Point (outlined on Figure 30; NASA NP-3A photographs). a. early flood tide.

Figure 32 (cont'd). b. late flood tide.

Figure 33. West Foreland during flood tide (outlined on Figure 30; NASA NP-3A photograph).

Figure 34. Area east of the North Foreland (outlined in Figure 30; NASA NP-3A photograph).

Suspended sediment concentration throughout the inlet is controlled primarily by the circulation described above and a generalized distribution can be presented (Fig. 35). Suspended sediment, mostly of glacial origin, is concentrated in the well-mixed northern inlet; it is nearly absent in the water of the east central and eastern portions of the inlet mouth. The inlet water from the mouth to the latitude of Cape Ninilchik and Chisik Island contains suspended sediment predominantly smaller than medium silt; medium silt or smaller particles dominate, but fine sand is present, north of Ninilchik to the area between the Susitna River mouth and Point Possession; silts predominate but fine sands become increasingly prevalent in the upper inlet east of Point Possession (Kinney et al. 1970b). This regional distribution is maintained year-round but the total suspended sediment load varies with season and with depth (Murphy et al. 1972, Kinney et al. 1970b). Subsurface measurements show that suspended load normally increases with depth (Sharma et al. 1974). Rosenberg et al. (1967) also indicate that the vertical sediment distribution varies with depth. Maximum values generally occur at approximately 10 m at the head of the inlet, load increases with depth south of the forelands.

ERTS MSS imagery from November 1972 (Fig. 30), April (Fig. 36) and September 1973 (Fig. 37) clearly shows many of the aforementioned sediment patterns produced by the movement of water types with different temperatures, salinities and suspended sediment concentrations. The distribution of and areas of mixing between the less turbid, more saline, oceanic water in the southeast and the turbid, fresher inlet water in the north and southwest are apparent. Zones of mixing along the boundary between the oceanic (1) and inlet (2) water are apparent based on changes in suspended sediment concentration (Fig. 36). This ERTS image was taken on 15 April 1973 during late flood tide in Seldovia and shows a clear distinction (3) between water types. The zone of intermediate sediment concentration (4) suggests extensive mixing at the northern end of the oceanic water.

Figure 37 shows surface patterns of suspended sediment distribution on 24 September 1973 during late flood tide in Seldovia and late ebb tide in Anchorage (lower low water in Anchorage occurred at 1204, approximately ten minutes after the imagery was taken). The oceanic water (1) on the southeast has migrated as far north as Kenai. The boundary (2) between this water and inlet water (3) is much less obvious on this imagery than that acquired on 15 April (Fig. 36). Surface runoff is probably reduced and less suspended sediment discharged into the inlet. Mixing between the two major water types appears to be more extensive at this time in the middle and southern inlet. The entire inlet south of the forelands is dominated by oceanic water and complex surface circulation patterns exist near Kalgin Island. The patterns differ from those observed on the November 1972 imagery. Flooding oceanic water

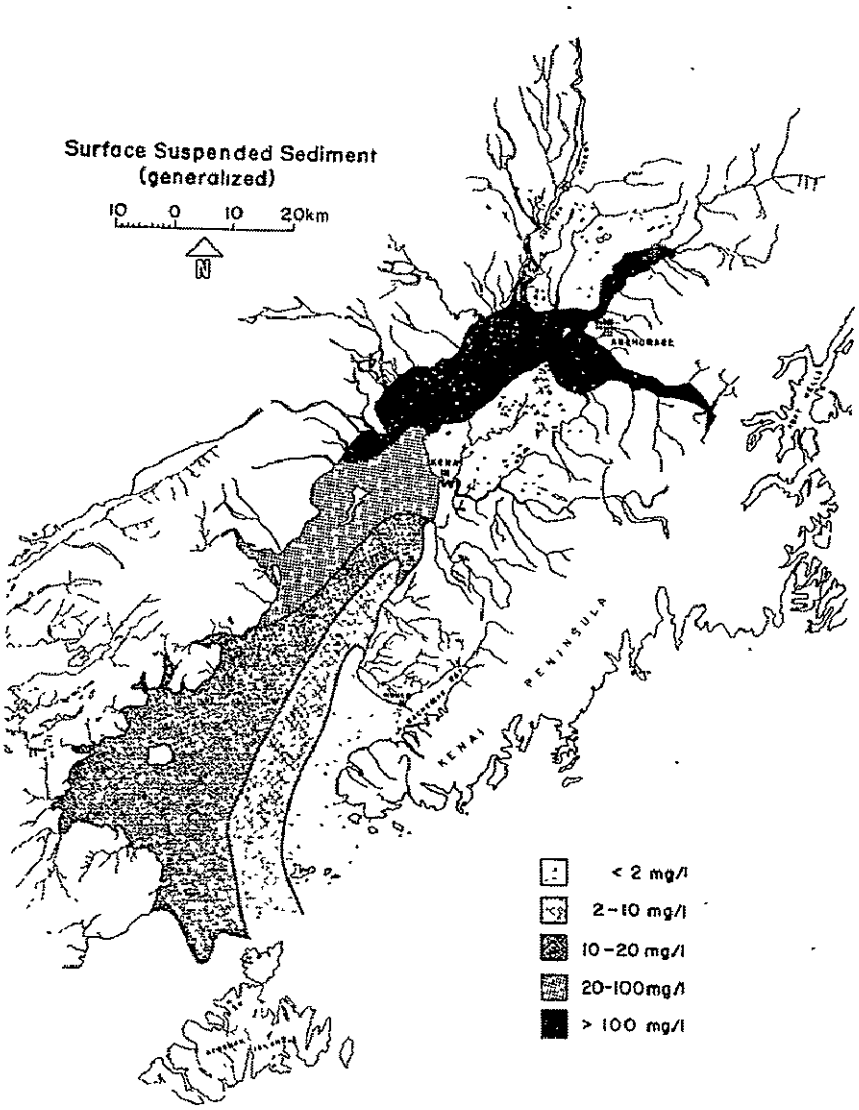

Figure 35. Generalized surface suspended sediment distribution (after Sharma et al. 1973).

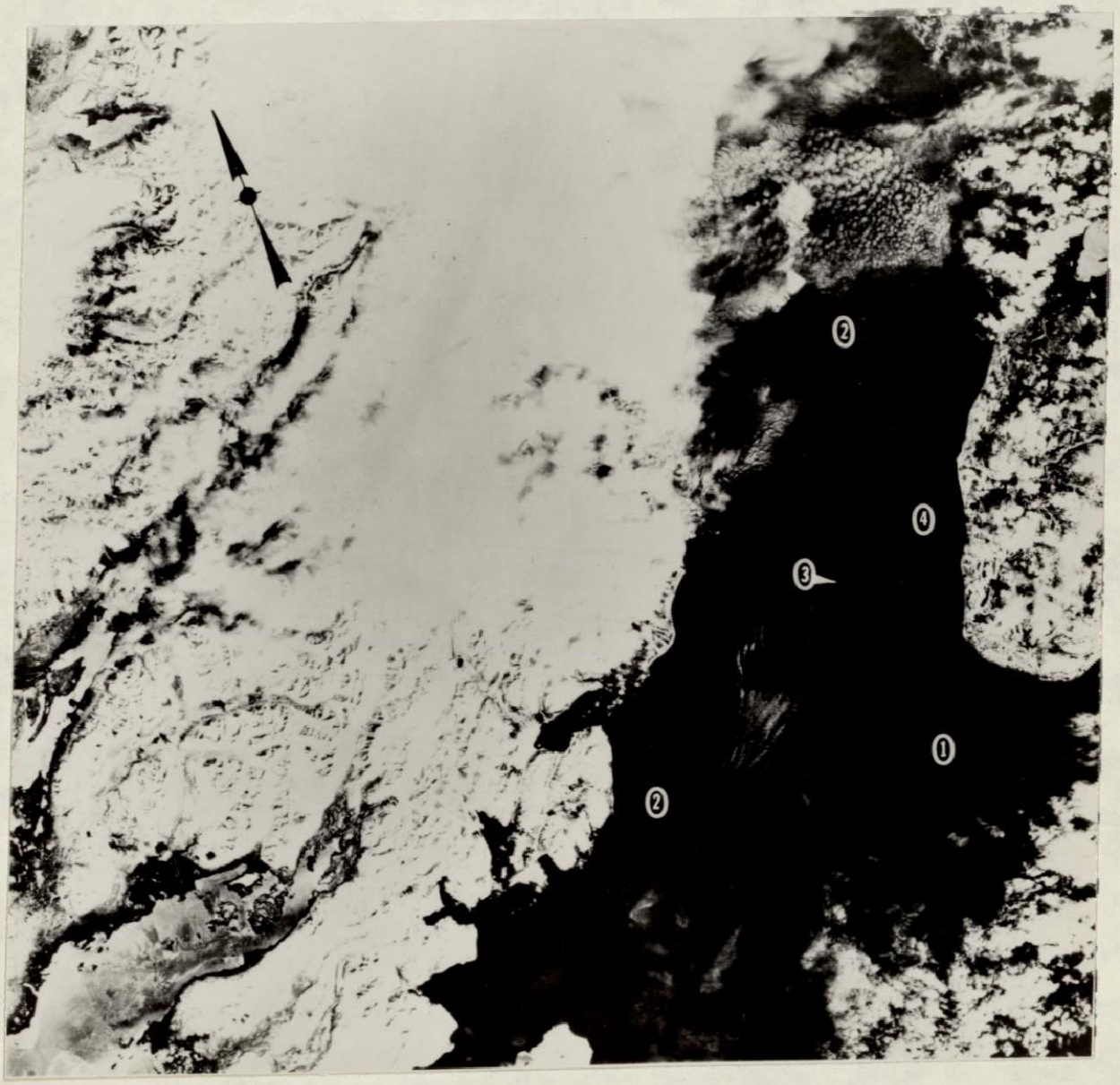

Figure 36. Surface water patterns in southern Cook Inlet.
MSS band 5 image 1266-20581, acquired 15 April 1973.

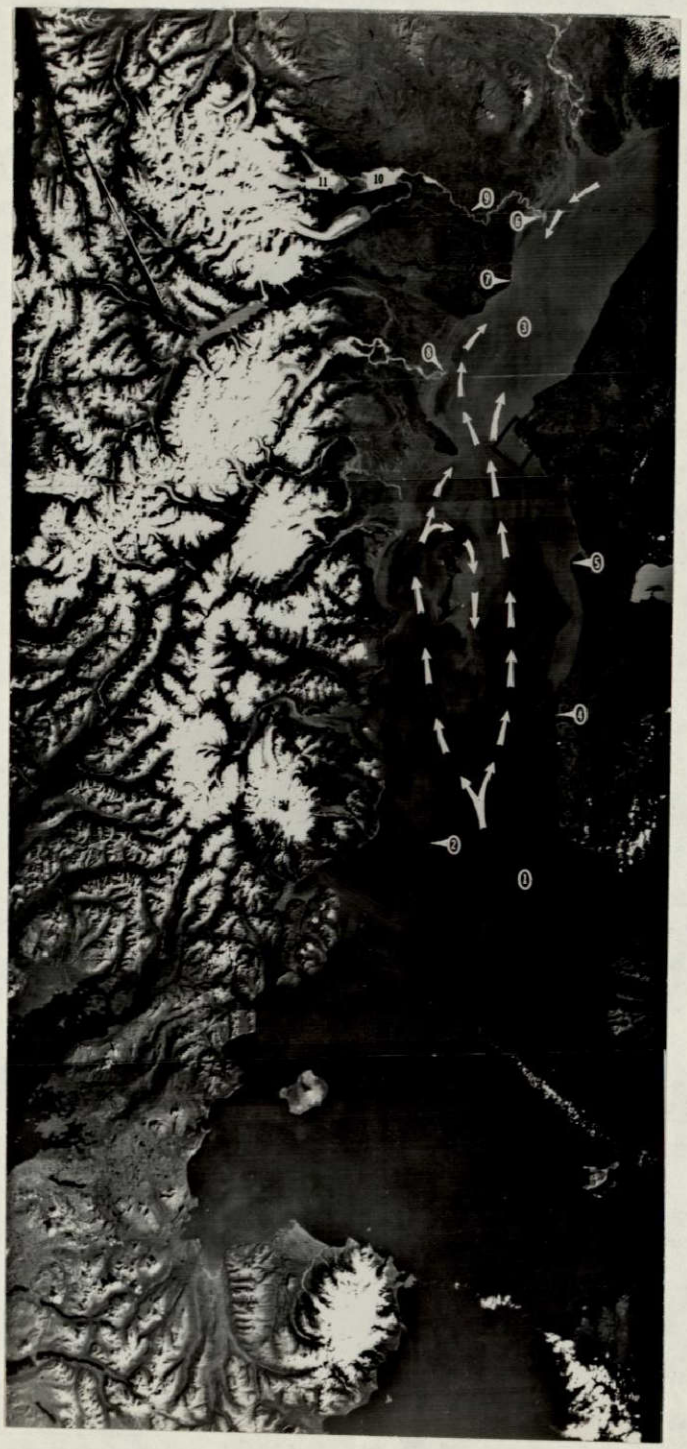

Figure 37. Surface water patterns in Cook Inlet. Mosaic made from MSS band 5 images 1428-20554, 1428-20560, and 1428-20563, acquired 24 September 1973.

appears to bifurcate near the latitude of Tuxedni Bay and move northward east and west of Kalgin Island. A nearshore counter current appears along the east coast of Kalgin Island. The high sediment concentration along the east coast between Cape Ninilchik (4) and Cape Kasilof (5) may be due to scouring of the bottom or a southerly counter current along the coast. A similar pattern was observed on 22 September 1973 (Fig. 20). North of the forelands the oceanic water has mixed extensively with the turbid inlet water but appears to continue up the inlet along the west shore and in the middle. McArthur River plume (8) indicates that coastal water here is moving north. Surface salinity data from August 1972 (Fig. 25) show a similar pattern north of the forelands. The Beluga River (9) is a meltwater stream flowing from Beluga Lake (10), a periglacial lake at the terminus of the Triumvirate Glacier (11). The river plume (6) indicates southerly nearshore currents. This coastal water may continue along the coast to the North Foreland (7) then move across the inlet and become mixed with flooding water.

Figure 38 shows details of water movement in the Anchor Point (1) area at flood tide conditions as shown in Figure 37. Clear water (2) dominates this area especially during flood. Anchor River (3) discharges clear water at the north end of the bay mouth bar (4) which has formed across the mouth of the river. Wave action and currents appear to rework the nearshore sediment producing a turbid zone (6) seaward of the bar. The dominant current direction is northerly as inferred from the orientation of the bar. Sea cliffs (5) are common along the coast.

Figure 39 shows the Nikiski wharf area (1) and the surface current patterns near the East Foreland during flood tide. These patterns are also apparent in Figures 30 and 37. Current velocities reach 8 knots here and current directions are parallel to the coast. Turbid streaks in the nearshore water (2) show northerly flow. A distinct line between this water and more turbid water (3) offshore is apparent in the west (also very apparent on Figure 30). Turbidity (4) on the north side of the foreland may result from bottom scouring. The light area (5) is due to sun glint on the water surface. Rosenberg et al. (1967) report the changes in local tidal currents based on drogue studies: a large eddy develops in the area of turbid water (4) north of the East Foreland during flood; this assists in lateral mixing and dispersion of wastes from the Nikiski outfalls. Water that misses this eddy is moved farther offshore during ebb, while nearshore ebb currents parallel the coast and carry effluents to the Kenai River area. The high current velocities and lateral mixing cause rapid dispersion of the local wastes.

Circulation patterns similar to those observed on 24 September 1973 (Fig. 37) were observed on 6 September 1973 during mid-flood at Anchorage and very early ebb at Seldovia (Fig. 40). Clear oceanic water

Figure 38. Anchor Point area during flood tide (outlined on Figure 37; NASA NP-3A photograph).

Figure 39. Nikiski wharf - East Foreland area during flood tide (outlined on Figure 37; NASA NP-3A photograph).

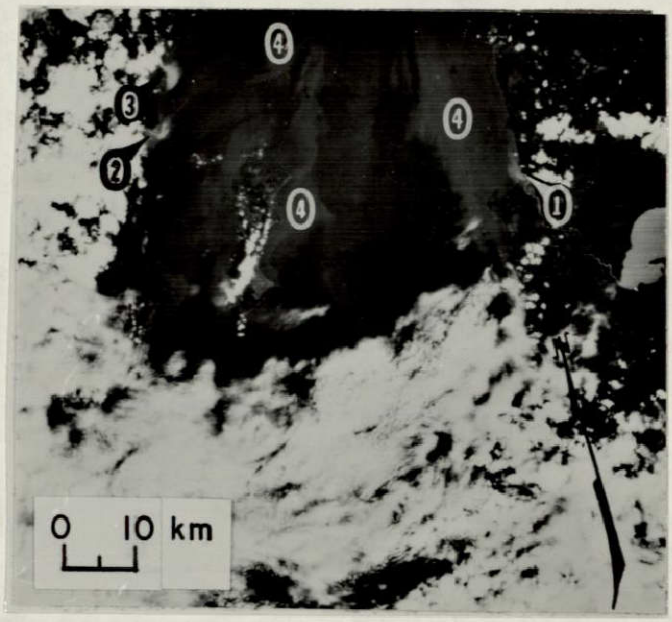

Figure 40. Surface water patterns near Kalgin Island. From MSS band 5 image 1410-20513, acquired 6 September 1973.

moves north on either side of Kalgin Island. Plumes from the Kasilof (1), Drift (2) and Big (3) Rivers indicate that nearshore currents are moving north. The turbid waters (4) near the coasts occur over shallow areas (refer to N.O.A.A. Navigational Charts 8554 and 8553) and the high concentration of suspended sediment may result primarily from bottom scouring and river discharge.

Repetitive ground truth observations of water characteristics in the southern inlet from 15 May to 9 September 1973 were provided by the National Ocean Survey, N.O.A.A. These data were used to prepare distribution maps, profiles and T-S diagrams; seasonal and tidal changes in characteristics were noted. These results were correlated with and verified many of the interpretations and observations made from the imagery. Surface temperature (Fig. 41) and salinity (Fig. 42) distributions from 22-26 May are comparable to the 1968 data (Fig. 24) although the 1973 temperatures are generally lower, salinities higher. Cold water ($\approx$5.0°C) enters the inlet on the southeast side while warmer water moves seaward along the west shore. The warmest water is found in Kamishak Bay and appears to circulate out of the Bay round Augustine Island. This circulation was observed on ERTS imagery acquired in November 1973 (Figs. 28 and 30) but was not previously recognized. The 1968 and 1973 salinity patterns in May are very similar. The more saline water is concentrated in the southeast and dilution by fresh water occurs primarily from the north and southwest. A very distinct shear zone is indicated by the 1968 and 1973 salinity data.

Differences in surface temperature (Fig. 43) and salinity (Fig. 44) distributions for flood and ebb tides from 17-26 May were prepared to illustrate changes in distributions and circulation due to tidal action. Surface temperatures of inlet water are colder than the oceanic water during this time, although this relationship reverses in the summer. Lowest salinities (29°/oo) are found in Kamishak Bay. Circulation in Kamishak Bay appears to be reduced during flood tide and fresh water tends to accumulate in this protected embayment. Surface temperatures in Kachemak Bay are generally higher than in the inlet while changes in salinity during different tides are minor. Circulation in the inner bay may be reduced because the narrow opening between the end of Homer spit and the south shore causes restricted water exchange.

Temperature and salinity data indicate that the shear zone (boundary) between the two water masses in the southern inlet is compressed toward the west during flood, being forced in that direction by the inflowing oceanic water. Surface circulation out of Kamishak Bay appears to be negligible during flood. The boundary migrates eastward during ebb, and southerly moving inlet water appears to spread over a larger portion of the lower inlet. The mixing zone between the water masses is moved toward the mouth and oceanic water is restricted to the lower southeast side of the inlet.

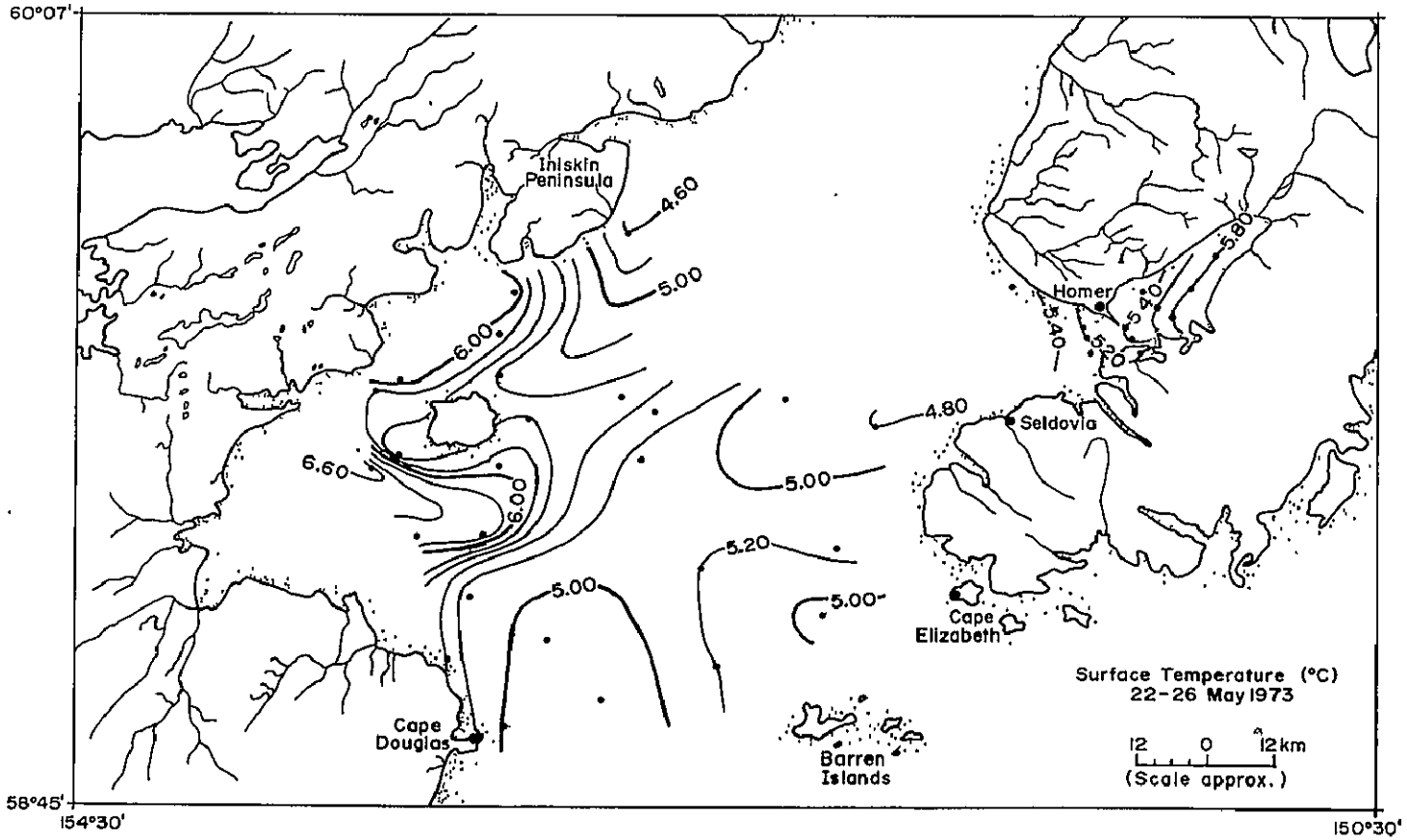

Figure 41. Surface temperature distribution, 22-26 May 1973.

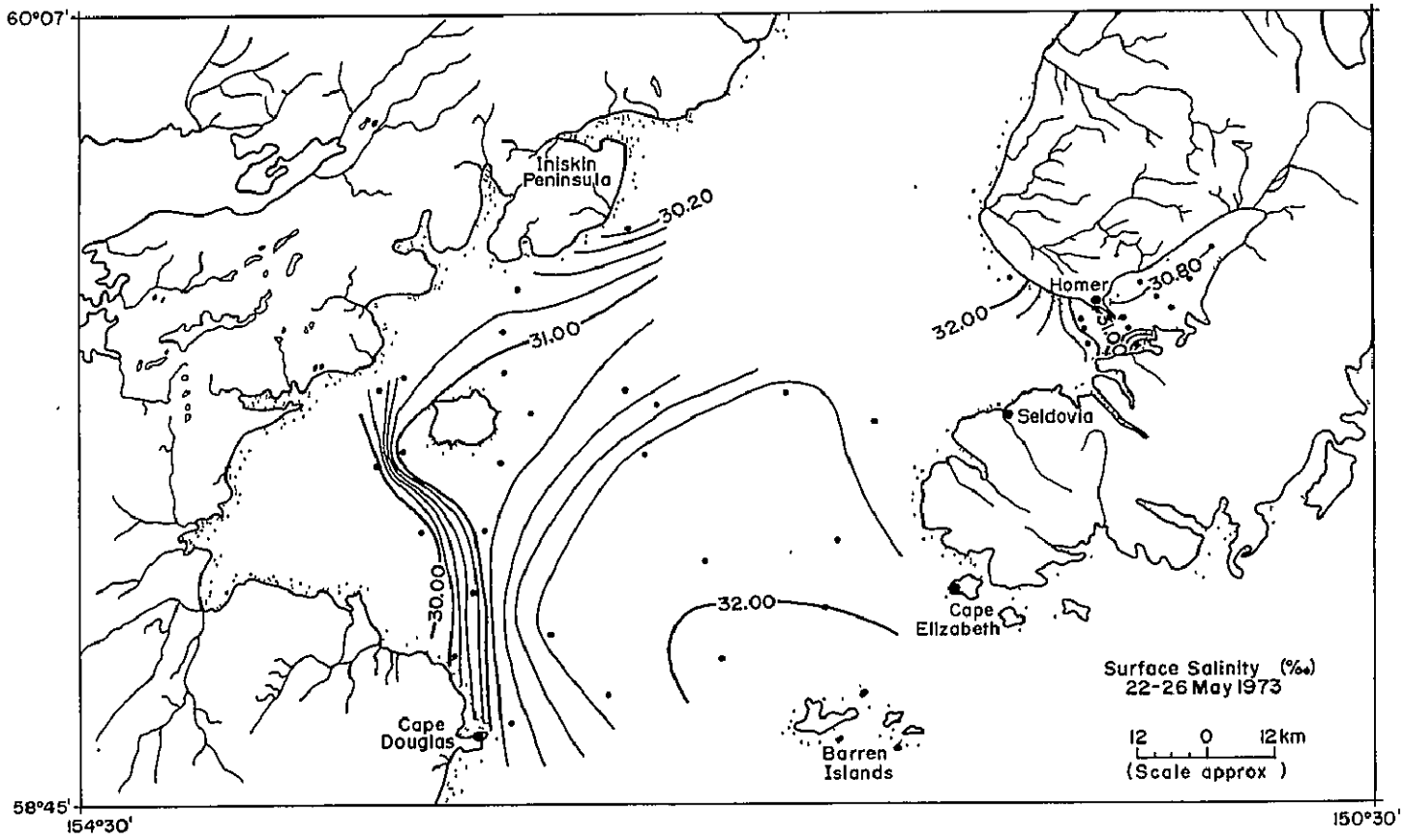

Figure 42. Surface salinity distribution, 22-26 May 1973.

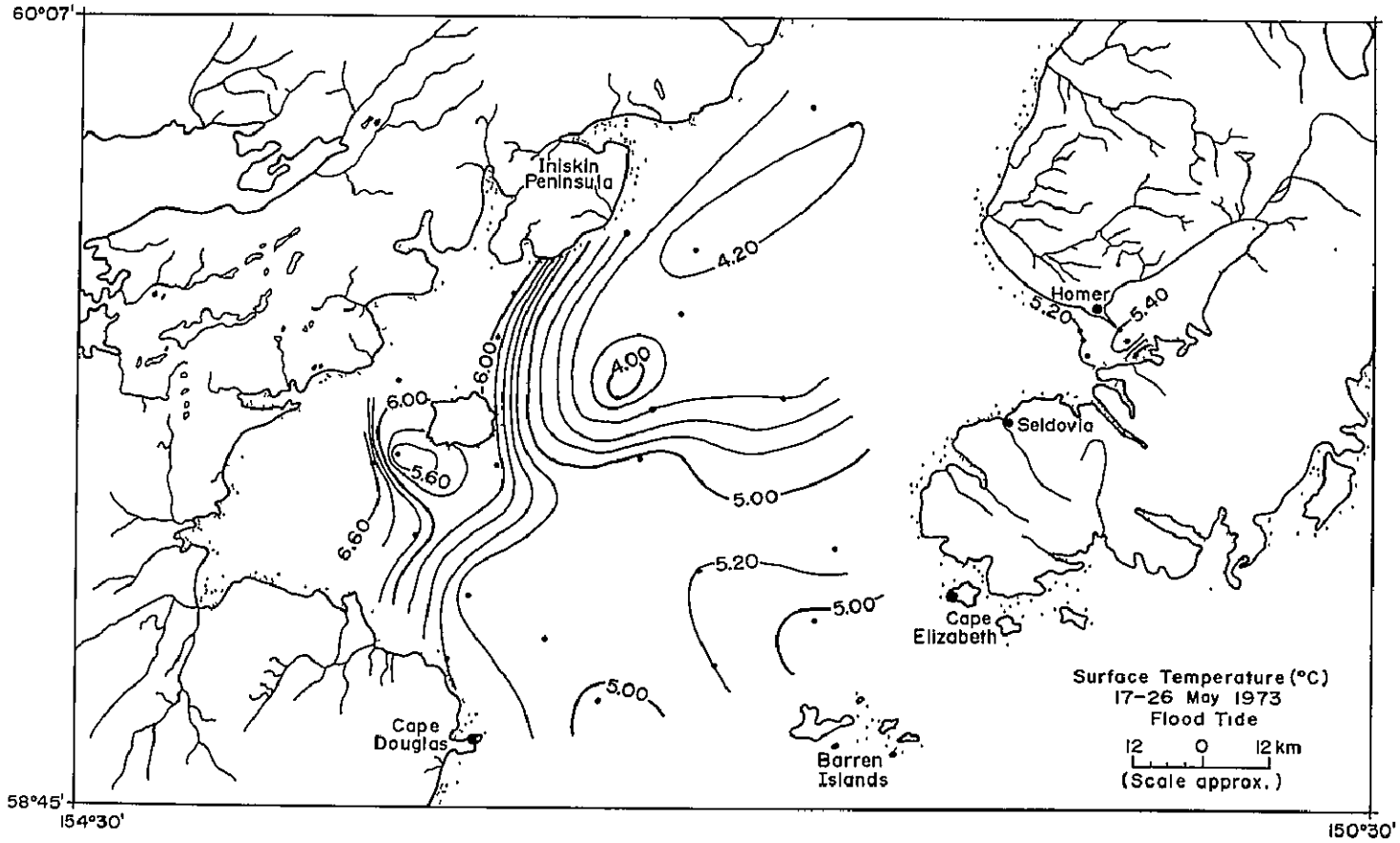

Figure 43. Surface temperature distribution, 17-26 May 1973. a. Flood tide.

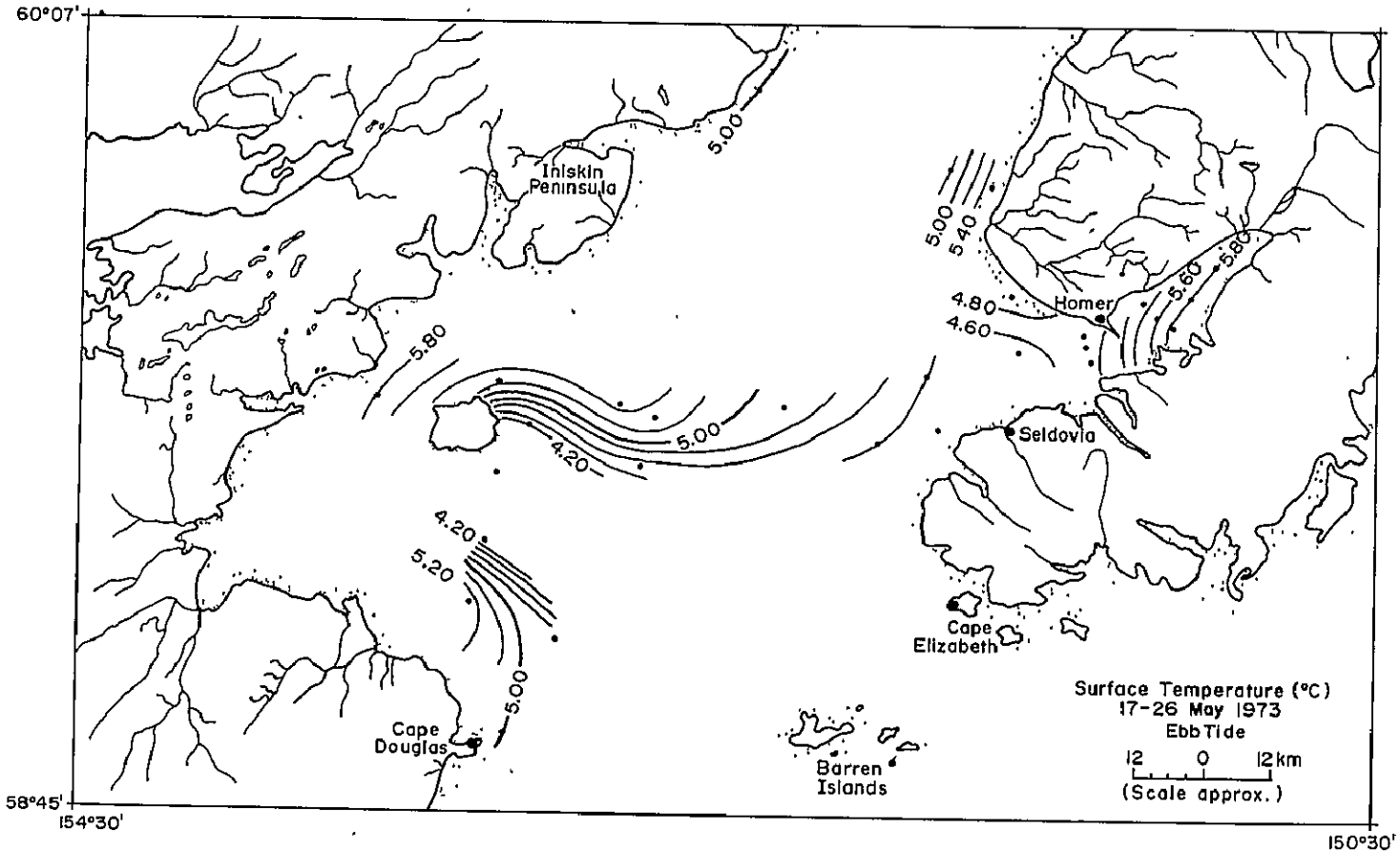

Figure 43 (cont'd). b. Ebb tide.

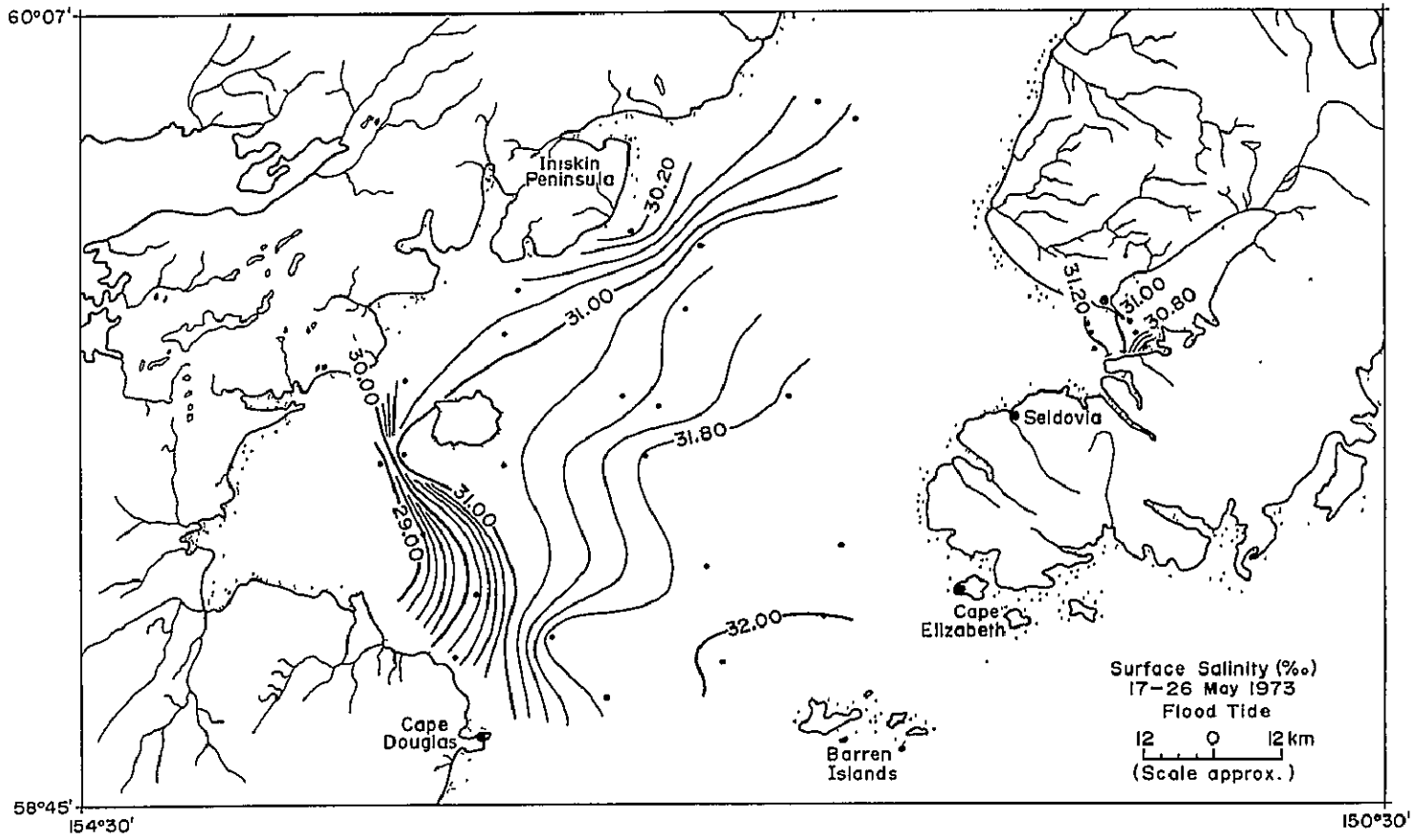

Figure 44. Surface salinity distribution, 17-26 May 1973. a. Flood tide.

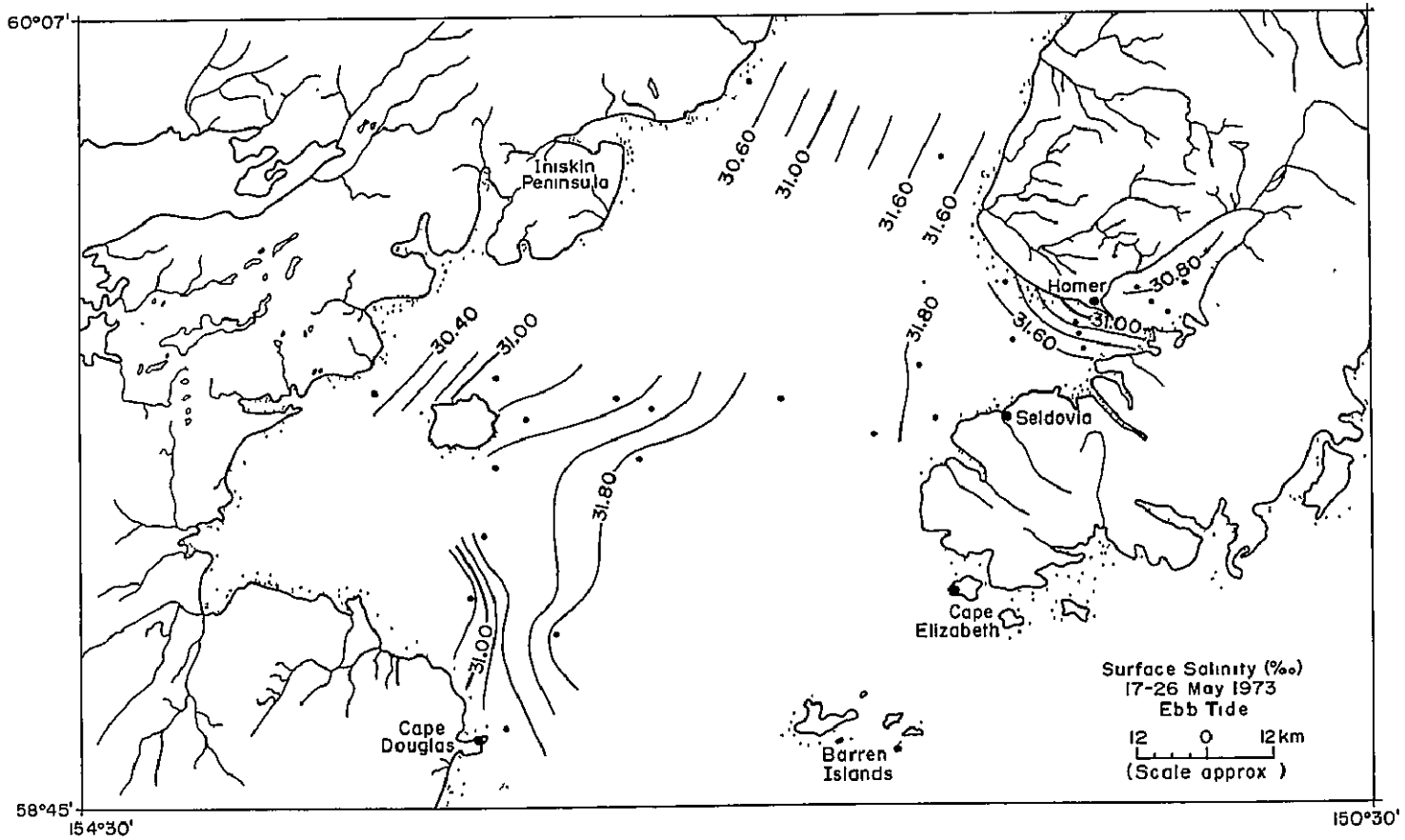

Figure 44 (cont'd). b. Ebb tide.

Temperature and salinity profiles (Fig. 45) indicate that a distinct thermocline and halocline occur between 5-10 m and 0-5 m, respectively, at location SP-2014 in Kamishak Bay. The surface water is ≈ 2°C warmer than the water at depth while the salinity is ≈ 2°/oo higher at depth. The water temperature and salinity below 10 m remain virtually constant. Strong stratification is not present at sites SP-2033, southwest of Homer, and SP-2021, in mid-inlet. In general, mixing of surface and lower waters appears to be more complete in these locations.

Data acquired from 8-15 June show several changes in water characteristics for flood and ebb tides. Surface water entering the inlet during flood tide in June (Fig. 46a) is approximately 2°C warmer than in May. The water temperature change across the mouth is greater (3°C), and the oceanic water appears to intrude less into the inlet during flood tide in June. Temperatures of the inlet water appear to be as cold as the oceanic water, possibly due to the increased discharge of glacial meltwater streams in summer. Surface temperatures during ebb (Fig. 46b) indicate less intrusion of oceanic water and a spreading of warmer water from Kamishak Bay.

Surface salinity distribution (Fig. 47) also indicates a greater restriction of oceanic water to the southeast than was evident in May. A more rapid salinity change across the mouth occurs and the less saline water in Kamishak Bay is confined during flood tide. The shear zone appears to be more compressed and slightly east of its location during flood in May. This shear zone or frontal zone becomes more diffuse and moves eastward during ebb flow. This migration with tides was also detected in tidal data acquired on 14 April 1973 (Sharma et al. 1973).

Water profiles at ST-2006, ST-2009 and ST-2020 indicate decreasing temperature and increasing salinity with depth (Fig. 48). Changes in temperature-salinity with depth are more pronounced and stratification is generally stronger in June than in May, except for the data at SP-2014 (Fig. 45) where a strong thermocline and halocline exist. Water at ST-2006 is more stratified than at the other sites, possibly because this site is in the area where Kamishak Bay and oceanic waters migrate with the tides. The water below 10 m in May has similar salinity and temperature values to the water below 30 m in June. This suggests that surface layers with high temperature/salinity variability have become thicker as surface runoff increased in June.

Temperature and salinity distributions for 3-8 July (Figs. 49 and 50) are comparable to those previously observed. Movement of warm surface water toward the inlet mouth from Kamishak Bay is well documented by the temperature patterns from 3-8 July and ebb tide data for 8-15 June (Figs. 46b and 47b). This circulation was also observed on the ERTS-1 imagery acquired 24 September 1973 (Fig. 37). Surface

L. 2

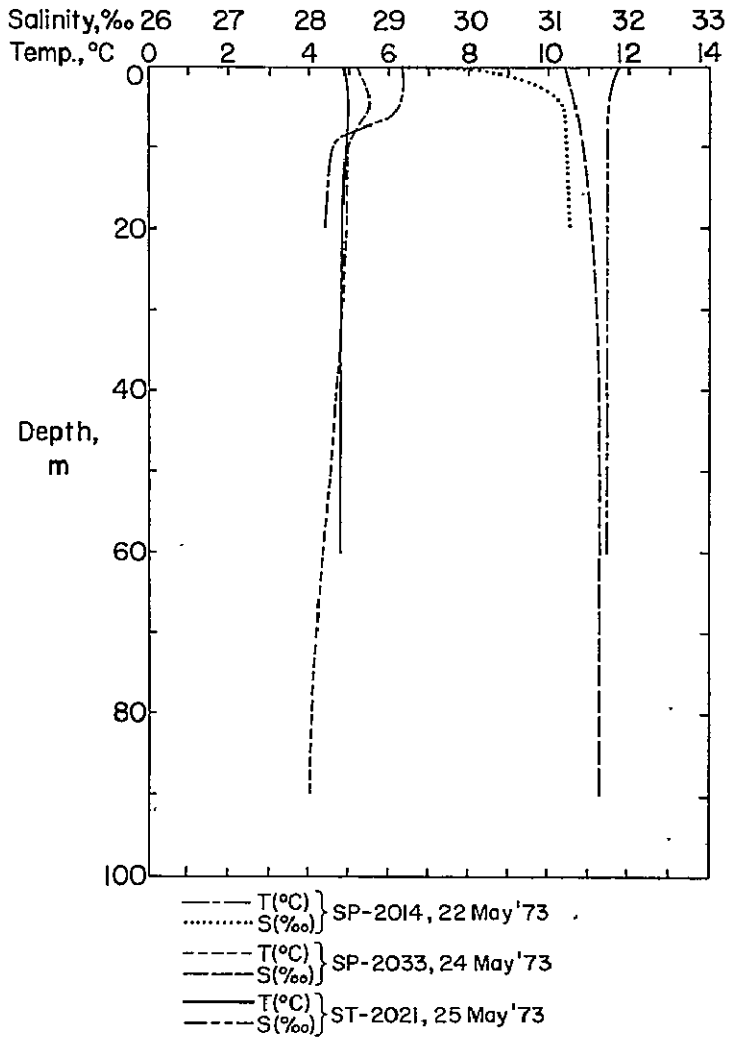

Figure 45. Temperature-salinity profiles, May 1973.

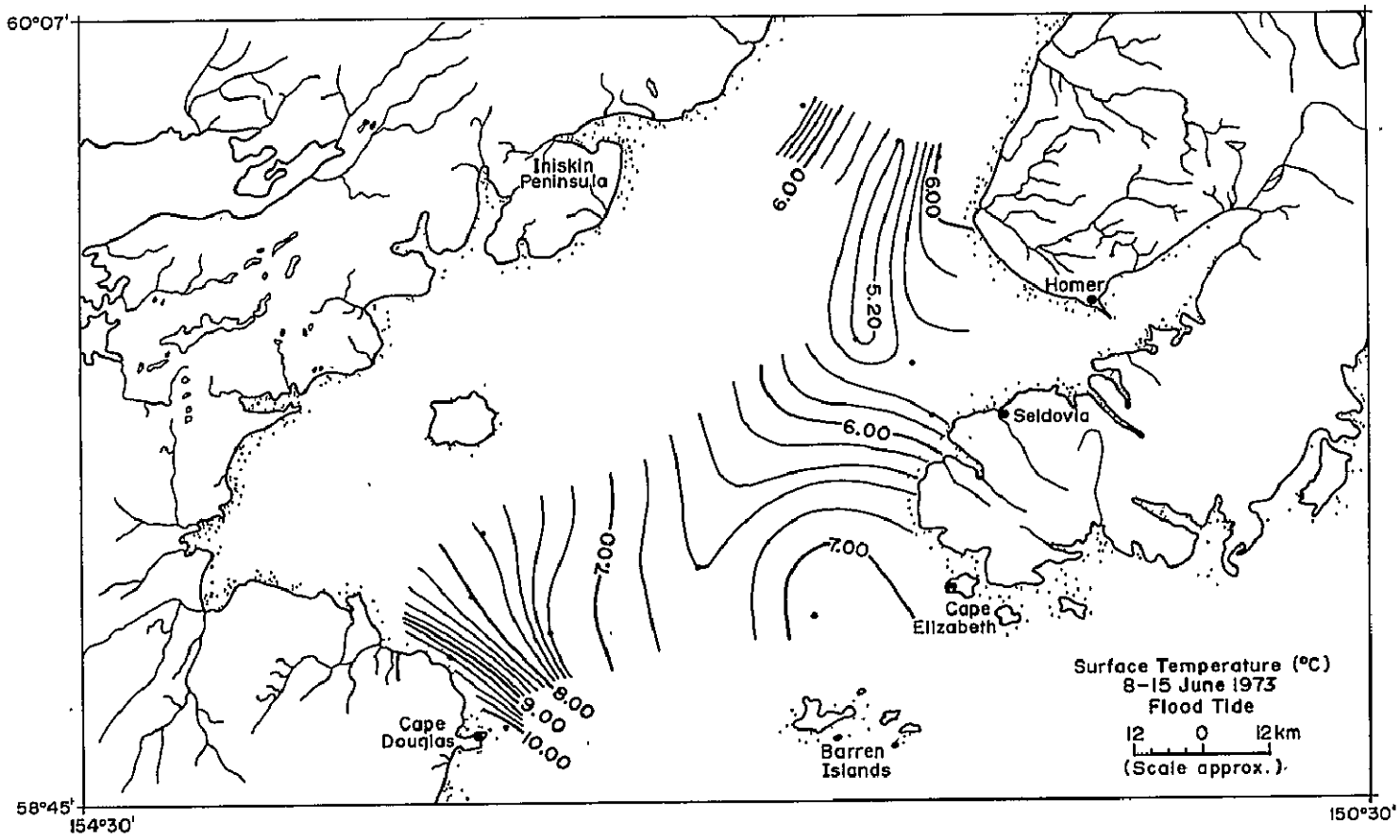

Figure 46. Surface temperature distribution, 8-15 June 1973. a. Flood tide.

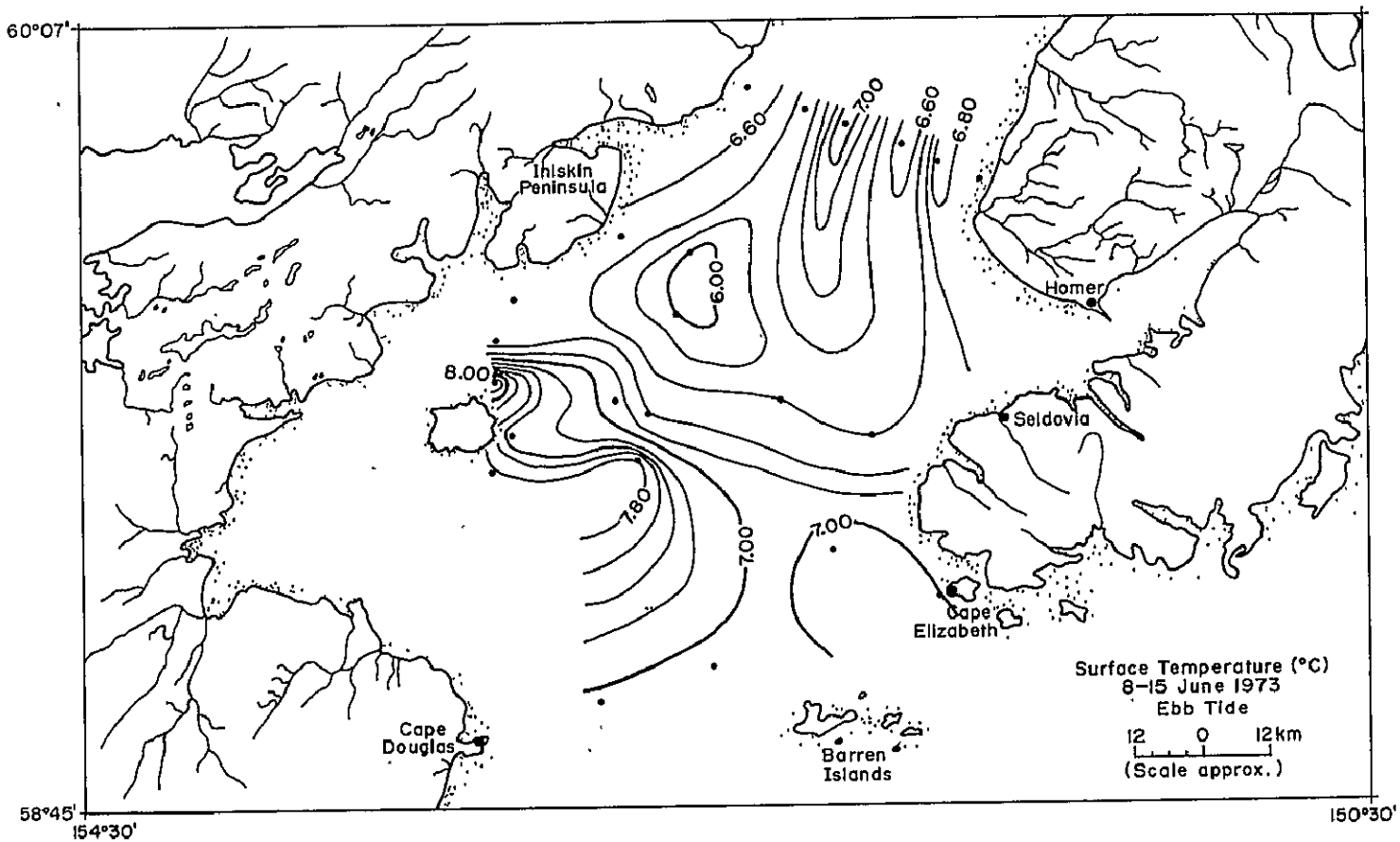

Figure 46 (cont'd). b. Ebb tide.

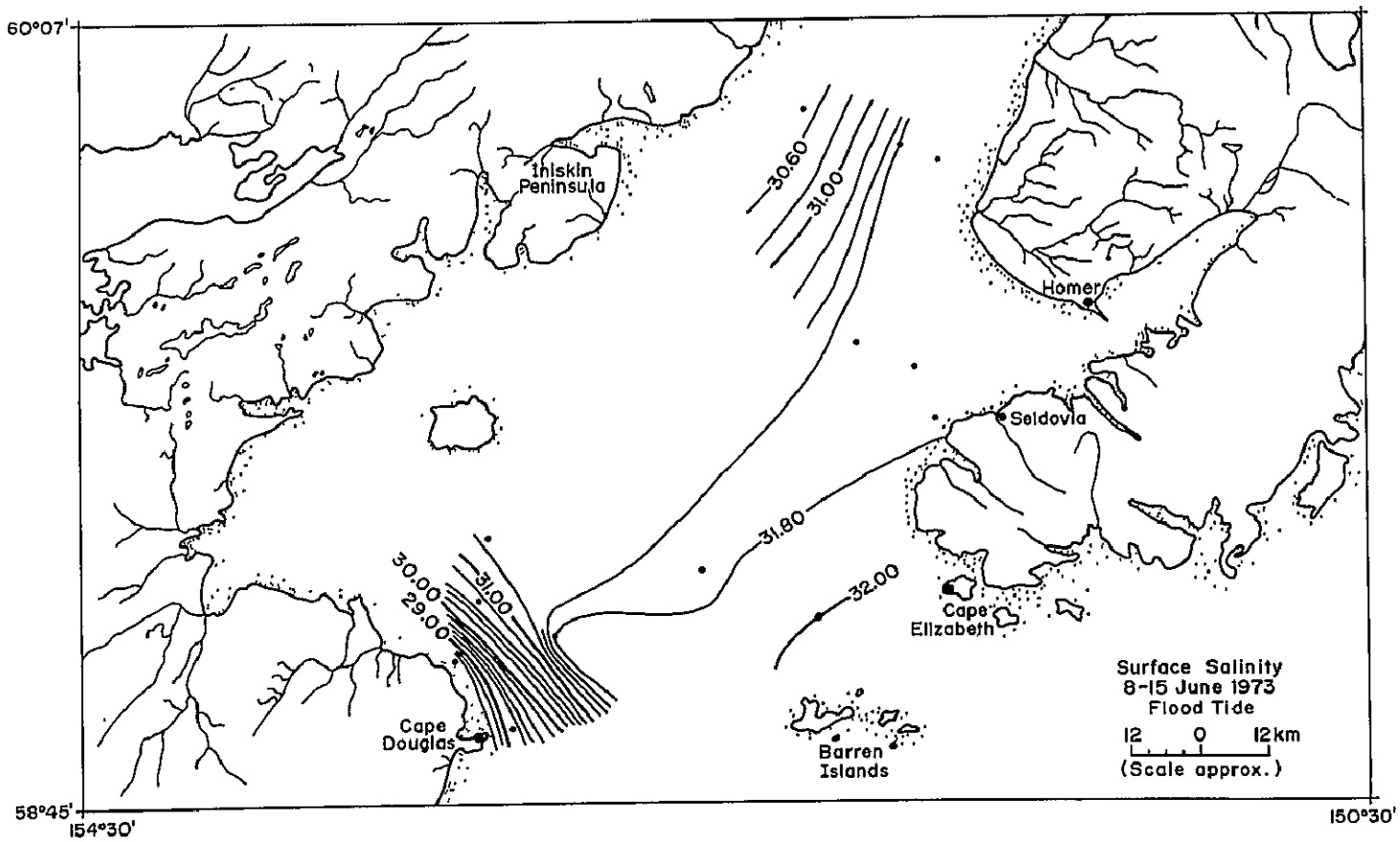

Figure 47. Surface salinity distribution, 8-15 June 1973. a. Flood tide.

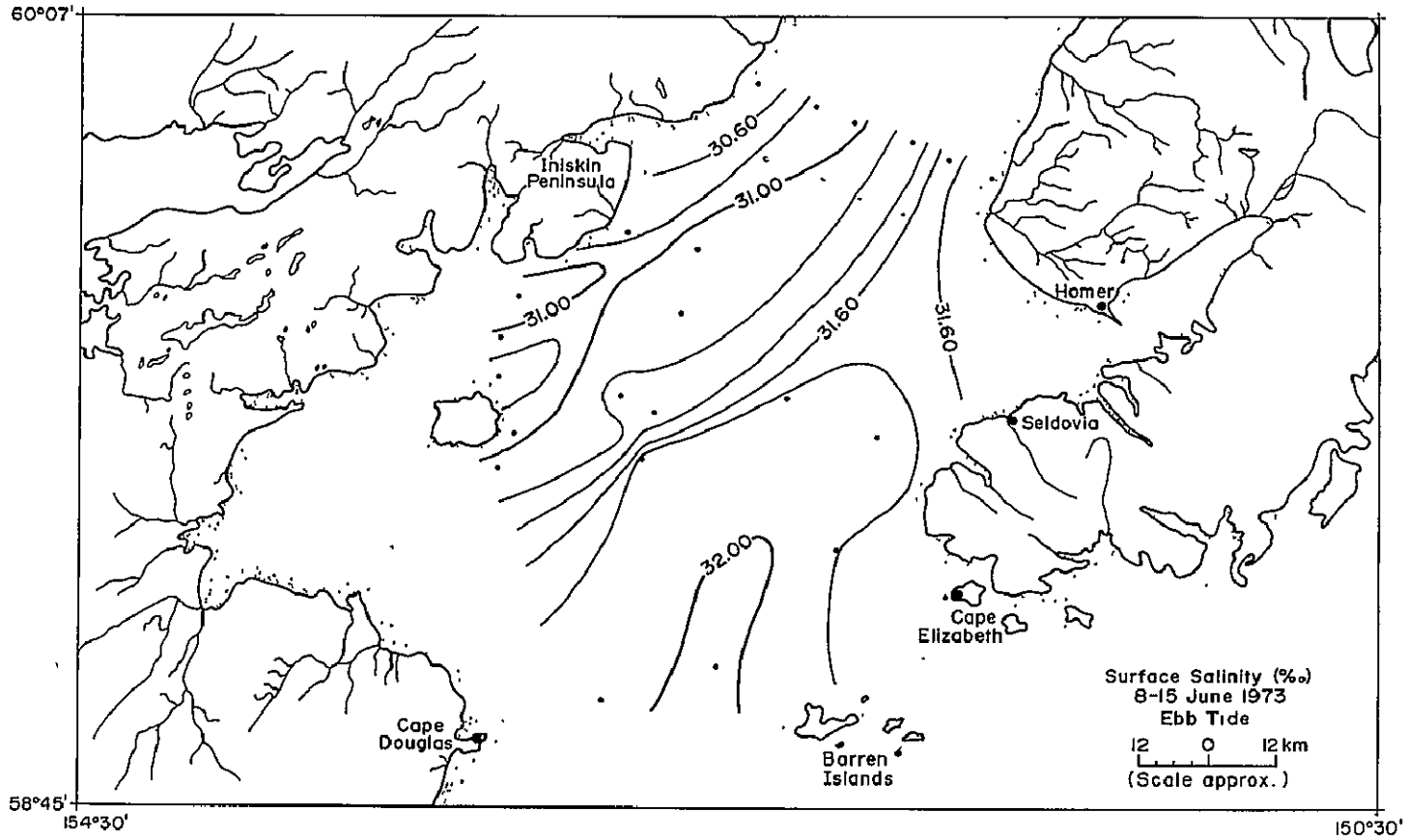

Figure 47 (cont'd). b. Ebb tide.

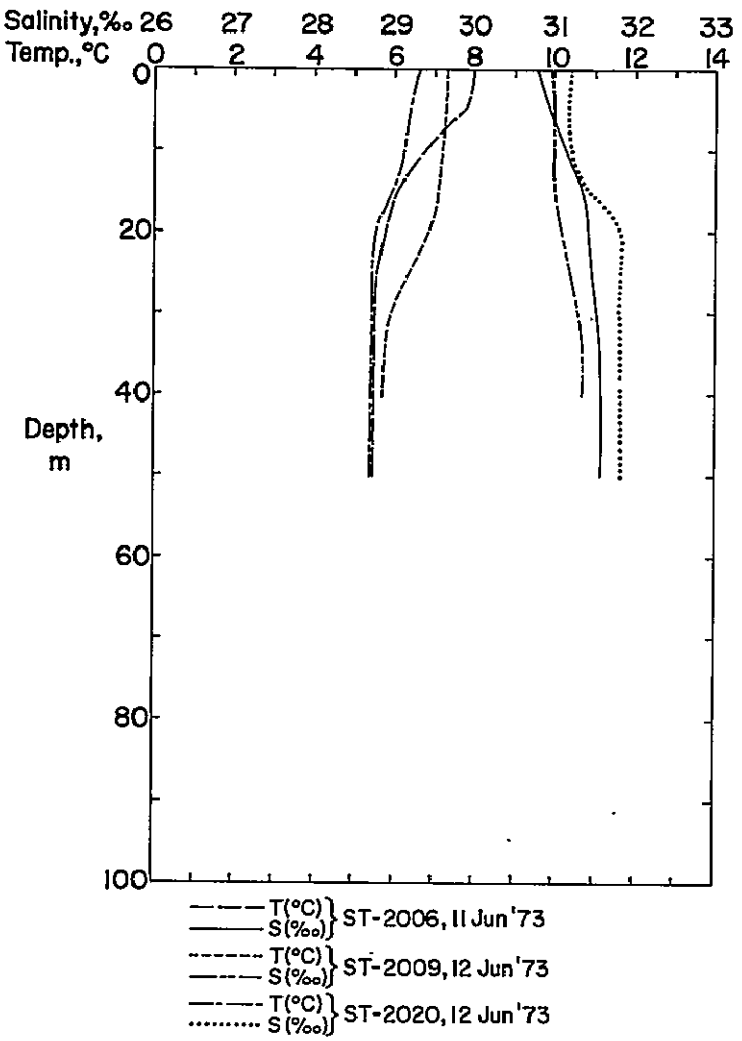

Figure 48. Temperature-salinity profiles, June 1973.

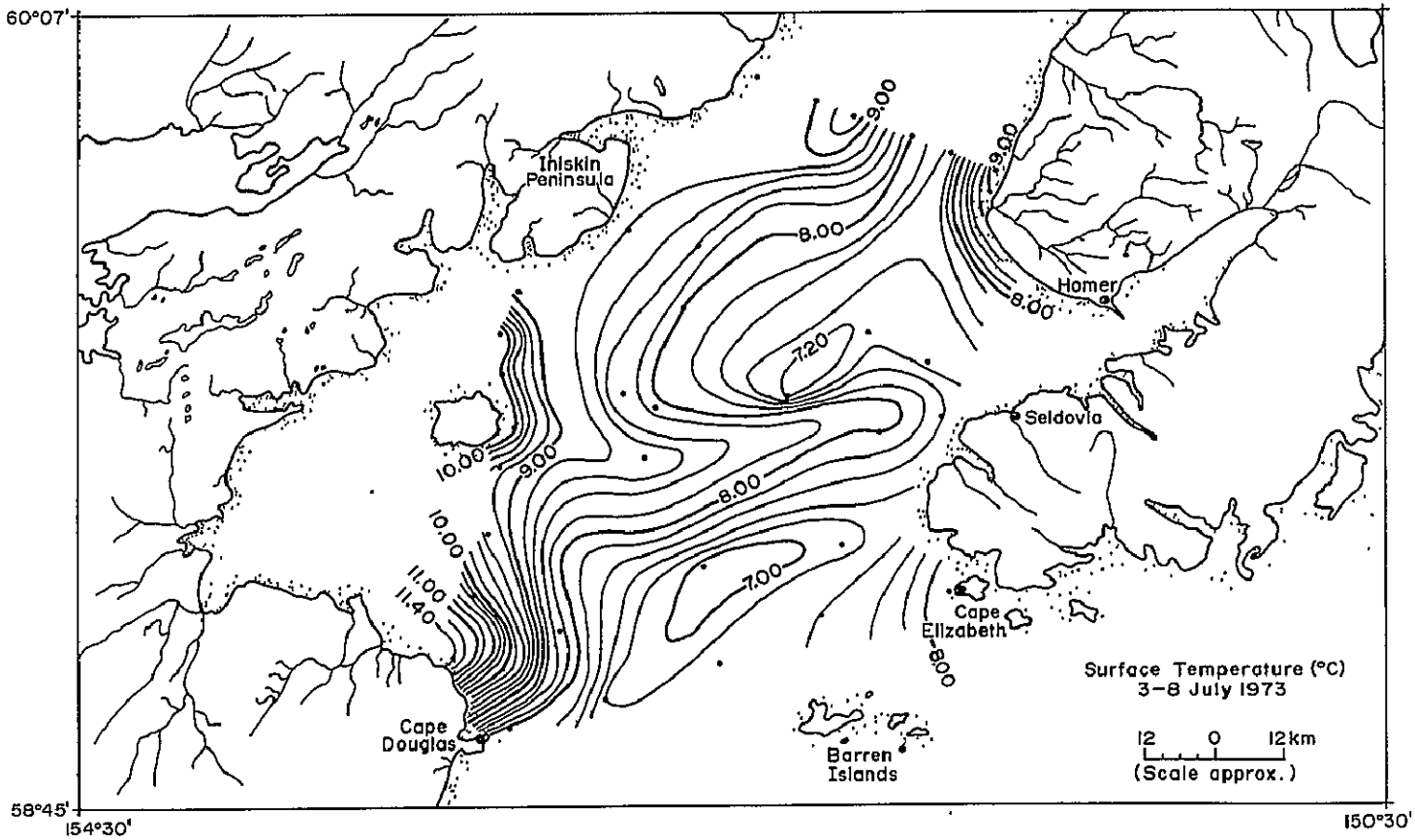

Figure 49. Surface temperature distribution, 3-8 July 1973.

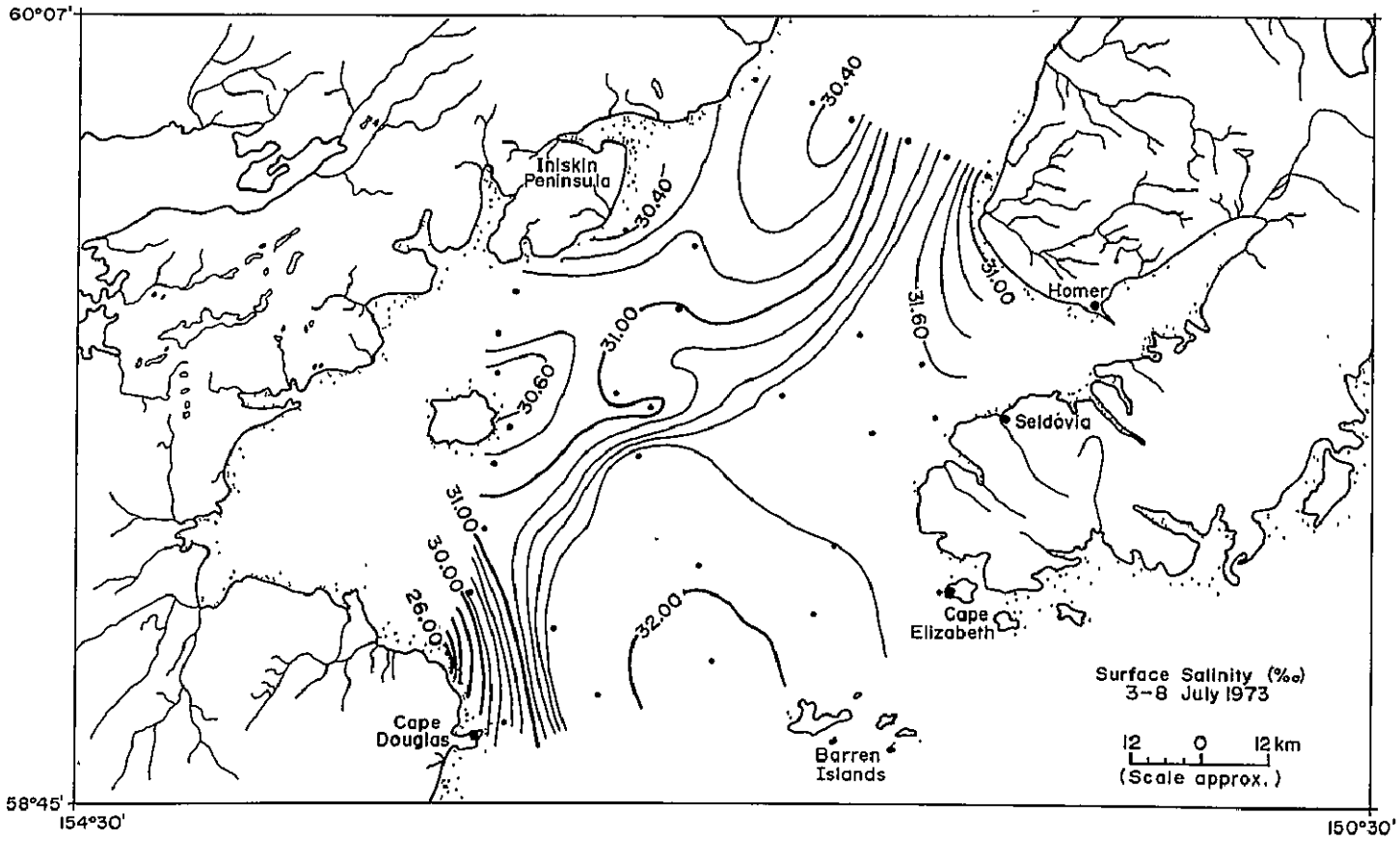

Figure 50. Surface salinity distribution, 3-8 July 1973.

temperatures of the inlet water and the water in Kamishak Bay have increased since June while the salinity has decreased, a result of increased fresh water runoff. Maximum runoff occurs in July - August (Fig. 23) and dilution of the surface water is near maximum.

Temperature profiles in July (Fig. 51) for ST-4,-5 and -25 indicate nearly complete mixing; temperatures change only 2°C from surface to near bottom and no distinct thermocline exists. Salinity variation is minor at ST-4 and -5, while at ST-25 salinity increases from 31°/oo at the surface to 32.2°/oo at 30 m depth. Below ≈30 m the water at ST-4, -5 and -25 is comparable. Strong stratification occurs at station ST-2001, north of Cape Douglas; turbulence is low in this area, resulting in a distinct thermocline and halocline from 0-20 m. Stratification is weak or absent at the other locations and water characteristics below 30-40 m are similar; water temperature at S-3 is generally higher throughout the water column than at other locations. Bottom water is slightly warmer and more saline in July than in June.

Surface temperature of the oceanic water and the inlet water north of Anchor Point increased approximately 2°C from 3-8 July to 7-9 August (Fig. 52). Surface salinities (Fig. 53) are similar to those in July. Salinity stratification is strong at station SP-2034 near Homer Spit (Fig. 54); less saline surface water (28.8°/oo) extends to 10 m where a strong halocline occurs from 10 m to 30 m (28.8°/oo to 31.5°/oo); temperature at this site changes from 10.5 to 9.2°C in this interval. Knull and Williamson (1969) report that stratification in Kachemak Bay is maximum in July when runoff is high. Below 30 m temperature and salinity remain virtually unchanged. This station is located near shore at China Poot Bay and surface water may be dominated by meltwater from the glaciers on Kenai Peninsula. ERTS image 1426-20444 (Fig. 20) shows highly turbid water at this location.

Time series data for station S-1 are also presented in Figure 54. Data are acquired every half hour through half a tidal cycle (generally 13 hours) at time series stations. The profiles show changes in water temperatures and salinities from the surface to near bottom at S-1 from late flood through early ebb on 30 August. The S-1a data were taken at 1328, 2:14 hrs. min. before high water and the S-1b at 1632, 0:50 hrs. min., S-1c, at 1731, 2:29 hrs. min., and S-1d, at 1830, 3:28 hrs. min. after high water (Table 7). Minor temperature and salinity changes

Table 7. Forecast tides at Seldovia, Alaska, 30 August 1973 (from U. S. Department of Commerce 1972).

Time (hrs. min.)	Height (m)
0325	6.3
0928	-0.6
1542	6.4
2154	-0.5

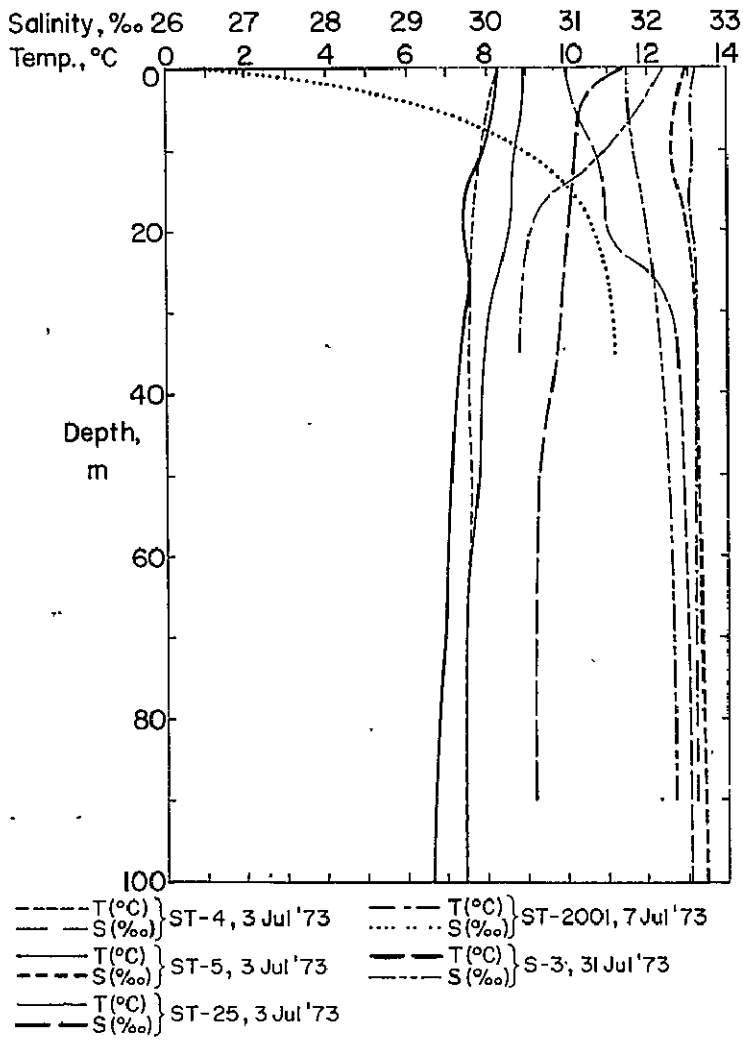

Figure 51. Temperature-salinity profiles, July 1973.

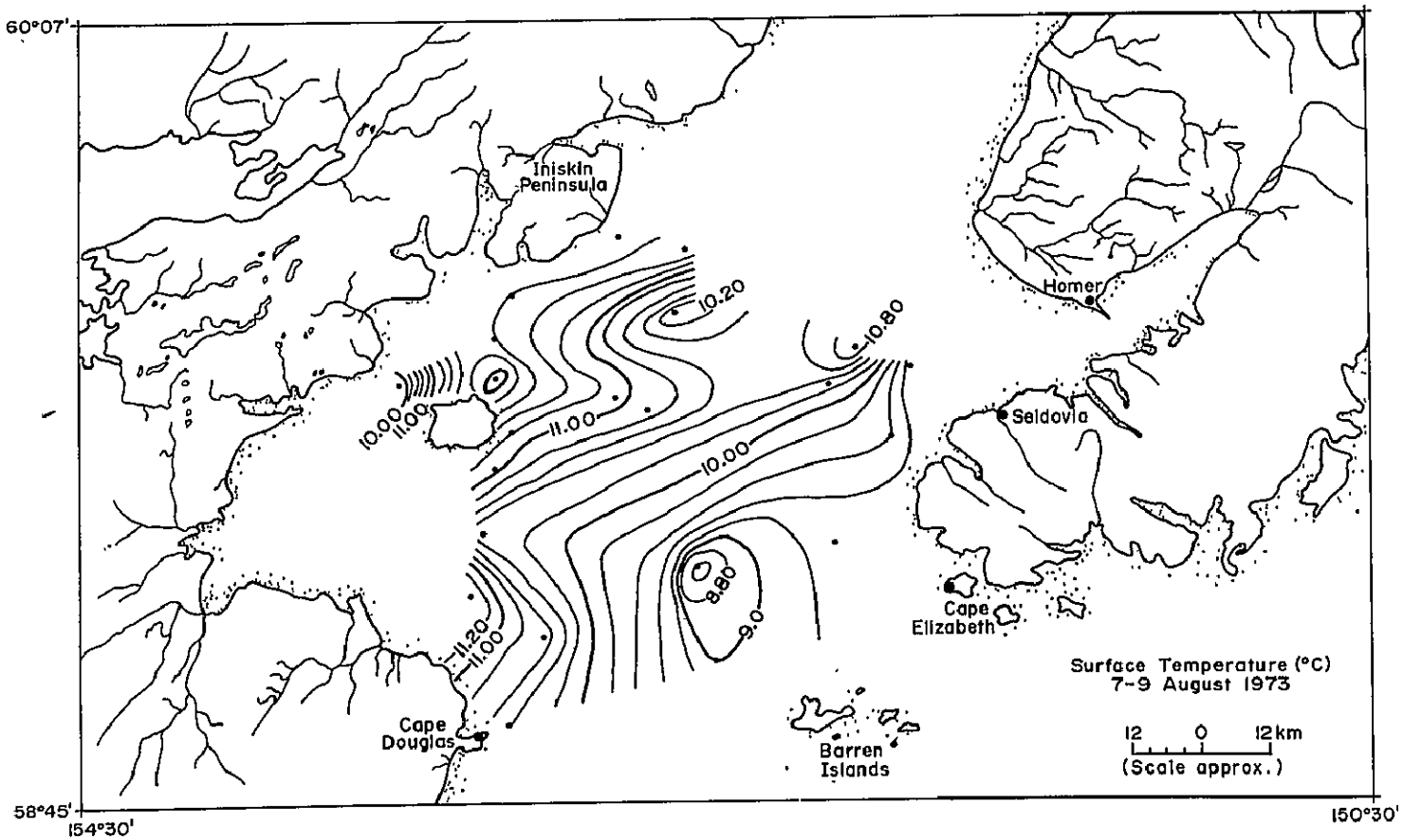

Figure 52. Surface temperature distribution, 7-9 August 1973.

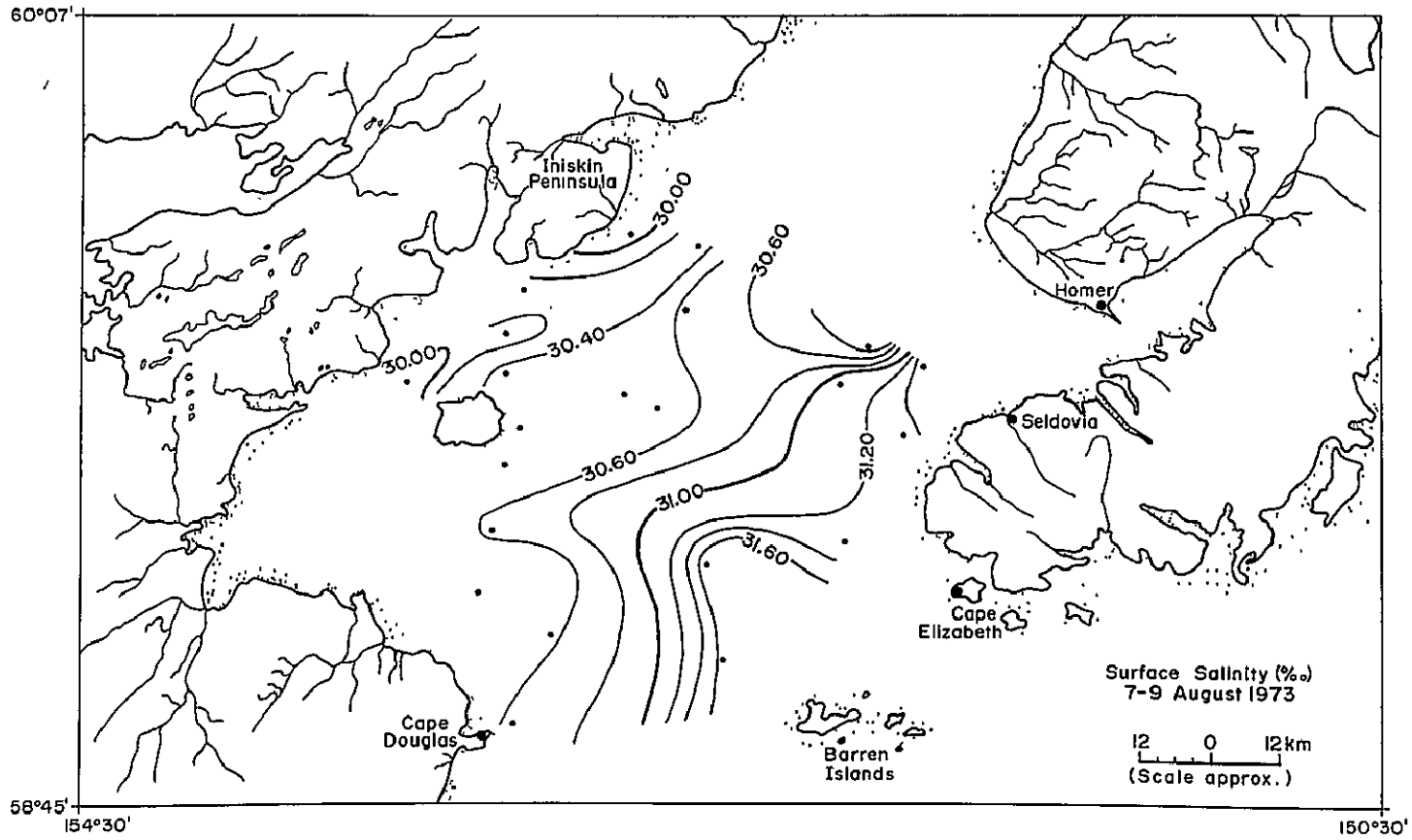

Figure 53. Surface salinity distribution, 7-9 August 1973.

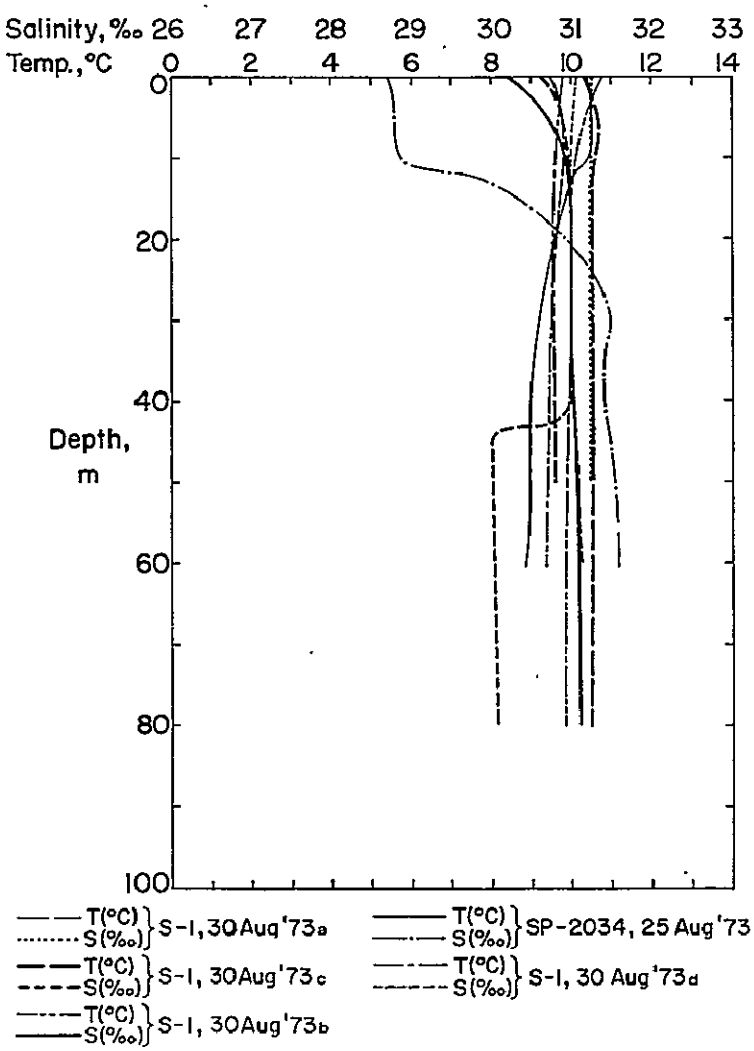

Figure 54. Temperature-salinity profiles, August 1973.

occur from the surface to 10 m; between 10 and 30 m the data are similar; below 30 m the variability increases with depth. Salinity at S-1c decreased rapidly from 31°/oo to 30°/oo at 42 m. This sudden decrease may have been caused by an instrument problem or by the rapid movement of less saline water past the station. This station is near the shear zone and considerable variation could occur throughout the water column along this frontal zone. This rapid change was not detected at 1830.

Surface temperatures from 5-9 September (Fig. 55) vary considerably from those acquired in August. Temperatures are 2°C warmer near the east side of the inlet mouth and ≈2°C cooler on the west. Kachemak Bay temperatures are ≈3°C warmer than in May (Fig. 41) and ≈2°C colder than the inflowing oceanic water (Fig. 55). Fresh water runoff during the summer has diluted and reduced the salinity of the water throughout the area, especially in Kachemak Bay with surface salinity 5°/oo lower in September (Fig. 56) than May 1973.

Water profiles in September are more variable than previously seen (Fig. 57). Water temperatures and salinities are variable from the surface to ≈40 m. The thermocline and halocline extend to this depth. Below 40 m variations continue to the bottom. Salinity at SP-17, south of Homer Spit, increases from 28.2°/oo at the surface to 31°/oo at 40 m; from 40 to 80 m it increases to 31.4°/oo. Temperature rapidly increases from 8.6°C at surface to 10.4°C at 5 m; from 5 to 80 m it decreases to 9.1°C. These halocline and thermocline characteristics are not present farther west. The temperature profile at ST-4 shows no thermocline and decreases gradually from 10°C at the surface to 7.5°C near the bottom; salinity decreases slightly from 0-5 m, then increases steadily to 31.8°/oo. Temperatures at ST-25 increase from 9.4°C at the surface to 10.4°C at 5 m, are relatively constant from 5 to 35 m, and decrease from 10°C to 8°C from 35 to 100 m.

T-S diagrams are especially useful in characterizing water at depth and in determining water types based on features and anomalies of temperature-salinity. Temperatures and salinities are plotted in reference to water density expressed as σ_T; the diagram indicates the stability and stratification of water by graphically illustrating density characteristics through the column (Sverdrup et al. 1942; von Arx 1962).

Water characteristics at location ST-2008 during early flood on 26 May (Fig. 58) produce a stable water column with very minor stratification. Salinity and temperature changes are minor, 31.1 - 31.6°/oo and 5.9 - 4.5°C, respectively. Strong stratification occurs at ST-2006 during late flood on 25 May. Surface water is colder, more saline and therefore more dense than the water immediately below. This reverse stratification may result from the intrusion of oceanic water during flood tide. The water type at ST-24 is generally less dense than at

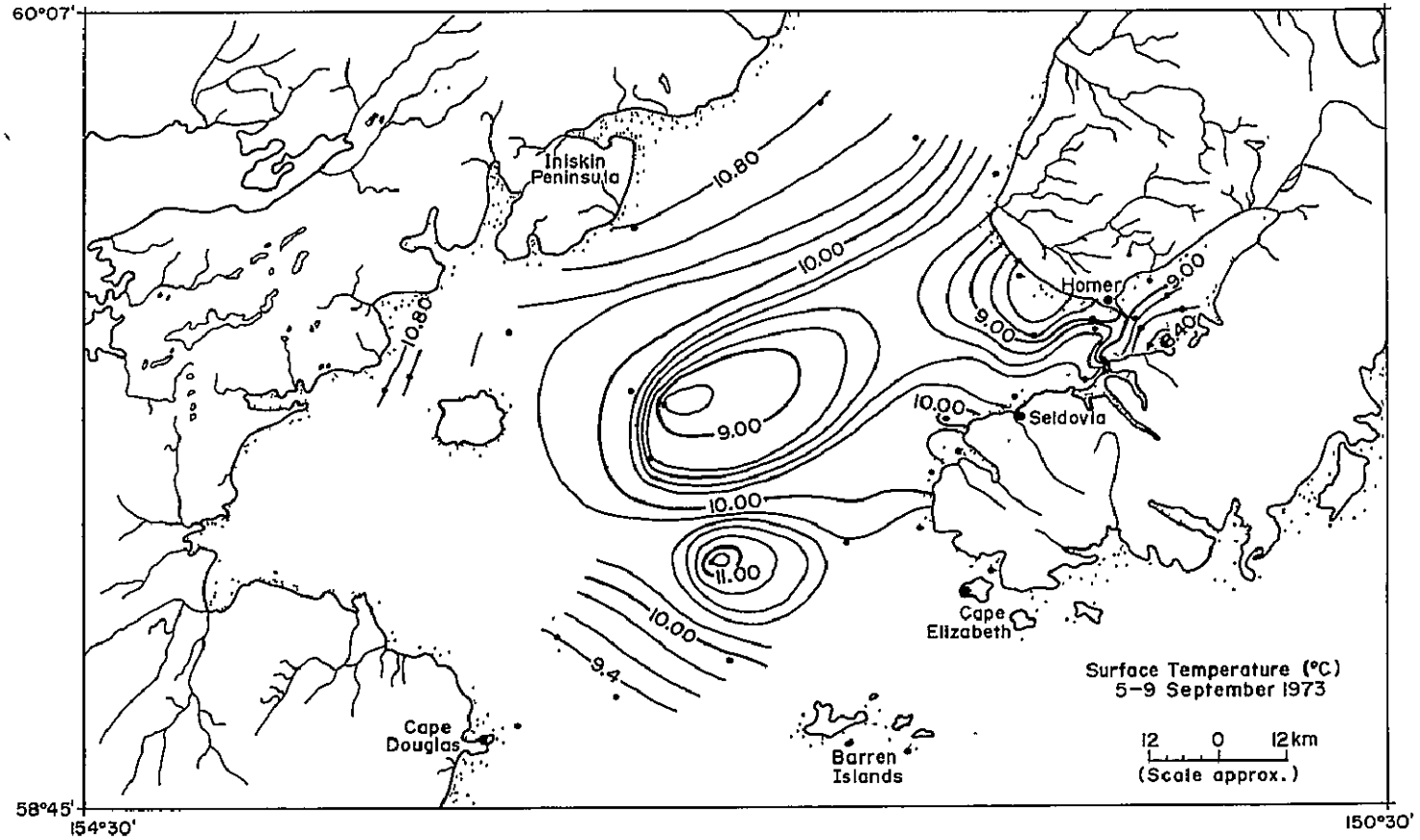

Figure 55. Surface temperature distribution, 5-9 September 1973.

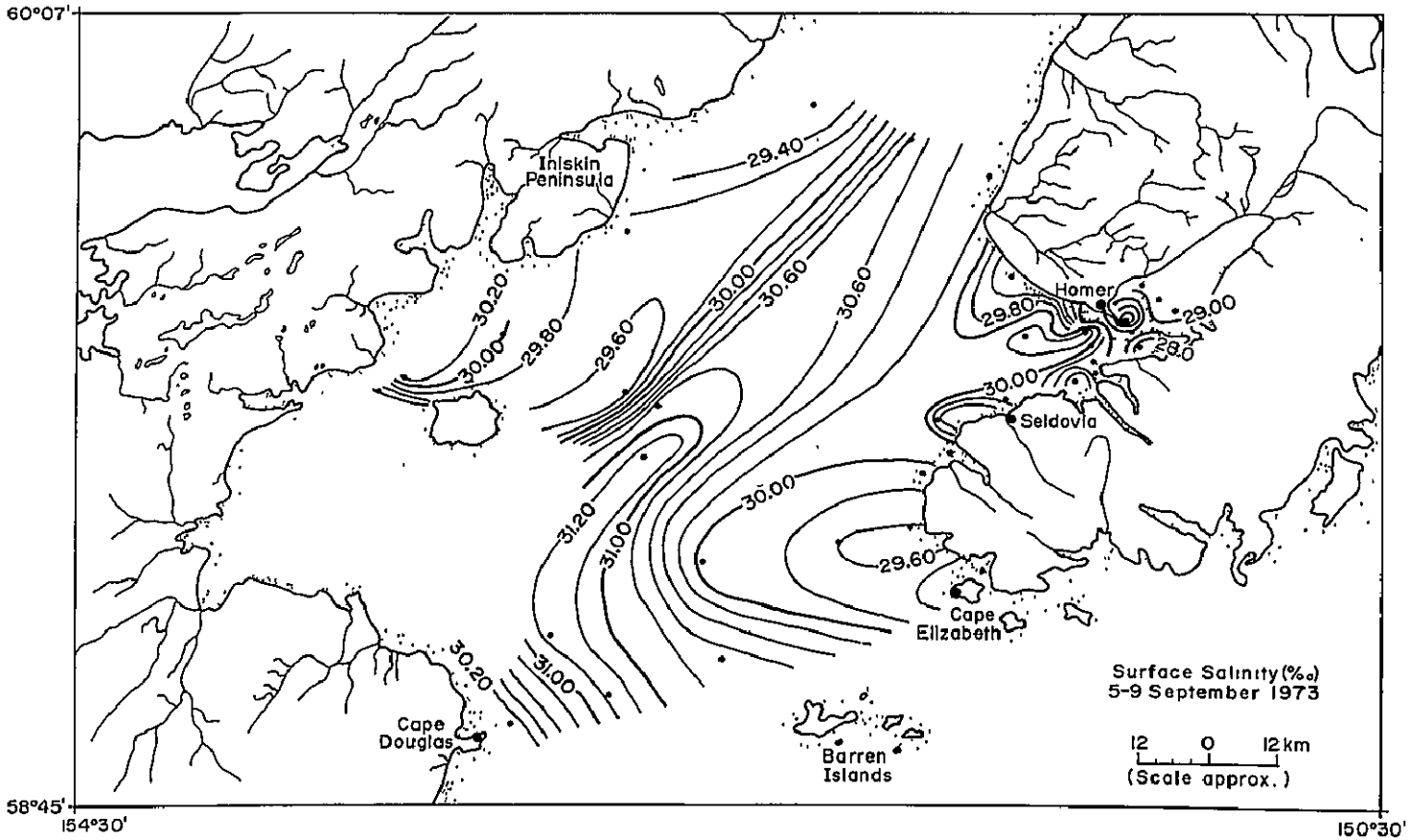

Figure 56. Surface salinity distribution, 5-9 September 1973.

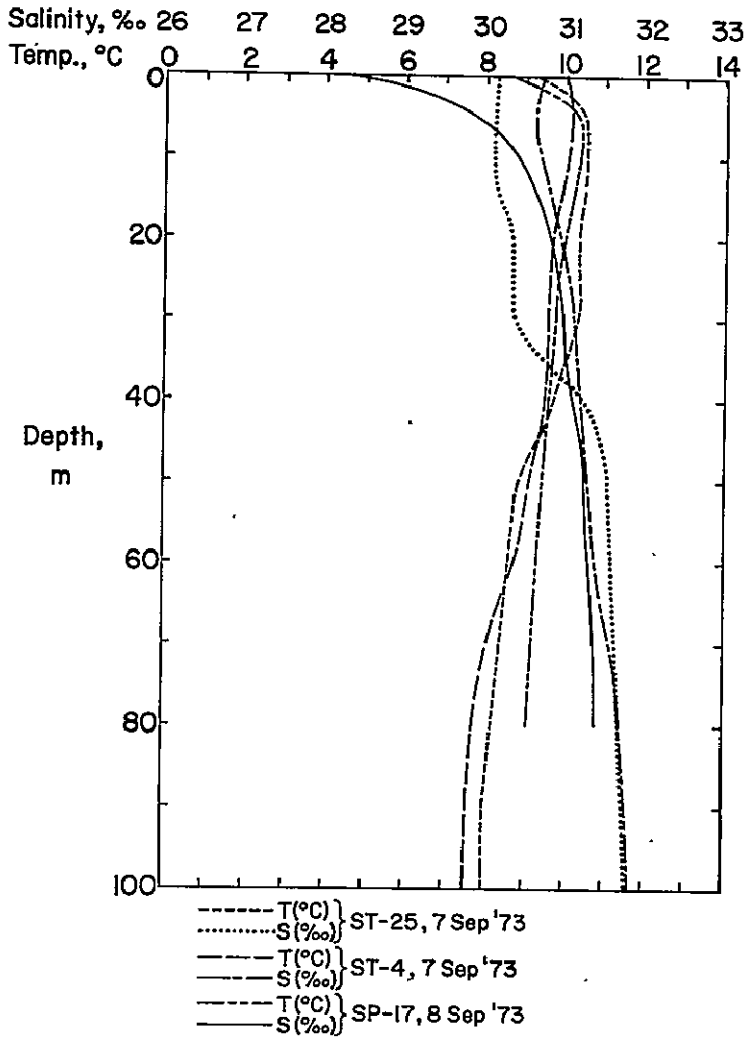

Figure 57. Temperature-salinity profiles, September 1973.

Figure 58. T-S diagrams, stations ST-2006, -2008, -24.

ST-2008 during flood; temperature is the controlling variable. Temperature at ST-2008 changes from 7.8°C at surface to 5.5°C at depth while the salinity range is only .3°/oo; density is comparable to the deeper water at ST-2006.

Water types at ST-2002 show considerable variation in stability from 3 to 31 July (Fig. 59). On 5 July, salinities are higher throughout the water column and temperatures lower. Salinity stratification occurs at several depths while temperature stratification is less pronounced. Rapid salinity changes are not as prominent on 31 July and the water is generally less dense.

Water characteristics at ST-25 on 3 July (Fig. 59) produce a deep salinity stratification and generally more dense water than present on 7 September (Fig. 60) when surface stratification is pronounced. Station SP-17 (Fig. 60) shows a slight change in temperature from surface to depth but a large salinity variation, 28.2 to 31.4°/oo. Temperature-salinity values at ST-4 (Fig. 60) are virtually the same as at ST-25; the water types are similar. The variability of the water characteristics, as shown by these T-S diagrams, illustrates the rapid changes that occur throughout the water column during different tidal stages and seasons.

Sea Ice

Sea ice is a navigational hazard particularly in the upper inlet north of the forelands for four to five months of the year (Marine Advisers 1964; Alaska District, Corps of Engineers 1948; Rosenberg et al. 1967). The movement and strength of the ice are important aspects of the inlet environment to be considered, especially in planning offshore construction. The ice is fine- to medium-grained (1-4 mm) with a salinity of .4-.6% and a ring tensile strength of 10-20 kg/cm^2. It exists as large floes which are commonly greater than 320 meters across with individual blocks generally less than 1 meter thick. Pressure ridges up to 6 meters in depth occasionally form on the floe peripheries due to frequent collisions with other floes (Blenkarn 1970). Large ice floes become scattered and move primarily up and down the upper inlet with the 6-8 knot tidal currents; some move as far south as Anchor Point on the east side (Wagner et al. 1969); large floes are commonly carried by winds and tides along the west side as far south as Kamishak Bay and beyond to Cape Douglas. Brash and frazil ice are common between the rounded floes. Previous reports (U.S. Department of Commerce 1964) suggest that ice occasionally closes Iliamna Bay for brief periods; however, repetitive ERTS-1 and N.O.A.A. -2 and -3 imagery indicate that large floes persist in Kamishak Bay for long periods and that many of the small embayments bordering the bay appear ice covered for a major portion of the winter.

Figure 59. T-S diagrams, stations ST-25 and -2002.

Figure 60. T-S diagrams, stations ST-25, -4 and SP-17.

Most of the ice forms by the freezing of river water as it flows over the tidal flats. Smaller amounts of ice are formed from sea water left on the flats during low tide (Sharma and Burrell 1970). Much of the ice on the flats is picked up during flood tide, moved out into the inlet and incorporated into the floe; the remainder is left on the flats and repeatedly refreezes to form sheets or stacks of ice (stanukhi) some as thick as 12 m. Some of these thick sheets are eventually transported to the floe while some remain on the flats throughout the winter.

ERTS-1 and NOAA-2 and -3 imagery are useful in observing the formation and ablation of inlet ice and in defining winter surface circulation patterns as inferred from sea ice movement. Although ERTS-1 imagery has better ground resolution, its utility is somewhat reduced by the 14 day gap between orbital cycles and by a two month period when data are not obtained due to low sun angles (<8°). NOAA-2 and -3 IR imagery supplements the ERTS data because of increased capability for haze penetration, the capability to show thermal differences and more frequent acquisition of data.

Cloud free ERTS imagery acquired on 29 January 1974 (Fig. 61) shows the distribution (1) of ice floes and frazil ice along the western coast from Chenik Head in Kamishak Bay north to Redoubt Bay. Westerly winds are moving the ice southeast (2) out of Kamishak Bay past Augustine Island (4) while winds and tidal currents produce complex patterns along the inlet coast farther north. These complex patterns may be influenced by tide rips which form 2 to 4 miles north of Chinitna Point with a strong westerly wind (U.S. Department of Commerce 1964). Lake Iliamna (3) is ice covered and the fractures are very distinct.

Although 80% cloud covered, ERTS image 1571-20472, acquired on 14 February 1974, shows ice floes concentrated in Redoubt Bay west of Kalgin Island, along the west side between Harriet Point and Tuxedni Bay, southeast of Chisik Island, in the eastern inlet south of the East Foreland to an area between Kenai and Kasilof and in the northern inlet. ERTS images 1572-20530 and 1572-20533, acquired 15 February 1974, are 50% cloud covered but show the ice distribution along much of the western shoreline between the West Foreland and Cape Douglas as observed on the previous day. Movement of the ice in this 24 hour period was strongly influenced by dominant westerly to southwesterly winds. Ice floes are still concentrated in Redoubt Bay but much of that southeast of Chisik Island has been aligned with the wind in long "stringers" and has been moved northeasterly away from the west coast. Similar elongated patterns have formed in the ice near Cape Douglas.

NOAA-2 and -3 imagery acquired on 18 February 1973 (Fig. 62), 12 March (Fig. 63) and 26 March (Fig. 64) 1974 show the distribution of sea ice throughout the inlet. The sea ice patterns are similar to the

Figure 61. Distribution of inlet ice along the southwest shore. MSS band 5 image 1555-20591, acquired 29 January 1974.

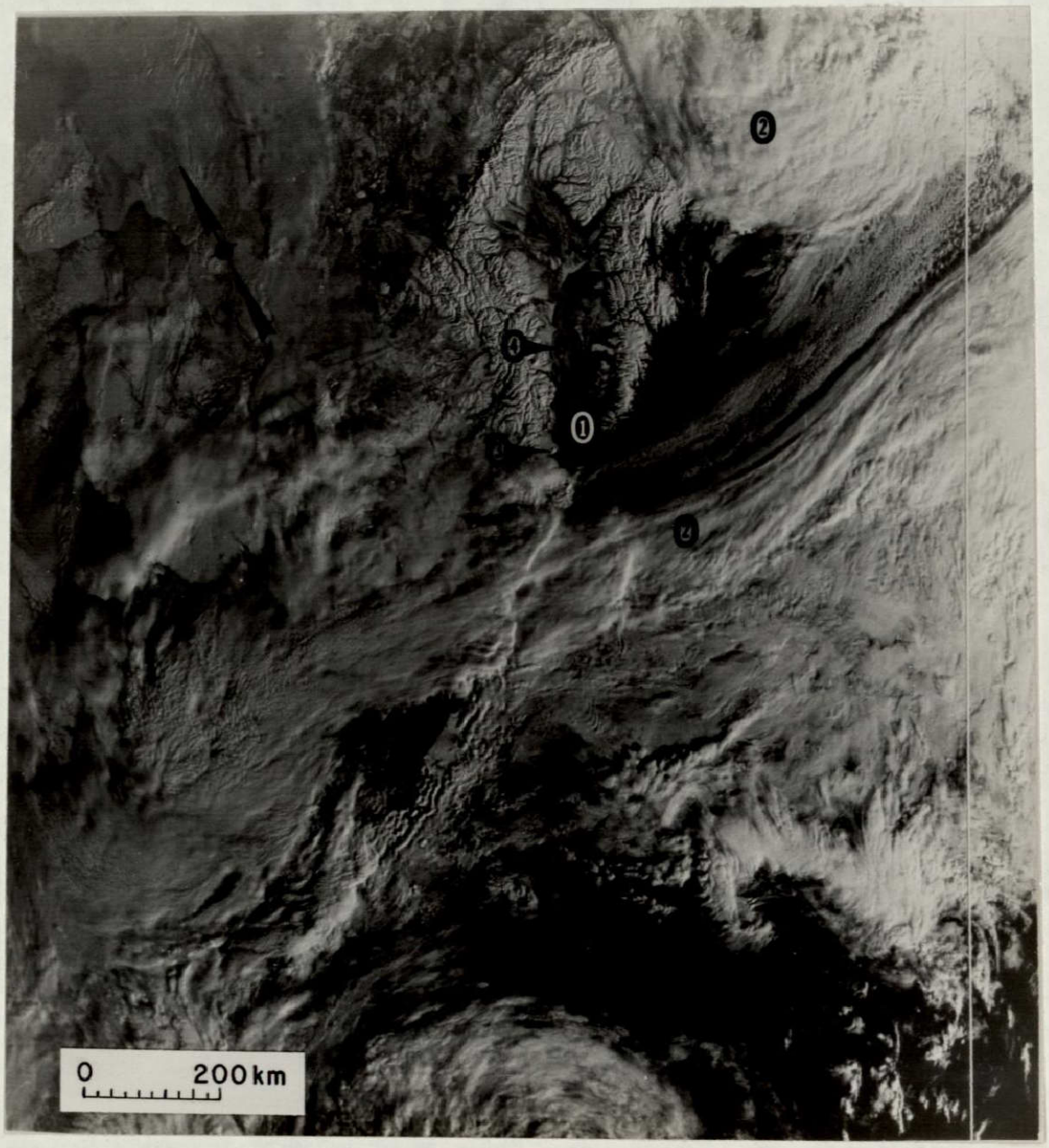

Figure 62. Sea ice in Cook Inlet on 18 February 1973, NOAA-2 VHRR visible image.

Figure 63. Sea ice in Cook Inlet on 12 March 1974, NOAA-3 VHRR visible image.

Figure 64. Sea ice in Cook Inlet on 26 March 1974, NOAA-3 VHRR visible image.

patterns of suspended sediment as observed on ERTS imagery. The highest concentrations of sea ice occur in the northern inlet and in the western portion of the southern inlet. The eastern portion south of the foreland is generally ice free because this area is characterized by the intrusion of sea water which is warmer than inlet water during winter months. There appears to be more ice present on 18 February 1973 than on 12 March 1974. The area near the inlet mouth (1) is ice free but ice is concentrated around Kalgin Island (4) and in Kamishak Bay around Augustine Island (3). Clouds (2) obscure portions of Kamishak Bay on 18 February 1973. There is less ice in Kamishak Bay on 12 March 1974 (Fig. 63) than on 29 January 1974 (Fig. 61). Notice the changes in distribution between 12 March and 26 March (Fig. 64) 1974. Less ice is present in the inlet but more is concentrated west of Augustine Island. Also the east side of the ice-cover on Tustumena Lake (5) appears to have melted by 26 March 1974. NOAA-2 imagery from 4 April 1973 and 6 April 1974 show that ice has ablated and the inlet is ice-free while ice and snow remain on land near the coast. This preliminary analysis of sea ice distribution and movement demonstrates that with certain limitations, satellite imagery can provide data required to aid navigation and guide construction of offshore facilities. An important advantage of satellite imagery is the synoptic view while the major limitation is the difficulty of obtaining sequential cloud free imagery coincident with the occurrence of significant ice movement.

The presence of this mobile ice cover is useful in making comparisons between analogous summer and winter circulation patterns. The highest concentrations of sea ice generally occur in the western portion of the lower inlet while the eastern portion remains ice free. Predominantly north winds in the winter also moves the ice to the west and southwest side of the inlet. Although large ice floes are a navigation hazard as they move up and down the inlet between the forelands during flood and ebb tide, extensive damage to shipping has generally been avoided although numerous reports of shipping difficulties have been made (Alaska District 1973).

Tidal Flushing Characteristics

The pollutant flushing time of an estuary is the time required for existing fresh water in an estuary to be replaced. The time depends basically on river discharge and salt water replacement due to mixing entrainment. Pollutant concentrations are also reduced by dispersion/diffusion mechanisms which move pollutants to other water masses in a high velocity regime and by fresh water input which moves entire water masses to sea by supplying new water (advective flow) (Murphy et al. 1972). Various methods are useful in determining the flushing rate but their utility is limited by the available data.

Rosenberg et al. (1967) calculated the concentration of an effluent introduced near Nikiski and determined its distribution considering removal by river flow and salt water replacement. Fresh water, as it migrates seaward from an estuary, entrains salt water from below; at steady state, seawater enters the inlet at the rate it is being entrained. The amount of entrained water is calculated knowing the mean salinity of the estuary. This value for Cook Inlet is 24.15°/oo as determined from data acquired in June 1967. The flow of entrained water is calculated as follows:

$$V_i = \frac{S_a(R)}{S_o - S_a} \qquad (1)$$

where V_i = entrained flow (ft^3/sec)

S_a = avg. salinity of inlet (°/oo) = 24.15°/oo

S_o = salinity of source waters at mouth (°/oo) = 32.00°/oo

R = river flow at time of observation (ft^3/sec) = mean monthly, 10.2×10^4 ft^3/sec

Assuming this to be the average per year, total water leaving the inlet per year is 1.13×10^{13} ft^3. Conclusions from this investigation indicate that soluble wastes introduced south of the East Forelands would be mixed throughout the inlet or removed by turbulent mixing, tidal changes, river flow, salt water replacement and waste decay.

Kinney et al. (1970a) investigated oil pollution in Cook Inlet and reported the flow of entrained salt water for June using equation 1 to be $V_i = 1.32 \times 10^6$ ft^3/sec when S_o = 32.0°/oo, S_a = 29.7°/oo and $R = 1.02 \times 10^5$ ft^3/sec. This is equivalent to 4.40×10^{13} ft^3/yr. Since winter river flow is significantly lower, the yearly flushing flow would be reduced if salinity remained constant. However, Bowden (1967) reports that flushing times are affected more by turbulence and mixing than seasonal river flow variations; therefore, Cook Inlet would maintain a relatively high V_i. With these values, Kinney et al. (1970a) conclude that tidal and river driven flushing reduces the hydrocarbon pollutants in Cook Inlet by 90% in about 10 months.

Since data for the entire inlet are sparse and coastal development is and will be concentrated along Knik Arm and Kachemak Bay, respectively, the flushing rates for these areas were determined by the simplest, but possibly the least precise, method, the tidal prism method (Ketchum 1950, Lauf 1967 and Dyer 1973). Flushing time in tidal cycles was calculated as follows:

$$T = \frac{V + P}{P} \qquad (2)$$

where V is the low tide volume and P the intertidal volume (tidal prism). Flood tide water is assumed to become totally mixed with estuary water; sea/river water introduced during flood equals the tidal prism. The same volume of water is removed on ebb and the amount of fresh water equals the increment of river flow. Generally this method yields faster rates than other methods because in reality mixing is incomplete. Fresher water near the inlet head does not reach the mouth during ebb and some of the water that escapes during ebb returns at flood.

The modified tidal prism method (Ketchum 1951) divides an estuary into segments determined by the average tidal excursion of a water particle on flood tide. This segmentation method requires that the innermost segment be defined as that which has an intertidal volume equal to the river discharge. River discharge data for Eagle, Chester, Matanuska, Cottonwood and Knik Rivers bordering Knik Arm were available from Wagner et al. (1969). Discharge data were available only for the Bradley River on the northeast coast of Kachemak Bay (U.S. Geological Survey 1971). To approximate the total river input for this bay (Fig. 65), the meltwater discharge from the Grewingk (6), Portlock (7) and Dixon (8) Glaciers was considered similar to that of Kachemak Glacier (9), the source of Bradley River (10); the Fox River (11) discharge was approximated as twice that of the Bradley River since two main tributaries of the Fox head at Dinglestadt (12) and Chernof (13) Glaciers.

The innermost segment is that with an intertidal volume (P_o) equal to the river flow (R) (Dyer 1973)

$$P_o = R \qquad (3)$$

V_o = low tide volume of segment

The limit of the next segment is placed so

$$V_1 = V_o + P_o = V_o + R$$

The low tide volume in each segment equals the total tidal prism with the next landward segment plus the low tide volume in segment 0, or

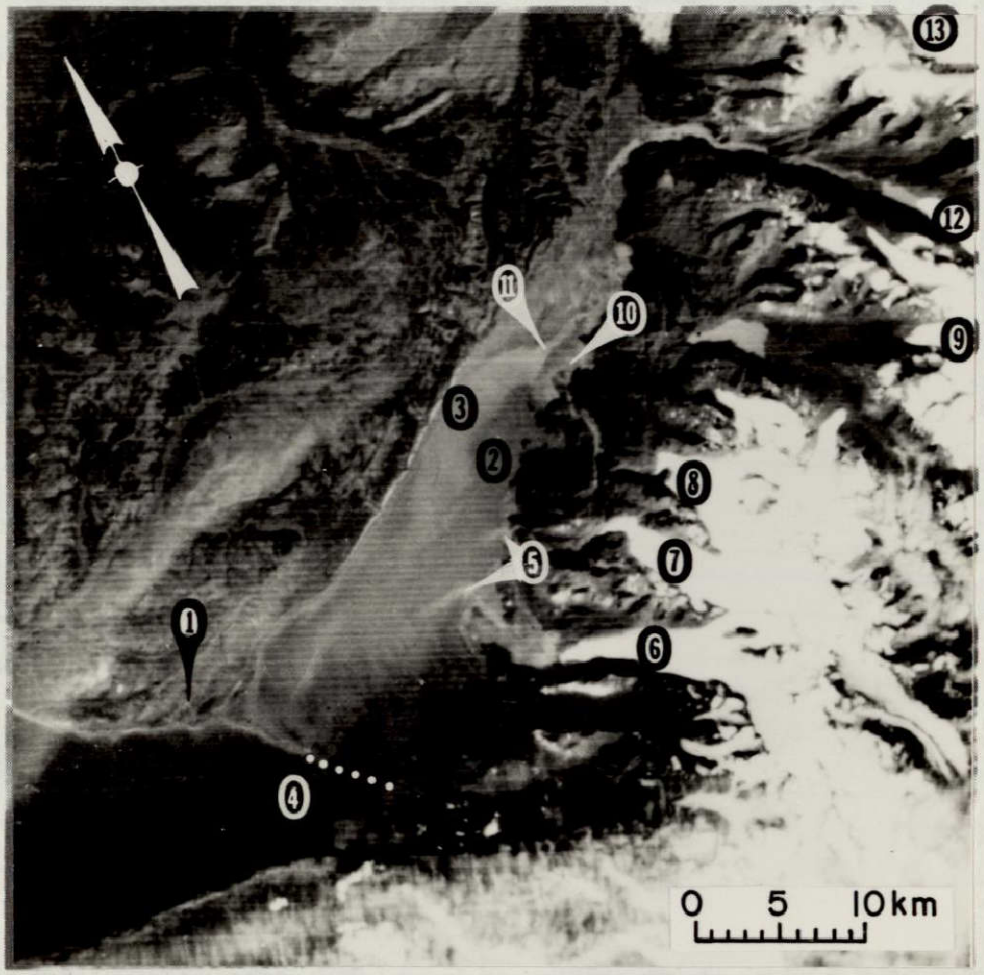

Figure 65. Kachemak Bay. 2x enlargement from ERTS MSS band 4 image 1066-20452, acquired 27 September 1972 (scale approximate).

$$V_n = V_o + R + \Sigma_1^{n-1} P \qquad (4)$$

Each segment at high tide contains the volume of water in the next seaward segment at low tide. With complete mixing at high tide, the proportion of water removed on ebb is the ratio between local intertidal volume and high tide volume and an exchange ratio can be defined for any segment "n" as

$$r_n = P_n/(P_n + V_n) \qquad (5)$$

The flushing time in tidal cycles will be $1/r_n$. In any segment the amount of river water removed during ebb equals $r_n(1-r_n)^{m-1} R$ where "m" is age in tidal cycles while the amount remaining equals

$$(1-r_n)^m R \qquad (6)$$

Total volume of river water, Q_n, accumulated in segment "n" equals

$$Q_n = R\,(1+(1-r_n) + (1-r_n)^2 \ldots (1-r_n)^m) \qquad (7)$$

The sum is

$$\frac{R}{r_n}\,(1-(1-r_n)^{m+1}) \qquad (8)$$

when m is large, $(1-r_n)^{m+1}$ approaches 0 when $r_n<1$, so that

$$Q_n = R/r_n \qquad (9)$$

Total flushing time for all estuary segments equals

$$\Sigma\ {}^{1}/_{r_n} \qquad (10)$$

The seaward limit of Knik Arm was defined by a north-south line from Point Woronzof (Fig. 66), that of Kachemak Bay from Gull Island to Coal Point (Fig. 65). Total areas of water for high tide, mean lower low tide and the 3 or 10 fathom depths in each bay were determined with a planimeter from National Ocean Survey navigation charts 8553 and 8554. Approximate volumes were calculated for lower low, intertidal and higher high water using tide tables (U.S. Department of Commerce 1972). The lower low water volume for Knik Arm was 4.5×10^8 m^3, the intertidal 5.7×10^8 m^3, and the higher high water 1.02×10^9 m^3. The river flow into Knik Arm in March is 1031 cfs and using the tidal prism method the flushing time was determined to be 205.3 hours, approximately 8.5 days. When freshwater runoff is highest in July, the flushing time decreases to 13.1 hours; the annual average is 47.9 hours. Using the modified tidal prism method, the resulting flushing times were higher, but compared favorably to that determined for March by the tidal prism method, 205.6 hours. The July value was calculated to be 13.2 hours; the annual average was 48.2 hours.

The lower low water volume for inner Kachemak Bay is 5.81×10^9 m^3, the intertidal 1.53×10^9 m^3. Using the tidal prism method, 773 hours or approximately 32 days was the flushing time in March when runoff was 30.5 cfs; flushing time using the modified method was 774.3 hours. In July the runoff was 1394 cfs, and with the two methods, 17.07 and 18.0 hour flushing rates were calculated, respectively. With an annual average discharge of 408 cfs, the flushing times were 58.8 and 59.3 hours, respectively.

The extremes in river discharge at both sites significantly influence the flushing of pollutants. In addition, at Knik Arm the tides are especially effective in increasing the dilution volume of the receiving waters by: 1) moving vast quantities of water past any point in the Arm; this produces an effect comparable to that obtained by a large diffuser installed in the same body of water without such tides; and, 2) the intense tidal currents increase the turbulence in the receiving water and create an ideal environment for rapid dilution of wastes through turbulent diffusion (Marine Advisers 1965). As a result the large tidal ranges and turbulence especially in Knik Arm would produce more rapid flushing rates.

The movement of surface water out of Knik Arm during ebb tide is observed in Figure 66. This ERTS image shows near IR reflected radiation (0.8-1.1 m); very little water penetration is achieved in this wavelength. Tidal flats (1) are apparent and variations in suspended sediment

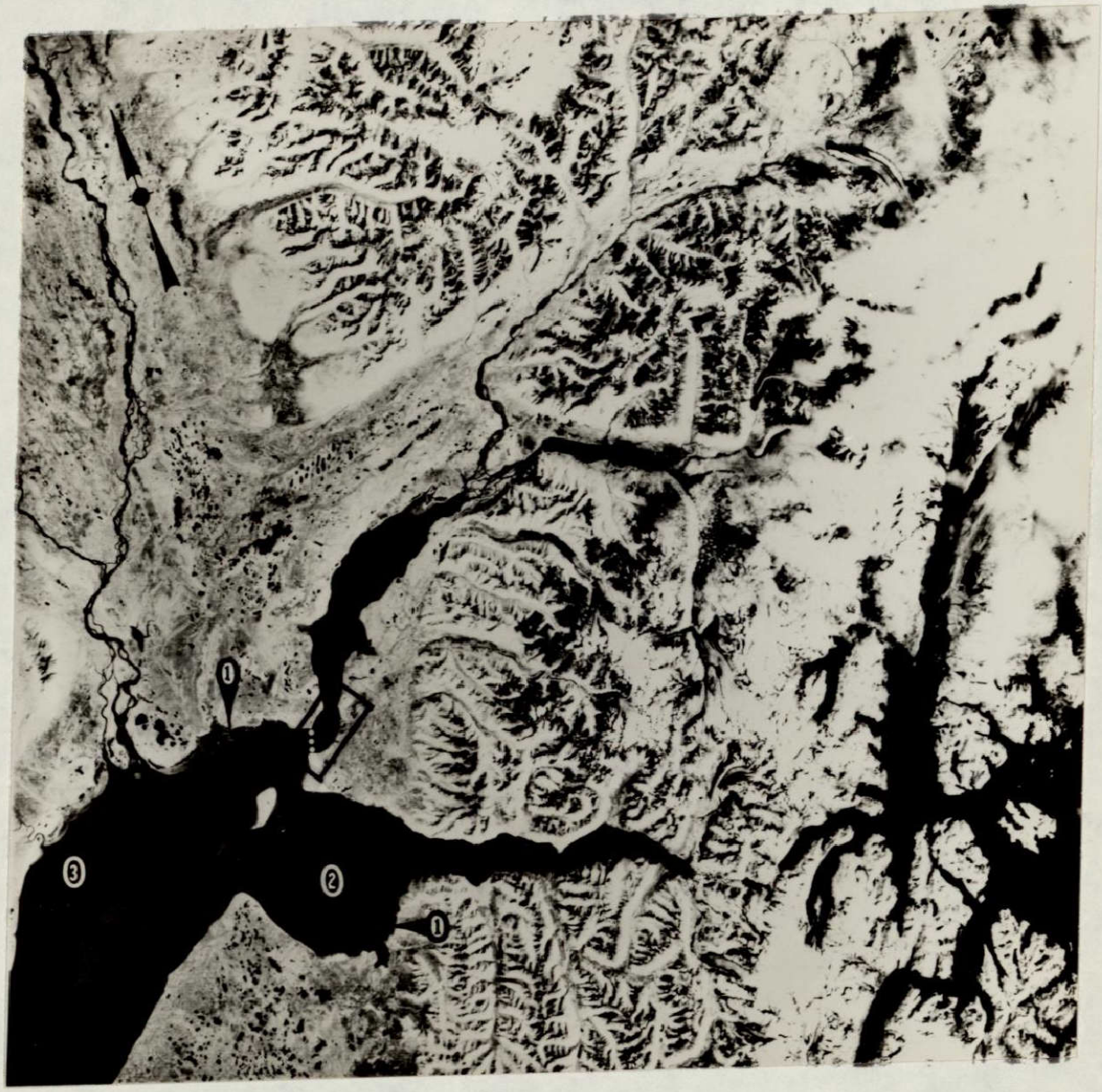

Figure 66. Northern Cook Inlet. ERTS MSS band 7 image 1390-20450, acquired 17 August 1973; ebb tide at Anchorage.

loads near the water surface enhance the current patterns. Turbid water (2) appears lighter than clear water (3). These patterns show the most likely path of pollutant transport and potential sites of dispersion or concentration can be distinguished. Ebbing water moves out of the Arm between Fire Island and the north shore and appears to stay on the north side of the inlet. Data from detailed studies at the mouth of Turnagain Arm indicate that tidal currents of 4-6 knots generally move directly up and down the Arm with the changing tides (Alaska Department of Highways, undated). There is minor lateral movement of water except at early flood and late ebb when bottom friction is greatest and eddies are common. These virtually straight patterns are also apparent on the ERTS image in Figure 66.

Figure 67 (location indicated on Figure 66) shows the location of the Anchorage Borough Sewage Treatment Plant (1) at Point Woronzof (2). The outfall is located northwest (3) of the Point in an area of high turbulence and mixing. Currents in this area are essentially rectilinear (to-fro) with weak transverse currents. This is reflected in the linear surface patterns (4) at the mouth of Knik Arm (Figs. 66 and 67). Model studies show that flow past the Anchorage Dock area (9) is approximately 2.5×10^6 cfs but varies with tide heights (Carlson 1970). Murphy et al. (1972) report that a large eddy current may form in the half-moon shaped bay east of Point Woronzof which may tend to concentrate wastes in this area. Detailed current studies verify that a clockwise gyre forms on the northeast side of Point Woronzof during flood, a counter-clockwise gyre on the southwest side during ebb (Marine Advisers 1965). Due to high turbulence in this area there is nearly complete mixing and little thermal stratification. The "feathered-edge" pattern (5) suggests that bottom scouring may occur west of Point MacKenzie during early flood. Clear water (6) occurs in the protected area; sun glint (7) shows the surface roughness; turbid mixed water (8)exists north of Anchorage.

Figure 65 shows Kachemak Bay on 27 September during early flood tide. Homer (1) is located at the base of the spit which divides the bay in half. Clear oceanic water (4) has begun to move into the inner bay and more turbid water (3) occupies the north side. Glacial meltwater (5) appears to be moving out and mixing with less turbid water (2). Flushing within this portion of the bay may be significantly reduced because of the narrow opening between the spit and south shore.

SUMMARY AND CONCLUSIONS

Sufficient observational data on transport-circulation processes were presented to develop a basic understanding of the regional relationships between river hydrology, sediment distribution and nearshore oceanography in Cook Inlet. Synoptic interpretations made from repetitive

Figure 67. Anchorage area during early flood tide (outlined in Figure 66; NP-3A photograph).

aircraft, ERTS-1 Multispectral Scanner (MSS), and NOAA-2 and -3 Very High Resolution Radiometer (VHRR) imagery with corroborative ground truth data provide for the first time, a means of analyzing on a regional basis, estuarine surface circulation, sediment distribution, water mass movement, coastal processes, areas of sediment deposition, tidal flat distribution, and coastal land forms. The distribution and configuration of tidal flats were mapped with MSS band 5 and 7 images. Coastal landforms and configuration are most apparent in band 6 and 7 images taken during the 6th ERTS-1 cycle; cultural features not previously mapped are also visible on the MSS band 5 images of these scenes. Areas of suspected upwelling, the distribution of suspended sediment and surface circulation patterns were mapped on MSS bands 4 and 5. Comparisons of these features and processes were made with color IR and thermal IR aircraft imagery. Sediment distribution, current directions, mixing patterns along river plume and water mass boundaries, tidal flats and coastal landforms show best on the color IR photography. The thermal IR scanner imagery was most useful in interpreting mixing zone patterns.

The regional circulation as inferred from suspended sediment patterns apparent on the imagery were verified by ground truth data. Clear ocean water moves into the inlet and progresses northerly along the east shore during flood tide at Seldovia, while ebb flow is occurring at Anchorage; near Ninilchik mixing increases with sediment laden inlet water. Clear oceanic water also progresses in an easterly direction along the south side of Kachemak Bay during flood tide. Water with higher suspended sediment concentration from the Fox River and Sheep Creek is confined to the northern portion of the bay. Turbid inlet water generally occurs in the western portion of the inlet and moves south towards the inlet mouth along the west side. Changes in the sediment concentration of these water masses and of rivers discharging into the inlet can be inferred from the tonal variations in the MSS imagery. Complex circulation patterns are produced around Kalgin Island because at this location ebbing and flooding waters meet, current velocities are high and coastline configuration causes strong cross-inlet currents. Several local circulation patterns not recognized before were identified: a clockwise back eddy observed during flood tide in the slack water area between Cape Ninilchik and Kenai offshore from Clam Gulch; a counterclockwise current north of the forelands during ebb tide at Anchorage; and, the movement of sediment laden, ebbing water past the west side of Augustine Island, out the inlet around Cape Douglas and through Shelikof Strait.

Imagery interpretations and ground truth data also indicate that turbulence and mixing are especially high along the southeast coast. The rivers along this coast contain less suspended sediment than those on the northwest shore; the high sediment concentration in these coastal

waters is probably due primarily to bottom scouring and resuspension during flood tide. A distinct mass of less turbid water was observed to intrude into the Kenai River more than a mile during flood tide. This may hasten the removal of pollutants from the river by increasing the volume of water available for mixing. Along the northwest coast between the Drift and Big Rivers, variability in water turbidity is distinct and the movement of water was traced through several tidal stages.

Stratification occurs in and around protected areas such as Kamishak and Kachemak Bays throughout the summer months but is weak in late spring and early fall when fresh water runoff is reduced. It is generally agreed however, that stratification in most of the inlet is weak due to high turbulence and mixing. The variable densities in stratified water provide boundaries along which pollutants move and disperse. Strong stratification could restrict diffusion and cause increased pollution concentrations. A summary of stratification in the lower inlet during summer 1973 follows: May, weak or absent in the central inlet, more developed in Kamishak Bay around Augustine Island, along or near the west shore and in outer Kachemak Bay (this is typical for all tides); June, weak in mid-inlet, decreases going north along the west shore, persists in Kamishak Bay, however, the thermocline is up to 25 m deeper near the inlet mouth on the west side; July, weak near mid-inlet mouth, stronger on west side of mouth, generally the thermocline varies within the 0-25 m depth; August, stratification persists in Kachemak and Kamishak Bays; September, stratification becomes stronger in the above areas.

The locations where most pollutants are presently discharged into the inlet are sites of high turbulence and mixing. Dissipation of the pollutants depends on freshwater inflow, which influences the net exchange of inlet and ocean water, and on the velocity of the tidal currents, which influences turbulent diffusion; where these factors are high, dispersion and diffusion are greatest. Current and mixing patterns in these areas were observed on the satellite and aircraft imagery.

This investigation has contributed to the NASA Earth Observations Aircraft Program by demonstrating the utility of aircraft and satellite imagery and current state-of-the-art remote sensing interpretation techniques in providing repetitive synoptic data on estuarine processes in the subarctic. This program was established in 1964 at NASA's Manned Spacecraft Center (MSC) to develop earth survey techniques using aircraft equipped with various combinations of photographic, infrared, and microwave remote sensing instruments. The program has grown in size and importance due primarily to increasing national interest in ecological problems and the current emphasis within the government in testing space science and technology for practical applications (National Aeronautics

and Space Administration 1972). The techniques utilized during this study can be useful in guiding improvements in sensor selection and interpretation methods in future satellite programs investigating arctic and subarctic oceanography.

APPLICATIONS

Demonstrations and speculations on the application of aircraft and satellite imagery to a wide variety of earth resources investigations are numerous in the literature. It would be redundant to cite these examples here. As an alternative the Congressional Acts which deal with subjects pertinent to this investigation and which form the basis for the principal civil works mission responsibilities of the Corps of Engineers are listed according to subject areas:

1. Water/land conservation:

   Federal Water Project Recreation Act, 1965

   Land and Water Conservation Act, 1965

   Outdoor Recreation Act, 1963

   Estuarine Study Act - Inventory of Estuaries, 1968

2. Environmental impacts:

   National Environmental Policy Act, 1969

3. Maintenance of waterways, shorelines and beaches:

   River and Harbor Act, 1962-1968

   Coastal Zone Management Act, 1972

4. Water quality:

   Clean Water Restoration Act, 1966

   Fish and Wildlife Coordination Act, 1946-1958

   Federal Water Pollution Control Act, 1948-1972

   Water Quality Act, 1965

   Marine Protection, Research and Sanctuaries Act, 1972

Simultaneously, these Acts deal with subjects for which the utility of aircraft and satellite imagery has been demonstrated or suggested by this or related investigations. A number of applications in earth resources studies recognized during this investigation and directly applicable to the requirements of the aforementioned Congressional Acts are shown in Table 8.

Table 8. Applications of aircraft and satellite imagery.

A. Data base
   1. Preliminary site selection
   2. Coastal Zone Management decisions
   3. Channel and harbor maintenance
   4. Regional environmental interpretations
   5. Ecosystem protection

B. Augment preparation and revision of hydrographic and navigation charts

C. Acquire engineering design criteria

D. Interpret coastal processes

E. Improved thematic mapping

F. Monitor estuarine circulation
   1. Dispersion of pollutants
   2. Movement of sea ice/ ice survey
   3. Sediment distribution
   4. Fish migration

In addition, data on circulation and sedimentation provided by this project and similar remote sensing investigations would be useful in several on-going Alaska District, Corps of Engineers investigations of: circulation and sedimentary processes at sites of proposed deep-draft harbors and/or small boat basins in Iniskin Bay, near Anchorage and at several locations along the southeast shore, resuspension of dredge material disposed at the site 300 m west of Anchorage in 12 m of water, sedimentation near Anchorage and Kenai, shoaling and littoral drift near Kenai, suspended sediment transport mechanisms, and beach erosion control at Ninilchik. The data could also be used in developing maintenance dredging schedules and in preparing environmental impact statements prior to the construction of offshore and coastal structures, especially in areas of active petroleum development.

Remote sensing techniques utilized in this investigation could also provide reliable repetitive data to state, local and federal agencies and private industry with interests in preserving the environmental quality of the inlet. One of the major objectives of the Coastal Zone Management programs being administered by N.O.A.A. is the acquisition of information on estuarine and coastal water circulation, waste assimilation capabilities of coastal water and coastal sediment transport. The U. S. Geological Survey is currently investigating the sources and deposition of sediment in estuarine and coastal environments. The National Ocean Survey, N.O.A.A. is actively updating existing navigational and tidal current charts. Private industry has increasing interest in developing and exploiting the resources and commercial potential of the Cook Inlet basin. Federal funds may become available

to study the regional impact of a proposed export dock at Point MacKenzie. A lumber chip mill has been proposed for construction in the Homer area. Interest has recently increased in coal reserves at Beluga and minerals along the west shore; petroleum exploration drilling in the southern Cook Inlet has been active since September 1974. Wise utilization of these resources with minimal environmental degradation is now acknowledged to be a primary concern of our society. With pressure mounting rapidly for extensive development, it is necessary to continue the environmental research required to increase our basic understanding of this region as soon and as vigorously as possible. Cook Inlet is the fastest growing area in industrial development in the state of Alaska. Increased pressures of population and industrialization make it imperative that investigations of the water resources of Cook Inlet be continued in order to manage these resources in the most efficient manner possible.

RECOMMENDATIONS

Based on the experience of this investigation it is considered appropriate to make some general recommendations relative to future NASA Earth Observations programs. First, there is a need to emphasize and improve provisions for technology transfer within user organizations. Greater awareness and participation from the operational personnel of the user agencies is needed. This, of course, is a responsibility of the user agencies, but NASA should recognize this need and take the lead in stimulating a greater awareness of this requirement and aid in devising means for implementing effective programs. Second, utilization of aircraft and satellite data must be increased in remote areas where ground surveys are seasonally impossible or prohibitively expensive. These aerial data provide repetitive, synoptic views of many dynamic environmental processes. Third, a cooperative program between the U.S. Geological Survey, the National Ocean Survey, NOAA, the Corps of Engineers, universities and state agencies should be instituted to develop a more complete data base on the water quality and processes of the inlet. Presently the above agencies and institutions have separate projects to provide data on several aspects of the inlet oceanography. The suggested unified approach would produce integrated baseline data in all pertinent oceanographic fields with minimal duplication and costs. As a result private industry and responsible state and federal governmental agencies could utilize the data package to more intelligently and efficiently plan, design and construct offshore engineering structures; to maintain existing harbors and navigable waters; and, to implement a coastal zone management program based on complete and up-to-date data. Fourth, additional research is required in several areas. Complex circulation patterns were observed in the middle inlet from Kalgin Island to just north of the forelands. Extensive mixing of the oceanic and inlet water masses occurs here and current directions change four times daily. A detailed analysis of tidal/seasonal changes in this area would provide a more complete understanding of the inlet circulation. Detailed

investigations of oceanographic processes should be completed prior to offshore exploration and drilling in southern Cook Inlet. Potential pollution from drilling muds is currently of particular concern to fishermen in the Kachemak Bay area. Repetitive aerial surveys of the bay would provide data on circulation which would be useful in selecting possible disposal sites for the muds. Fifth, the utility of imagery in measurement of suspended sediment concentrations should be investigated as a method for estimating deposition rates, dredging schedules, and ultimately, the longevity of harbors and small boat basins.

BIBLIOGRAPHY

Alaska Construction and Oil, 1973, Big Anchorage sewer job nears completion: November, p. 45-48.

Alaska Department of Highways, undated, Engineering geology and foundation report, Field and laboratory soils data, Turnagain Arm Crossing, 37 p.

Alaska District, Corps of Engineers, 1948, Engineering data, survey of Cook Inlet and Anchorage Harbor, Alaska: Preliminary Report, Anchorage, Alaska, 21 p.

Alaska District, Corps of Engineers, 1973, Operation and maintenance of the Anchorage Harbor, Anchorage, Alaska: Draft Environmental Impact Statement, 56 p.

Anderson, D. M., L. W. Gatto, H. L. McKim and A. Petrone, 1973, Sediment distribution and coastal processes in Cook Inlet, Alaska: Symposium on Significant Results obtained from the Earth Resources Technology Satellite-1, NASA SP-327, March, p. 1323-1339.

Armstrong Associates, 1968, Causeway studies, Turnagain Arm crossing, Alaska: Report for Alaska Department of Highways, November, 27 p.

Barnes, F. F., 1958a, Cook Inlet-Susitna Lowland: in Landscapes of Alaska: Their Geologic Evolution: ed. Howell Williams, Berkeley, California, University of California Press, p. 43-47.

Barnes, F. F., 1958b, Talkeetna Mountains: in Landscapes of Alaska: Their Geologic Evolution: ed. Howell Williams, Berkeley, California, University of California Press, p. 38-42.

Barnwell, W. W., R. S. George, L. L. Dearborn, J. B. Weeks, C. Zenone, 1972, Water for Anchorage, an atlas of the water resources of the Anchorage area, Alaska: U.S. Geological Survey, Water Resources Division, Alaska District, 77 p.

Barnwell, W. W. and C. Zenone, 1969, Hydrologic studies in northern Cook Inlet, Alaska using color photography and thermal imagery: Second Annual Earth Resources Aircraft Program Status Review, vol. III, Hydrology and Oceanography, Report 36, 16-18 September 1969, p. 3-16.

Bartlett, G. A., 1973, Sediment source and processes of transport and deposition in estuaries: presented at 9th Canadian Hydrology Symposium, University of Alberta, Edmonton, Alberta, 7-11 May, 39 p.

Blenkarn, K. A., 1970, Measurement and analysis of ice forces on Cook Inlet structures: Offshore Technology Conference, 22-24 April, Houston, Texas, p. 365-378.

Bowden, K. F., 1967, Circulation and diffusion: in Estuaries, American Association for the Advancement of Science, Publication No. 83, Washington, D.C., p. 15-36.

Burrell, D. C. and D. W. Hood, 1967, Clay - inorganic and organic-inorganic association in aquatic environments, Part II: Institute of Marine Science, University of Alaska, Fairbanks, Alaska.

Carlson, R. F., 1970, The nature of tidal hydraulics in Cook Inlet: The Northern Engineer, vol. 2, no. 4, p. 4-7.

Carlson, R. F. and C. E. Behlke, 1972, A computer model of the tidal phenomena in Cook Inlet, Alaska: Institude of Water Resources Report IWR-17, University of Alaska, Fairbanks, Alaska, 69 p.

Carter, L. V., 1973, An "understanding" on offshore oil: News and Comment, Science, vol. 182, no. 4112, p. 564.

Childers, J. M., 1968, Hydrologic estimates for Turnagain Arm of Cook Inlet, Alaska: based on data collected by the U.S. Geological Survey, 23 May, 2 p.

Coleman, J. M., L. D. Wright, and J. N. Suhayda, 1972, Density gradients at river mouths: Naval Research Reviews, vol. 25, no. 10, p. 9-20.

Cravat, H. R. and R. Glaser, 1971, Color aerial stereograms of selected coastal areas of the United States: National Ocean Survey, National Oceanic and Atmospheric Administration, Rockville, Maryland, 93 p.

Crick, R. W., 1971, Potential petroleum reserves, Cook Inlet, Alaska: in Future Petroleum Provinces, North America, Amer. Assoc. Pet. Geol. Memoir 15, vol. 1, p. 109-119.

Dyer, K. R., 1973, Estuaries: a physical introduction: John Wiley and Sons, London, 140 p.

Environmental Currents, 1972, Environmental Science and Technology, vol. 6, no. 12, p. 965.

Evans, C. D., E. Buch, R. Buffler, G. Fisk, R. Forbes and W. Parker, 1972, The Cook Inlet environment, a background study of available knowledge: Resource and Science Service Center, University of Alaska, Anchorage, Alaska.

Federal Field Committee for Development Planning in Alaska, 1971, Economic outline for Alaska: Anchorage, Alaska.

Feulner, A. J., 1971, Water-resources reconnaissance of a part of the Matanuska-Susitna Borough, Alaska: U.S. Geological Survey Hydrologic Investigation Atlas HA-364.

Feulner, A. J., J. M. Childers, V. W. Norman, 1971, Water Resources of Alaska: U.S. Geological Survey, Water Resources Division, Alaska District, Open File Report, 60 p.

Grantz, A., I. Zietz and G. E. Andreasen, 1963, An aeromagnetic reconnaissance of the Cook Inlet area, Alaska: U.S. Geological Survey Prof. Paper 316G, p. 117-134.

Hansen, J. A., 1973, Symposium on the physical processes responsible for dispersal of pollutants in the sea; a summary of proceedings: Water Research, vol. 7, p. 927-928.

Horrer, P. L., 1967, Methods and devices for measuring currents: in Estuaries, American Association for the Advancement of Science, Publication No. 83, Washington, D.C., p. 80-89.

Johnson, P. R. and C. W. Hartman, 1969, Environmental Atlas of Alaska: Institute of Arctic Environmental Engineering, University of Alaska, Fairbanks, Alaska, 111 p.

Karlstrom, N. V., 1964, Quaternary geology of the Kenai lowland and glacial history of the Cook Inlet Region, Alaska: U.S. Geological Survey Prof. Paper 443, 69 p.

Ketchum, B. H., 1950, Hydrographic factors involved in dispersion of pollutants introduced into tidal streams: Journal Boston Soc. Civil Engineers, vol. 37, p. 296-314.

Ketchum, B. H., 1951, The exchange of fresh and salt water in tidal estuaries: Journal Marine Research, vol. 10, p. 18-38.

Ketchum, B. H. and B. W. Tripp, 1972, Pre-publication summary of the coastal zone workshop: Institute of Ecology and Woods Hole Oceanographic Institution, Woods Hole, Mass., 22 May - 3 June, 43 p.

Kinney, P. J., D. K. Button, D. M. Schell, B. R. Robertson and J. Groves, 1970a, Quantitative assessment of oil pollution problems in Alaska's Cook Inlet: Institute of Marine Science Report R-169, University of Alaska, Fairbanks, Alaska, 116 p.

Kinney, P. J., J. Groves and D. K. Button, 1970b, Cook Inlet Environmental data, R/V Acona Cruise 065 - May 21-28, 1968: Institute of Marine Science Report R-70-2, University of Alaska, Fairbanks, Alaska, 120 p.

Knecht, R. W., 1973, Coastal zone management act: a broader scope for state initiative: Water Spectrum, vol. 5, no. 1, p. 32-36.

Knull, J. R. and R. Williamson, 1969, Oceanographic survey of Kachemak Bay, Alaska: U.S. Department of Interior, Fish and Wildlife Service, Bureau of Commercial Fisheries, Biological Laboratory Auke Bay, Alaska, Manuscript Report - File Nos. 60 (April), 70 (July) and 76 (October), 53 p., 76 p., 29 p., respectively.

Lauf, G. H. (ed), 1967, Estuaries; American Association for the Advancement of Science, Publication 83, Washington, D.C., 757 p.

Lawrence, F. F., 1949, Preliminary report on water power resources of Little Susitna River and Cottonwood Creek, Alaska: U.S. Geological Survey, Tacoma, Washington, 24 p.

MacKevett, E. M. and G. Plafker, 1974, The Border Ranges fault in south-central Alaska: U.S. Geological Survey Journal of Research, vol. 2, no. 3, p. 323-329.

Marine Advisers, Inc., 1964, Oceanographic conditions at Beshta Bay, Cook Inlet, Alaska: Report prepared for Humble Oil Company of California, La Jolla, California, May, 37 p.

Marine Advisers, Inc., 1965, A study of the oceanographic conditions in the Anchorage area relevant to sewage outfall planning: Report prepared for Tryck, Nyman and Hayes and Stevens and Thompson, La Jolla, California, October, 34 p.

Marine Advisers, Inc., 1966a, Currents near the mouth of Drift River, Cook Inlet, Alaska: Report prepared for Cook Inlet Pile Line Company, La Jolla, California, August, 7 p.

Marine Advisers, Inc., 1966b, Hydrographic survey in Trading Bay, Cook Inlet, Alaska: San Diego, California, September, 10 p.

Marine Advisers, Inc., undated, Oceanographic survey of Beluga-Moose Point pipeline route across Cook Inlet, Alaska: Report prepared for Standard Oil Company of California, La Jolla, California, 50 p.

Miller, D. J., 1958, Gulf of Alaska Area: in Landscapes of Alaska: Their Geologic Evolution: ed. Howell Williams, Berkeley, Calif., University of California Press, p. 19-29.

Mungall, J. C. H. and J. B. Matthews, 1970, A variable-boundary numerical tidal model: Institute of Marine Science Report R70-4, University of Alaska, Fairbanks, Alaska, 163 p.

Murphy, R. S., R. F. Carlson, D. Nyquist, and R. Britch, 1972, Effect of waste discharges into a silt laden estuary, a case study of Cook Inlet, Alaska: Institute of Water Resources Report IWR-26, University of Alaska, Fairbanks, Alaska, 42 p.

National Aeronautics and Space Administration, 1972, Earth observations aircraft remote sensing handbook, volumes I, II and III: Report MSC - 04810, prepared for Earth Observations Aircraft Program Office, Manned Spacecraft Center, Houston, Texas.

Oil and Gas Journal, 1974a, Wildcatting near in lower Cook Inlet: August 5, vol. 72, no. 31, p. 32.

Oil and Gas Journal, 1974b, Local spudding middle Cook Inlet well: September 9, vol. 72, no. 36, p. 53.

Owens, M. E. and B. R. Allard, 1970, Installation and operation of hydraulic pumping systems on Cook Inlet: Offshore Technology Conference Preprints, vol. 1, April 22-24, p. 469-480.

Payne, T. G., 1955, Mesozoic and Cenozoic tectonic elements of Alaska: U.S. Geological Survey Misc. Geol. Inv. Map I-84.

Pluhowski, E. J., 1972, Hydrologic interpretations based on infrared imagery of Long Island, New York: U.S. Geological Survey Prof. Paper 2009-B, 20 p.

Porter, O'Brien, Armstrong and Tryck, Nymam and Associates, 1963, Feasibility Study Turnagain Arm Crossing, Phase 1, Research of Existing Data: Preliminary Report for State of Alaska, March 8, 47 p.

Porter, O'Brien, Armstrong and Tryck, Nymam and Associates, 1964, Feasibility Study, Turnagain Arm Crossing, Phase 2, Alternative Crossing Studies: Preliminary Report for State of Alaska, January 6, 20 p.

Pritchard, D. W., 1967, What is an estuary: physical viewpoint: in Estuaries, American Association for the Advancement of Science, Publication No. 83, Washington, D.C., p. 3-5.

Rosenberg, D. H. (Ed.), 1972, A review of the oceanography and renewable resources of the northern Gulf of Alaska: Institute of Marine Science Report R72-23, University of Alaska, Fairbanks, Alaska, 690 p.

Rosenberg, D. H., D. C. Burrell, K. V. Natarajan, and D. W. Hood, 1967, Oceanography of Cook Inlet with special reference to the effluent from the Collier Carbon and Chemical Plant: Institute of Marine Science Report No. R67-5, University of Alaska, Fairbanks, Alaska, 80 p.

Rosenberg, D. H., D. V. Natarajan and D. W. Hood, 1969, Summary Report on Collier Carbon and Chemical Corporation Studies in Cook Inlet, Alaska, Parts I and II, November 1968-September 1969: Institute of Marine Science Report No. 69-13, University of Alaska, Fairbanks, Alaska.

Rosgen, D. L., 1973, The use of color infrared photography for the determination of sediment production: presented at 9th Canadian Hydrology Symposium, Universtiy of Alberta, Edmonton, Alberta, 7-11 May.

Schoephorster, D. B., 1968, Soil Survey of Matanuska Valley Area, Alaska: U.S. Department of Agriculture, Soil Conservation Service, June, 67 p.

Scott, J. T. and R. Stewart, 1968, The role of Langmuir circulations in mixing of Lake George: Atmospheric Sciences Research Center Report 60, State University of New York at Albany, Albany, N.Y., 68 p.

Selkregg, L. l., E. H. Buck, R. T. Buffler, O. E. Coté, C. D. Evans and S. G. Fisk (editors), 1972, Environmental atlas of the Greater Anchorage Area Borough, Alaska: Resource and Science Services, Arctic Environmental Information and Data Center, University of Alaska, Anchorage, Alaska, 105 p.

Sharma, G. D. and D. C. Burrell, 1970, Sedimentary environment and sediments of Cook Inlet, Alaska: Amer. Assoc. Pet. Geologists Bull. vol. 54, no. 4, p. 647-654.

Sharma, G. D., F. F. Wright, and J. J. Burns, 1973, Sea-ice and surface water circulation, Alaskan Continental Shelf: 2nd Semi-Annual Report for ERTS Project 110-H, University of Alaska, Fairbanks, Alaska, Feb.-July, 31 p.

Sharma, G. D., F. F. Wright, J. J. Burns, and D. C. Burbank, 1974, Sea surface circulation, sediment transport, and marine mammal distribution, Alaska continental shelf: Final Report of ERTS Project 110-H, University of Alaska, Fairbanks, Alaska, 77 p.

Sverdrup, H. U., M. W. Johnson and R. H. Fleming, 1942, The Oceans, their physics, chemistry, and general biology: Prentice-Hall, Inc., Englewood Cliffs, N.J., 1087 pp.

Tabata, S., 1972, The movement of Fraser River - influenced surface water in the Strait of Georgia as deduced from a series of aerial photographs: Pacific Marine Science Report No. 72-6, Marine Sciences Branch, Pacific Region, Victoria, B.C., Canada, 69 p.

Totspeich, F. B. 1969, Water pollution in Alaska, Present and Future: Science, vol. 166, p. 1239-1245.

Trainer, F. W., 1953, Preliminary report on the geology and ground-water resources of the Matanuska Valley agricultural area, Alaska: U.S. Geological Survey Circular 268, 43 p.

U.S. Department of Agriculture, U.S. Department of Commerce, U.S. Department of Interior, State of Alaska, 1968, Alaska Conservation Needs Inventory: A Cooperative Report, 57 p.

U.S. Department of Commerce, 1964, U.S. Coast Pilot 9, Pacific and Arctic Coasts, Alaska, Cape Spencer to Beaufort Sea: U.S. Government Printing Office, Washington, D.C., 347 p.

U.S. Department of Commerce, 1971, Tide Table, High and Low Water Predictions 1972, West Coast of North and South America: National Ocean Survey, National Oceanic and Atmospheric Administration, p. 126-133.

U.S. Department of Commerce, 1972, Tide Table, High and Low Water Predictions 1973, West Coast of North and South America: National Ocean Survey, National Oceanic and Atmospheric Administration, p. 120-127.

U.S. Department of Commerce, 1973, Local Climatological Data, Environmental Data Service.

U.S. Geological Survey, 1970, Water resource data for Alaska: Water Resources Division, Anchorage, Alaska, 263 p.

U.S. Geological Survey, 1971, Water resource data for Alaska: Water Resources Division, Anchorage, Alaska, 319 p.

von Arx, W. S., 1962, An introduction to physical oceanography: Addison-Wesley Publishing Co., Reading, Mass., 422 pp.

Wagner, D.G., R.S. Murphy and C.E. Behlke, 1969, A program for Cook Inlet, Alaska for the collection, storage and analysis of baseline environmental data: Institute of Water Resources Report No. 1WR-7, University of Alaska, Fairbanks, Alaska, 284 p.

Wahrhaftig, C., 1958, The Alaska Range: in Landscape of Alaska: Their Geologic Evolution: ed. Howell Williams, Berkeley, California, University of California Press.

Wahrhaftig, C., 1965, Physiographic divisions of Alaska: U.S. Geological Survey Prof. Paper 482, 52 p.

Walsh, D., 1969, The Mississippi River delta: in Oceans from Space, Gulf Publishing Company, Houston, Texas, p. 171-187.

Wright, F. F. and G. D. Sharma, 1973, Earth Resources Technology Satellite observations of high latitude estuarine circulation: Preprint for Second International Conference on Port and Ocean Engineering Under Arctic Conditions, University of Iceland, September, 14 p.

Wright, F. F., G. D. Sharma and D. C. Burbank, 1973, ERTS-1 observations of sea surface circulation and sediment transport, Cook Inlet, Alaska: Symposium on Significant Results obtained from the Earth Resources Technology Satellite-1, NASA SP-327, March, p. 1315-1322.